M.D. Simmons, K.G. Miller, D.C. Ray, A. Davies, F.S.P. van Buchem and B. Gréselle

Chapter 13

Phanerozoic Eustasy

Chapter outline

Abstract

Isolation of the eustatic signal from the sedimentary record remains challenging, yet much progress is being made toward understanding the timing, magnitude, and rate of eustasy on both long-term (10^7–10^8 years) and short-term (10^5–10^6 years) scales throughout the Phanerozoic. Long-term eustasy is primarily driven by a number of factors relating to plate tectonics. The magnitude and rate of short-term eustatic change strongly suggests glacio-eustasy as the key driving mechanism, even in episodes of the Earth's history often typified as having "greenhouse" climates. This notion is, in turn, supported by a growing body of both direct and proxy evidence for relatively substantial polar glaciation in many periods of the Earth's history (with the possible exception of the Triassic). An understanding of eustasy is important for the development of the geologic time scale because it contributes to the sequence stratigraphic organization of sedimentary successions (including chronostratigraphic reference sections) and helps to understand the often incomplete nature of the geologic record. The integration of eustasy with our evolving knowledge of the Earth systems science (e.g., paleoclimate evolution, orbital forcing of sedimentary systems, geochemical evolution of the oceans, and biological evolutions and extinctions) will help to provide the tools to develop a context for the subdivisions of the geologic time scale.

13.1 Introduction

Ever since the great Austrian geologist Suess (1888, 1906) introduced the term "eustatic movements" to describe globally recognizable and synchronous transgressions and regressions in the geological past, geoscientists have sought to better understand eustasy and its expression in the rock record. The early 20th century pioneers, such as Chamberlin (1909) and Grabau (1936a,b, 1940), argued for a "rhythm of the ages," the global signature of eustasy in the rock record (Johnson, 1992; Pemberton et al., 2016; Simmons, 2018).

The study of eustasy became somewhat neglected in the 1950s and 1960s, with the attention of many geologists focused on the development of the plate tectonics paradigm [although see Hallam (1963) for an early example of the integration of eustasy with the developments in marine geology that would shape plate tectonics]. Eustasy returned to the forefront of thinking in sedimentary geology in the late 1970s with the publication of the seminal paper on eustasy and its relationship to the concepts of sequence stratigraphy by Vail et al. (1977) at Exxon Production Research (EPR). Vail et al. published a much cited Phanerozoic global sea-level curve that would continue to be substantially revised in later years (Haq et al., 1987, 1988; Hardenbol et al., 1998; Haq and Schutter, 2008; Haq, 2014, 2017, 2018).

Much of the original work by Vail, Haq, and the EPR team was based on subsurface geology: the perceived expression of eustasy in biostratigraphically calibrated seismic and wire line log data. Because confidentiality restrictions prevented much of this data from being published, the proofs of the early eustatic models from this team were not available, which was a cause of significant criticism

Geologic Time Scale 2020. DOI: https://doi.org/10.1016/B978-0-12-824360-2.00013-9

(e.g., Miall, 1991, 1992; Miall and Miall, 2001). This uncertainty led many other stratigraphers worldwide to seek supporting evidence of the EPR models, or to develop alternative models, often based on outcrop geology (e.g., Embry, 1988, 1997; Hallam, 1992, 2001; Sahagian et al., 1996; House and Ziegler, 1997; Johnson et al., 1998; Izart et al., 2003; Miller et al., 2005a; Simmons et al., 2007; and see Section 13.4).

Eustasy refers to global sea level that is independent of local factors, namely, the position of the sea surface with reference to a fixed datum (Myers and Milton, 1996) (Fig. 13.1). Because such a datum level is often lacking or equivocal, geologists who use the term eustasy are often referring to global mean sea level (GMSL) (Gregory et al., 2019; Miller et al., 2020). Nonetheless, the terms eustasy, eustatic sea level, and eustatic change are persistent in the geological literature (Rovere et al., 2016) and are maintained here.

Geoscientists continue to seek to understand the timing, magnitude, pace, and drivers of eustasy in the rock record. Beyond simple scientific curiosity, there are practical reasons for this. For example, identifying the eustatic component of sequence stratigraphic models enhances their use by improving the ability to predict the likely lateral and vertical variation in sedimentary facies with the framework of stacking patterns (van Buchem and Simmons, 2017) and aids correlation. These factors have value in the search for hydrocarbon source rocks and reservoirs, which is why the study of eustasy has resonated with industry geologists. However, the application of eustasy is not without its challenges. For example, assuming eustasy as a basis for correlation can become a self-fulfilling prophecy; consequently, there is a danger of circular reasoning (see Miall, 2010 and references therein). Nonetheless, *if* a eustatic signal can be isolated in the rock record and constrained using biostratigraphy and other chronostratigraphic proxy techniques, then it can be used as a *guide* to the correlation of transgressive and regressive sedimentary successions (bearing in mind the controls of tectonics and sediment supply on the nature of local sedimentary successions).

Within the context of the geologic time scale an understanding of eustasy is important because it emphasizes the typically incomplete nature of the stratigraphic record, especially in facies deposited from alluvial plains to continental shelves and epicontinental seas (Barrell, 1917; Ager, 1981, 1993). High-amplitude eustatic changes will drive the presence of widespread unconformities and attendant hiatuses and assist in understanding whether or not chronostratigraphic reference sections [Global Boundary Stratotype Sections and Points (GSSPs)] are likely to contain continuous stratigraphy. An understanding of whether such sections are placed in transgressive or regressive settings can also help to facilitate their correlation. Furthermore, as understanding of eustasy evolves, it can assist in the placement of chronostratigraphic boundaries by relating them to widely correlatable events in the rock record that can have a distinctive expression (Simmons, 2012). Peter Vail's comment "using global cycles with their natural and significant boundaries, an international system of geochronology can be developed on a rational basis" (Vail et al., 1977) has failed to find much favor with the chronostratigraphic community, mainly because the expression of eustasy in the rock record is variable in time and space, and thus continues to be debated. Nonetheless, as Phanerozoic eustatic models become stable,

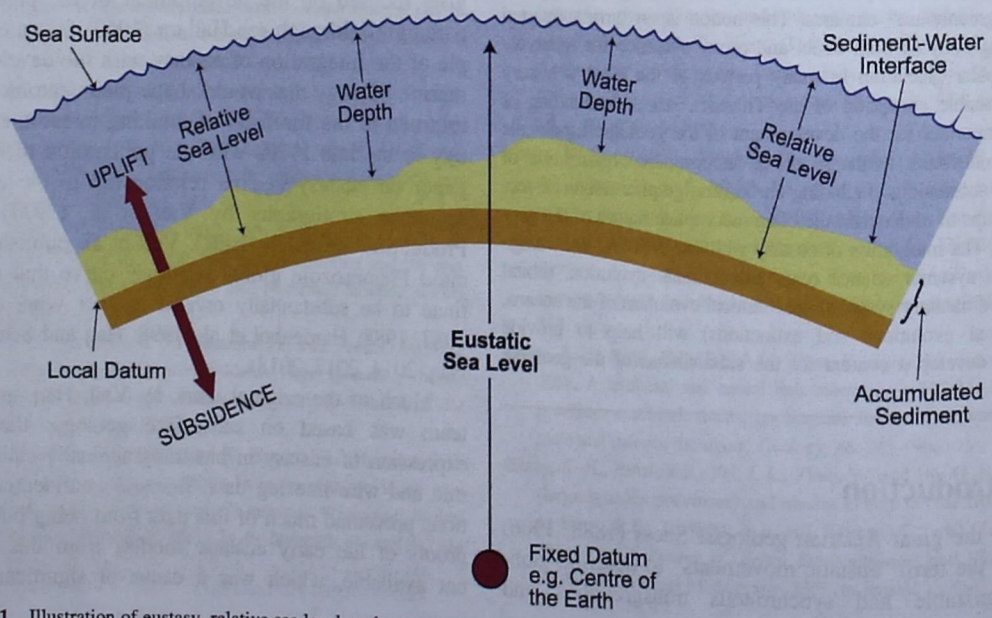

FIGURE 13.1 Illustration of eustasy, relative sea level, and water depth. After Myers and Milton (1996).

then eustasy can provide a clear guide to the formal subdivision of geologic time.

Indeed, there is an increasing integration of eustasy with chronostratigraphic definitions. For example, Babcock et al. (2015) noted that the first appearance datums of agnostoid trilobites, which are the primary correlation events for the bases of the Drumian, Guzhangian, Pabian, and Jiangshanian stages of the Cambrian, are associated with eustatic rises, and with oceanographic and climatic cycles. Such holistic approaches to chronostratigraphic definition that integrate GSSPs with various aspects of the Earth system science (including eustasy) are to be applauded: the proposed GSSP for the base of the Lopingian (Permian) stage is a further example (Jin et al., 2006), whereas Triassic stages have long been linked to eustatic cycles (Embry, 1997).

Identifying eustasy in the rock record is not easy. Major challenges exist to prove synchroneity, magnitude, and pace. Driving mechanisms are much debated outside of the well-established episodes of major polar glaciation that Chamberlin (1899) first recognized as a driver of sea-level change. Entire books (e.g., Miall, 2010) have been published justly emphasizing how difficult these challenges are. Although much work is still needed to improve our understanding of Phanerozoic eustasy, here we hope to demonstrate that knowledge of the timing, magnitude, duration, and drivers of eustasy is evolving, at least in the sense of what Johnson et al. (1991) termed "practical eustasy," and that this can provide insight into the development of the stratigraphic record and geologic time scale.

13.2 The sequence stratigraphy paradigm and eustasy

13.2.1 Sequence stratigraphy

The recognition of eustasy in the rock record is possible through an understanding of the principles of sequence stratigraphy. Sequence stratigraphy relies on recognizing changes in the space available for sediments to accumulate (accommodation), of which eustasy is but one driver, versus sediment supply. The technique builds upon the long-established geologic concept that the sedimentary rock record displays cycles that can be linked to water depth changes (e.g., Barrell, 1917). It enables the identification of packages of strata that were deposited during similar conditions of accommodation change (stationary, increasing, or decreasing) in relation to sediment supply, and the key stratigraphic surfaces that bound them.

Changes in accommodation relate to the interplay of various independent factors. In the marine realm, accommodation relates to relative sea level (RSL) that, in turn, is primarily controlled by tectonism (subsidence or uplift, including the effects of thermal subsidence, sediment loading, flexure, isostasy, and dynamic topography); changes in the height of the geoid driven by the changing distribution of ice and ocean mass; and short-term (10- to 1000-year scale) oceanographic effects and eustasy. Sediment supply also has a large effect on depositional architecture because changes in sedimentation affect how accommodation is filled. For example, the modern Mississippi delta is currently entering a phase of retrogradation in response to a 50% reduction in the sediment load of the river resulting from the construction of numerous dams (Maloney et al., 2018). These factors control the sequence stratigraphic architecture in every sedimentary basin (Catuneanu, 2019a, 2019b). Consequently, when making a sequence stratigraphic interpretation, it is necessary to consider changes in both the rate of accommodation (A) change (creation or destruction) and changes in the sediment supply (S). Therefore the A:S relationship is critical in determining stratigraphic architecture.

RSL is defined as a change in accommodation (vertical space) relative to the crust, determined by rates of sea-level change and subsidence/uplift (Jervey, 1988; Posamentier and Vail, 1988), although it can be defined more precisely as the difference in height between the sea surface and the solid Earth (Milne et al., 2009; Gregory et al., 2019) (Fig. 13.1). RSL is important because it is the local/region expression of sea-level change, from which the eustatic component must be extracted to develop a view on the timing, magnitude, and rate of eustasy. Subsequent subsections discuss the complexities of this undertaking. However, local sequence stratigraphic models are effectively built from knowledge of change in RSL.

The organization of the stratigraphic record is multiscale. The genetic unit, or parasequence, is the basic building block. Facies distribution within parasequences and how parasequences stack can differ. The characteristic stratal stacking patterns resulting from changes in accommodation and sediment supply are classified as (Fig. 13.2):

- "Aggradational," when sediments of the same facies stack broadly vertically. Here, the creation of accommodation and sediment supply are broadly in balance ($A = S$).
- "Retrogradational," when facies belts display a landward movement. Here, accommodation creation exceeds sediment supply ($A > S$). This can often occur during RSL rise.
- "Progradational," when facies belts display a basinward movement. Here, sediment supply exceeds accommodation creation ($A < S$) and can often occur when RSL is stationary. "Forced progradation" is a type of progradation related to the active destruction of accommodation (by a drop in RSL), when sediments are forced to prograde, irrespective of sediment supply.

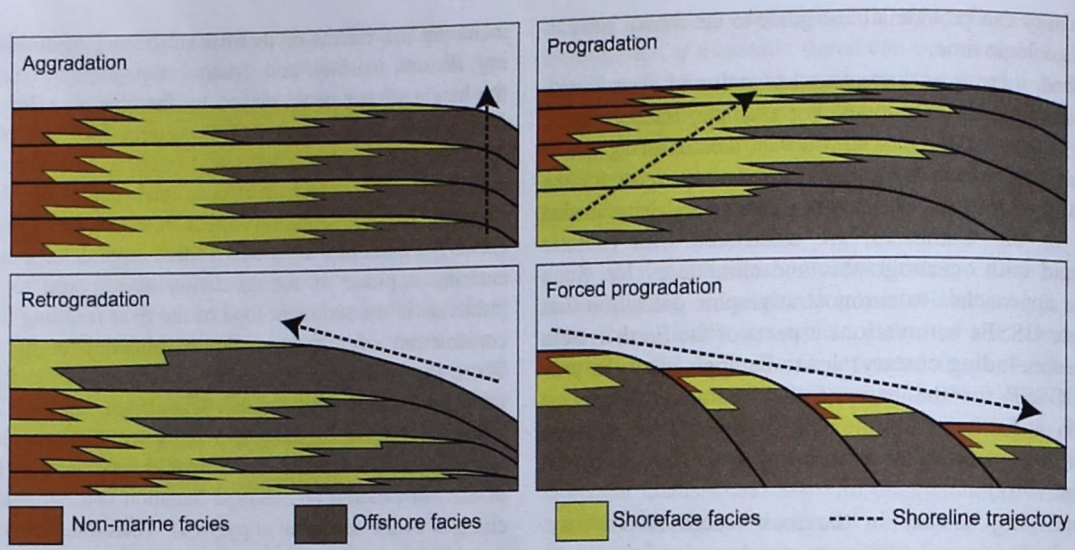

FIGURE 13.2 Stratal stacking patterns relating to the evolution of accommodation versus sedimentation rate over time. Modified after Van Wagoner et al. (1988).

A systems tract (Vail, 1987) represents a series of linked contemporaneous facies, deposited during a particular regime of accommodation creation or reduction (and consequently very often a particular state of RSL change). It is important to note that depositional systems will react differently to accommodation change and will produce and/or transport sediment in different ways. A key distinction can be made between clastic and carbonate systems because carbonates can grow rapidly in situ (Schlager, 2005). Similarly, evaporite systems react distinctively to variations in A/S. However, many of the basic principles are common and can be summarized as follows (Fig. 13.3):

- *Transgressive systems tract (TST).* When the creation of accommodation outpaces sediment supply, such as during periods of rapid sea-level rise or when sediment supply is dramatically reduced, stratal stacking patterns display a retrogradation pattern. Sediments deposited under these conditions are grouped into a TST. TST deposits display a rising shoreline trajectory (the path taken by the shoreline as it changes position in response to accommodation change; see Fig. 13.3) as the shoreface transgresses toward the land. The top of the TST is marked by a maximum flooding surface (MFS) that represents the most landward migration of the shoreline and the maximum amount of accommodation creation. In carbonate systems, different types of response are possible to RSL rise (e.g., Schlager, 2005), one of which is the development of isolated carbonate buildups during the TST that may be drowned, if the creation of accommodation is sufficiently rapid.
- *Highstand systems tract* (HST). Above the TST, sediments occur that comprise the HST. They are characterized by initial aggradation, reflecting a balance between accommodation creation and sediment supply, and later by progradation, as sediment supply outpaces any new accommodation creation. In the marine realm, HST sediments record the slowing of RSL rise. HST sediments display a rising, followed by flat, shoreline trajectory.
- *Lowstand systems tract (LST) and falling stage systems tract (FSST).* The top of the HST is marked by the sequence boundary (SB), which reflects the onset of the active destruction of accommodation, resulting from a drop in RSL. Sediments deposited under these conditions are forced to prograde, irrespective of sediment supply, and display a falling shoreline trajectory. They may form part of the LST or be classified into a discrete FSST. After baselevel fall has ceased, sediment supply may outpace accommodation creation, so that sediments continue to prograde. Sediments deposited under these conditions form part of the LST and display a rising shoreline trajectory. The top of the LST is marked by a maximum regression surface (MRS) or transgressive surface (TS), representing the most basinward migration of the shoreline. Although the MRS or TS is locally erosional, it can be usually distinguished from the SB by its local distribution and stacking patterns; in the absence of LSTs, MRS merge with SB.

At the larger scale, when several sequences are stacked together, the same descriptive terminology as defined previously (Fig. 13.2) can be used to describe the sequence stacking pattern. This notion of scale is important because the application of the principle of systems tracts applies at different scales. Although the expression of changing accommodation versus sediment supply is well understood, the exact means of classifying the different systems tracts

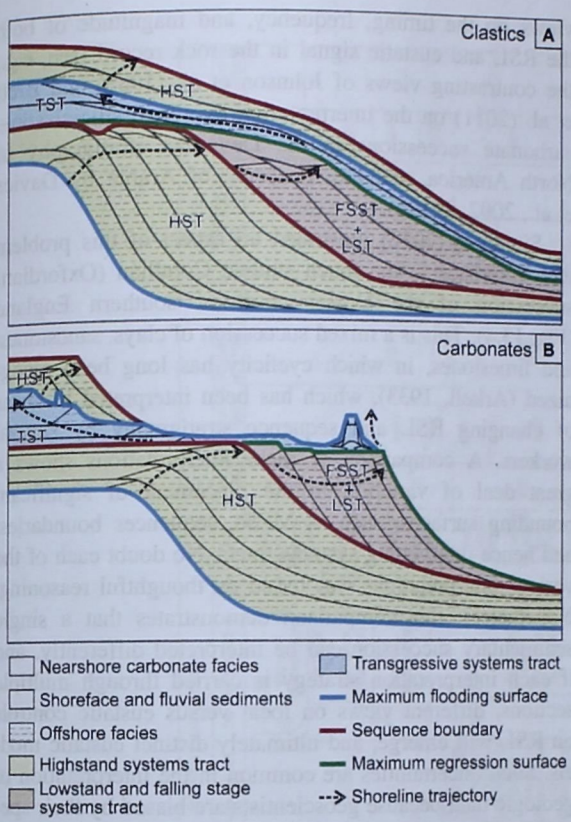

FIGURE 13.3 The typical response of a clastic depositional system (A), and one of the possible responses of a carbonate depositional system (B) to changes in accommodation. Stratal stacking patterns and shoreline trajectory help define three systems tracts (the FSST has been grouped into the LST) and their bounding stratal surfaces. Note the potential to form isolated carbonate buildups during transgression. *FSST*, falling stage systems tract; *HST*, highstand systems tract; *LST*, lowstand systems tract; *TST*, transgressive systems tract.

and stratal surfaces remains a subject of preference and debate (see Catuneanu et al., 2009; Donovan et al., 2010; Catuneanu, 2017, 2019a,b; Miller et al., 2018 and discussion in Simmons, 2012). For example, some authors do not recognize an FSST, and others place the SB at the top of the FSST. The identification of systems tracts and key stratal surfaces in various data types (outcrops, seismic, well logs) and the relationship of these features to position on a RSL curve can vary between different schools of thought, as recently reviewed by Neal and Abreu (2009), Miller et al. (2018), and Catuneanu (2019a). One commonality is the salience and pervasive nature of the MFS, which has led some to propose defining "sequences" not on SBs (unconformities) but on MFS ("genetic stratigraphy"; Galloway, 1989). Previous studies have shown that these approaches are useful on longer time scales and larger spatial scales for regional basin scale stratigraphy (e.g., Sharland et al., 2001) but lack the resolution for reservoir-scale interpretations (Miller et al., 2018).

13.2.2 Synchronous sea-level change

As previously noted, eustasy is one of several factors that control sequence stratigraphic organization of a sedimentary succession. The ongoing challenge is to disentangle eustatic influences from the various local controls to demonstrate that synchronous sequence stratigraphic surfaces exist in multiple sedimentary basins worldwide. Therefore a key challenge to recognizing eustasy in the rock record is the ability to confirm the synchroneity of changes in sea level through chronostratigraphically significant calibration, typically using biostratigraphy (Armentrout, 2019). Such techniques have inherent limitations. These include:

- Do biozones offer sufficient precision to unequivocally confirm synchroneity? For many biozonation schemes based on planktonic fossils, individual biozones can be of a duration of 500,000 years or less, but this is variable. In well-studied basins, such as the Neogene Gulf of Mexico, biostratigraphic resolution approaches that of cyclostratigraphy with average biozonal duration being 144,000 years (Bergen et al., 2019). Although the recognition of biozones defined by bioevents (typically extinctions and inceptions of taxa) remains the default method of conducting biostratigraphy, other approaches, including quantitative and semiquantitative methods, consider the whole fossil assemblage present, rather than the presence or absence of marker species. Such techniques include graphic correlation (e.g., Edwards, 1989) and constrained optimization (CONOP; Sadler, 2004). Such techniques, where applicable, provide a much higher temporal resolution for correlation than traditional biostratigraphy (Cooper et al., 2001).
- How well-calibrated are different biozonation schemes and bioevents to one another and to the geologic time scale? The correlation of RSL events in multiple sections around the globe often requires the use of a variety of biozonation schemes and fossil groups. For example, nearshore successions will contain different fossil assemblages to basinal successions; consequently, the correlation between them requires the calibration of different biozonation schemes. At a global scale, endemism may complicate calibration. Although the calibration of biozonal schemes against one another and the geologic time scale has progressed greatly in recent years (see, e.g., the charts within this book), inherent uncertainties exist (e.g., Luber et al., 2019 provides an example of calibration uncertainty between Cretaceous ammonites, planktonic foraminifera, and the subdivisions of the Aptian stage).
- Issues around reworking, caving (in well-based samples), identification of fossils, and knowledge of their stratigraphic range.

Put simply, the use of fossils for precise correlation and age calibration is not straightforward (Simmons, 2015).

Nonetheless, numerous examples exist in which biostratigraphy can provide high-resolution correlation within astronomically calibrated time scales in the order of 10^5 years (e.g., Gale et al., 2002, 2008).

The use of stable isotopes (e.g., $\delta^{13}C$ and $\delta^{18}O$) holds great promise for precise correlation (Saltzman and Thomas, 2012; Grossman, 2012; Jarvis et al., 2006; Bergström et al., 2008; Cramer et al., 2010a,b), but trends in the variation of these isotopes may be nonunique and can be subject to diagenetic alteration. As a result, they tend to be supported by biostratigraphy and require a good understanding of sedimentology and diagenesis. The $^{86}Sr/^{87}Sr$ ratios of sedimentary rocks, especially carbonates, are another potential correlation technique (McArthur et al., 2012). Again, the values are nonunique and, for some parts of the geologic record, the values remain constant for periods of significant duration. In other intervals, such as the Miocene, the $^{86}Sr/^{87}Sr$ ratio values change significantly through time, and the methodology has been applied to great effect for age determination and correlation (Ehrenberg et al., 2007; van Buchem et al., 2010a).

Despite these limitations, meaningful correlations of sections can be made with the overlap of the age range of an event in different sections pointing toward its precise timing (Sharland et al., 2001; Armentrout, 2019). Even in undated sequences (e.g., barren of fossils), superposition between well-dated sequences can provide resolution of a fraction of a biozone (e.g., Browning et al., 2013). Error bars will always exist, but within the current limitations of correlation techniques, many sea-level events in the Phanerozoic appear to be synchronous, being tied to a single, reasonably short-duration biozone or isotopic excursion event (see, e.g., worked examples from the Paleozoic in Simmons et al., 2007 and Simmons, 2012; and from the Mesozoic in Gale et al., 2002, 2008; Simmons, 2012).

13.2.3 Challenges in recognizing sea-level change and the eustatic signal

Interpretations of the sedimentary record in terms of changing depositional environments (that in a marine setting, we would relate to changing water depth) date back to the early history of geoscience (e.g., Cuvier and Brongniart, 1811). Nonetheless, the interpretation of a succession of facies can be challenging and requires an interpretation strategy. This strategy must be used consistently if multiple successions are to be studied and commonality recognized. Such an approach is a prerequisite to isolating the eustatic signal that also requires high-resolution chronostratigraphic calibration. Differences in interpretation strategy of facies successions and of chronostratigraphic proxies can ultimately lead to different views on the timing, frequency, and magnitude of both the RSL and eustatic signal in the rock record (see, e.g., the contrasting views of Johnson et al. (1985) and Brett et al. (2011) on the interpretation of mixed siliciclastic–carbonate successions in the Devonian stratigraphy of North America, and the Mesozoic of Arabia by Davies et al., 2002, 2019b).

Simmons (2012) illustrated an aspect of this problem with reference to the much studied Corallian (Oxfordian) succession of the Dorset coast of southern England (Fig. 13.4). This is a mixed succession of clays, sandstones, and limestones, in which cyclicity has long been recognized (Arkell, 1933), which has been interpreted in terms of changing RSL and sequence stratigraphy by several workers. A comparison of these interpretations shows a great deal of variation in the placement of significant bounding surfaces, such as MFSs, sequences boundaries, and hence intervening systems tracts. No doubt each of the various interpretations was based on thoughtful reasoning. Nonetheless, this comparison demonstrates that a single sedimentary succession can be interpreted differently, and if each interpretation strategy is carried through multiple sections, different views on local versus eustatic controls on RSL will emerge, and ultimately distinct eustatic models. Such uncertainties are common in the interpretation of geologic data because geoscientists are biased by their specialist skills and experience (Bond et al., 2007).

The recognition of RSL change in good resolution seismic data at an appropriate scale is arguably less contentious (Christie-Blick et al., 1990; Catuneanu, 2006; Neal and Abreu, 2009; Miller et al., 2018). This is because seismic data demonstrates the geometrical relationship of sedimentary systems within two-dimensional transects or within three-dimensional volumes. In other words, the progradational, aggradational, or retrogradational response of sediments to changes in accommodation and sedimentation is clear from the geometries visible within the seismic data. More importantly, the shelf-edge and shoreface trajectories can be recognized, providing clear insights into RSL and sediment supply.

In addition, the stratal geometries visible within seismic data can be replicated in flume tank experiments, computer models, and observed in large-scale outcrops, allowing a straightforward interpretation of RSL change (Miller et al., 2018). Indeed, it was the assessment of large amounts of seismic data that first led Peter Vail and his coworkers at EPR to develop the modern sequence stratigraphy paradigm (Vail, 1992).

However, the timing of the changes observed can be less easy to determine because it requires biostratigraphic calibration from well data that intersects the seismic lines. This may be of variable resolution depending, for example, on the quality of samples (e.g., cuttings versus cores) and the types of microfossil used. Nonetheless, where there is

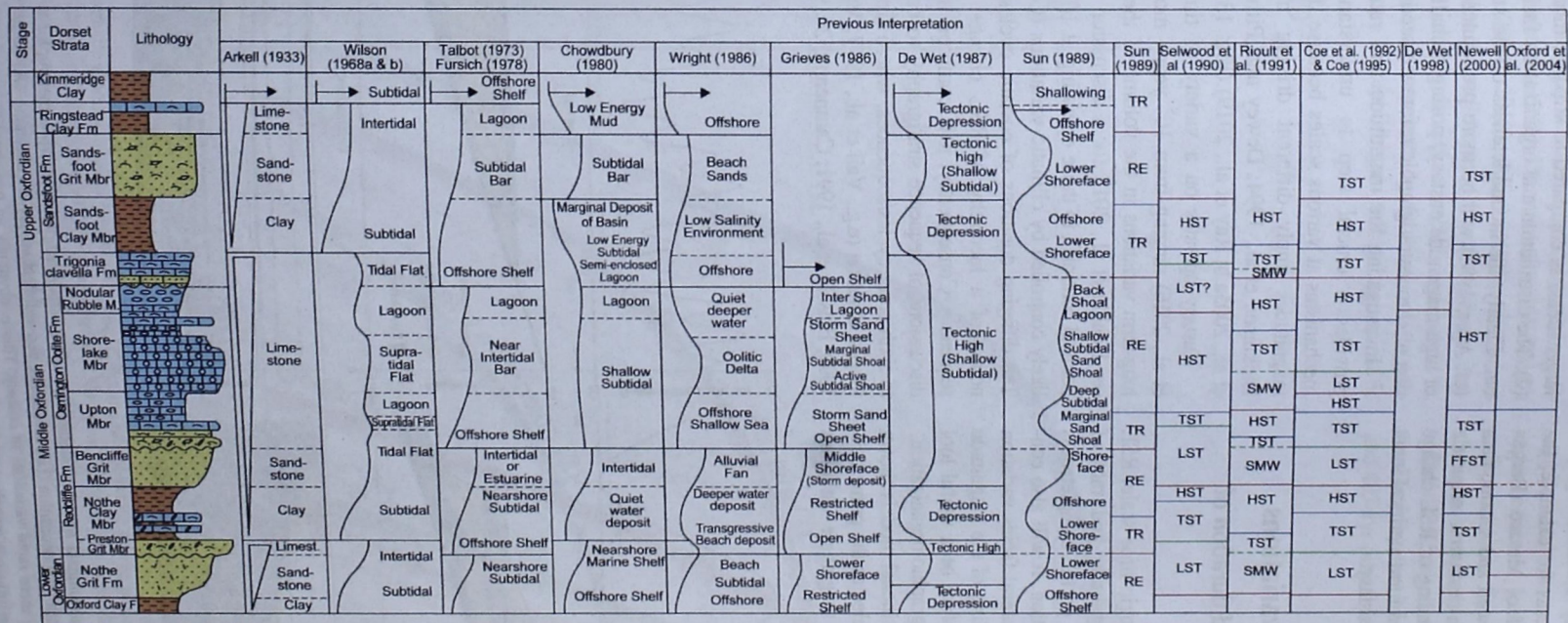

FIGURE 13.4 Comparison of different interpretations of the Corallian (Oxfordian) succession of the Dorset coast, southern England (following earlier comparisons by Sun, 1989; Newell, 2000; Oxford et al., 2004). Different strategies can exist for the interpretation of sea-level variation in the same succession of facies. An internally consistent and robust strategy needs to be developed when attempting to develop a global model of eustasy from a compilation of individual synchronous stratigraphic sections. Differences in interpretation strategy can explain differences between global sea-level curves. After Simmons (2012).

abundant, high-quality, and precisely chronostratigraphically calibrated biostratigraphic data, as for example, the Cenozoic sediments of the US Gulf of Mexico (Bergen et al., 2019), then the integration of well and seismic data can lead to the generation of high-resolution sequence stratigraphic models and an understanding of RSL change (e.g., Armentrout, 1996, 2019) that can form a critical input into developing an understanding of eustasy.

13.3 Anatomy of eustatic variations

13.3.1 The magnitude, rate, and duration of eustatic cycles

In the context of developing a geologic time scale, RSL change (as influenced by the magnitude and rate of eustasy) will be a controlling factor on the completeness of the rock record at any given location. It will also control the stratal stacking pattern and lateral facies variation within systems tracts. An understanding of the magnitude and rate of eustatic cycles can therefore be a useful tool for those engaged in predicting stratigraphic organization.

Consider the two simple 2D depositional models shown in Fig. 13.5, in which eustasy is modeled as the prime control on RSL. Large, relatively slow magnitude variations (1) produce more stratigraphically incomplete sections over larger areas, as compared to smaller, more rapid variations (2). The distribution and organization facies are also different. Clearly, the incompleteness of the stratigraphic record (cf. Ager, 1981) will be more pronounced during episodes of high-magnitude eustasy, posing a challenge to the selection of chronostratigraphic reference sections.

Investigating the magnitude and rate of eustasy also provides a crucial step to understanding its driving mechanisms at various scales because different rates and magnitudes imply different driving mechanisms (e.g., Dickinson et al., 1994; Dewey and Pitman, 1998; Miller et al., 2005a,b; Ray et al., 2019) (Fig. 13.6).

Eustasy operates on a variety of time scales (Rovere et al., 2016) ranging from 10^8 years, mostly controlled by long-term variations in the volume of the oceans (although see Boulila et al., 2018 for a discussion of possible astronomical controls), to those operating at 10^4–10^5 years, most likely controlled by climatic variations (Guillocheau, 1995). The differing durations of eustatic cycles contribute to the notion of a hierarchy of RSL change and the resulting sequences. Consequently, it is common in the literature for discussions of sequence stratigraphy to be in terms of first- to sixth-order cycles/sequences, where first order are of the longest duration (e.g., Vail et al., 1977; Van Wagoner et al., 1990; Einsele et al., 1991; Catuneanu, 2019b). Short-duration

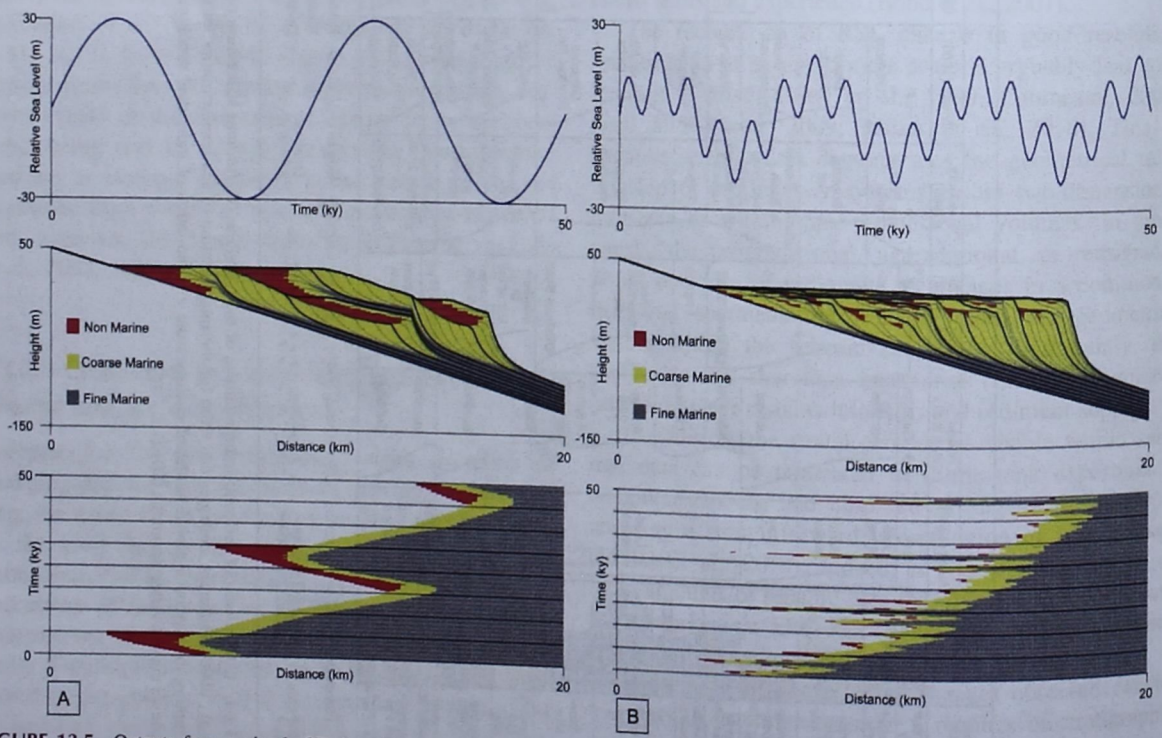

FIGURE 13.5 Outputs from a simple 2D depositional model of clastic deposition (http://nm2.rhul.ac.uk/wp-content/uploads/2015/03/DeltaModel3.html), where eustasy is the dominant factor controlling deposition (i.e., subsidence and sediment supply are constant). (A) Large, relatively slow magnitude variations of eustasy; versus (B) smaller, more rapid variations in eustasy. This is obviously an oversimplification from what controls the rock record in reality but is useful to demonstrate the influence magnitude and rate of eustasy can have on depositional completeness and facies distribution.

fifth- and sixth-order cycles can also be termed parasequences and will be strongly controlled by variations in sediment supply. Carter et al. (1991), Drummond and Wilkinson (1996), Schlager (2004, 2010), Allen (2017), and others have pointed out that the sedimentary record shows the characteristics of scale invariance (i.e., is fractal), and moreover, that ordering or ranking sequences by duration shows significant inconsistency in application within the scientific community. This is in part related to differences in sediment supply, which can result in the thickness of fifth- or sixth-order sequences greatly exceeding that of "typical" third-order sequences. In contrast, Miller et al. (2018) concluded that the stratigraphic record of sea-level changes largely reflects composites of sea-level cycles nested together. The bundling together of sea-level cycles controlled by c. 100- and 405-kyr orbital forcing yields a predictable packaging of

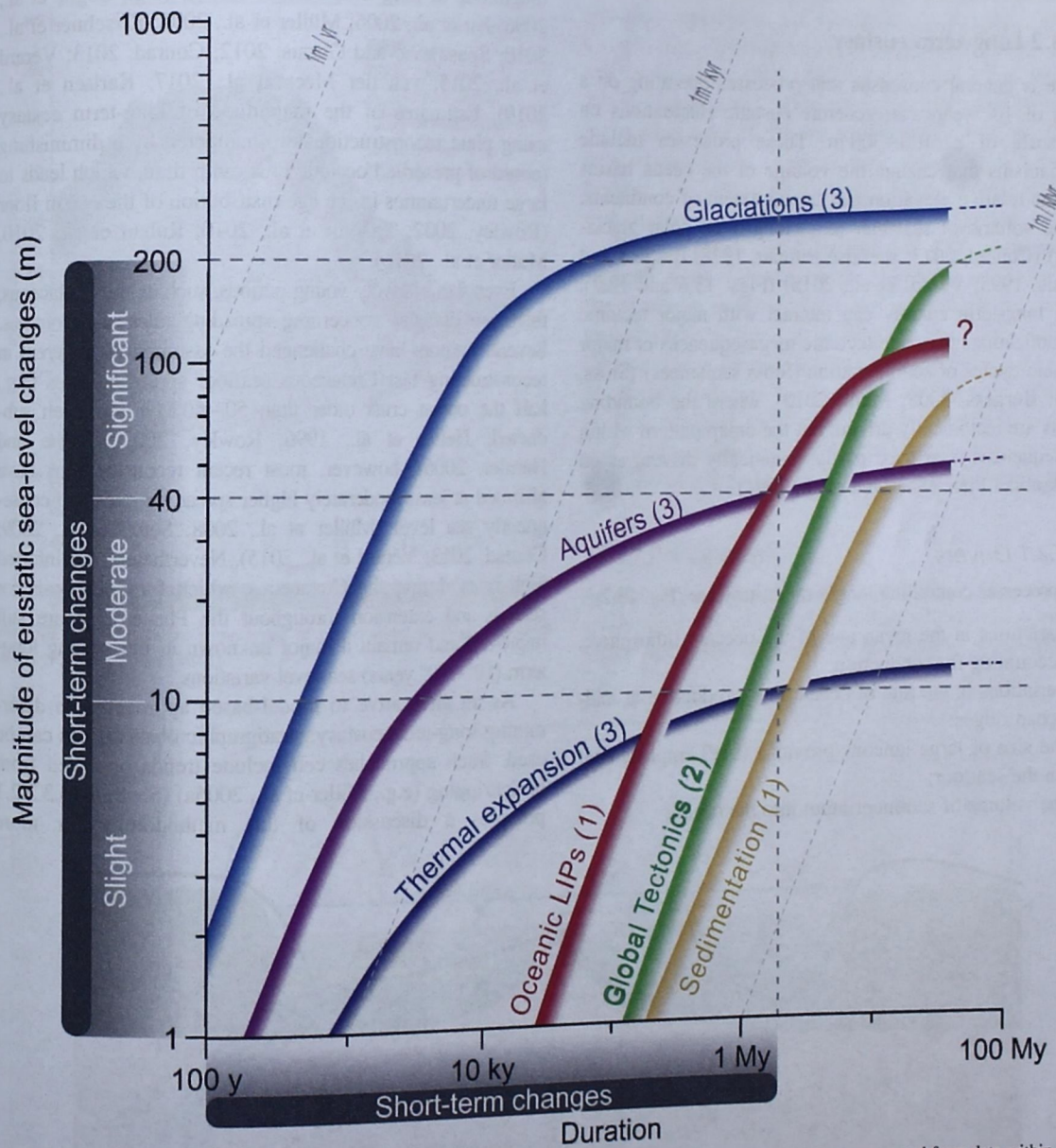

FIGURE 13.6 A schematic representation of the duration, magnitude, and rate of known drivers of eustatic changes, created from data within Emery and Aubrey (1991), Jacobs and Sahagian (1993), Immenhauser and Matthews (2004), Miller et al. (2011), Cloetingh and Haq (2015), Sames et al. (2016), and Wendler and Wendler (2016). The curves reflect the upper limits of durations, magnitudes, and rates that are reflective of the drivers of eustasy. Note that because of the different nature of the drivers, they can cause (1) sea-level rise; (2) sea-level rises and falls; and (3) regular, high-frequency, cyclic sea-level rises and falls. The "?" shown for LIPs represent the upper duration limit of continuous activity for a LIP. For an updated view on the magnitude of aquifer-eustasy see Davies et al. (2020). *LIPs*, Large igneous provinces. After Ray et al. (2019).

longer term sequences on the Myr scale. Given these uncertainties, we simplify our consideration of the magnitude and rate of eustasy to that operating on long-term time scales (10^8 years, largely forced by tectonics) and short-term time scales (10^5–10^6 years, largely controlled by astronomical forcing) (see also Sames et al., 2016), although make mention of ordering when citing from previous studies that use that terminology.

13.3.2 Long-term eustasy

There is general consensus that processes operating on a scale of 10^8 years can generate eustatic fluctuations on the scale of c. 100–300 m. These processes include mechanisms that change the volume of the ocean basins and the relative elevation and lateral extent of continents, or the volume of seawater (e.g., long-lived polar glaciations) (Conrad, 2013; see also Pitman, 1978; Burgess and Gurnis, 1995; Vérard et al., 2015) (Figs. 13.6 and 13.7). Such long-term eustasy can interact with major tectonic reorganizations to create tectonic megasequences or major cratonic cycles of sedimentation (Sloss sequences) (Sloss, 1963; Burgess, 2008; Miall, 2010), where the bounding events are tectonically driven, but the onlap pattern within the sequences is at least partly eustatically driven, as on the Arabian Plate (Sharland et al., 2001).

13.3.2.1 Drivers

The processes controlling long-term eustasy are (Fig. 13.7):

1. variations in the mean age of the oceanic lithosphere, accounting for subduction;
2. variations in the rate of ocean crust production at mid-ocean ridges;
3. the size of large igneous province (LIP) emplacement on the seafloor;
4. the volume of sediment input into the ocean;
5. dynamic topographic considerations;
6. the long-term creation and destruction of polar ice sheets; and
7. long-term variations in groundwater storage.

Of these, Conrad (2013) concluded that ocean ridge spreading volume was the most important (Fig. 13.8). Geodynamic (plate reconstruction) models can therefore be powerful tools for determining the likely timing, rate, and magnitude of long-term eustatic change (e.g., Cogné et al., 2006; Xu et al., 2006; Müller et al., 2008; Kirschner et al., 2010; Spasojevic and Gurnis, 2012; Conrad, 2013; Vérard et al., 2015; van der Meer et al., 2017; Karlsen et al., 2019). Estimates of the magnitude of long-term eustasy using plate reconstructions are hampered by a diminishing record of preserved oceanic crust with time, which leads to large uncertainties in the age distribution of the ocean floor (Rowley, 2002; Torsvik et al., 2010; Ruban et al., 2010, Müller et al., 2016).

Even for relatively young periods, such as the Cretaceous, there are disputes concerning spreading rates and volumes. Several authors have challenged the assumptions inherent in reconstructing fast Cretaceous seafloor spreading rates (e.g., half the ocean crust older than 50–60 Myr has been subducted: Heller et al., 1996; Rowley, 2002; Cogné and Humler, 2006); however, most recent reconstructions have affirmed at least moderately higher spreading rates and consequently sea level (Müller et al., 2008; Seton et al., 2009; Conrad, 2013; Vérard et al., 2015). Nevertheless, the inferred high rates during the Cretaceous, which form the basis for scaling and extension throughout the Phanerozoic are still unproven and remain a major unknown in interpreting long-term (10^7–10^8 years) sea-level variations.

As an alternative to model-based approaches to determining long-term eustasy, stratigraphic observations can be used. Such approaches can include trends observed from backstripping (e.g., Miller et al., 2005a) (Section 13.3.3.2.1 provides a discussion of this methodology) or more

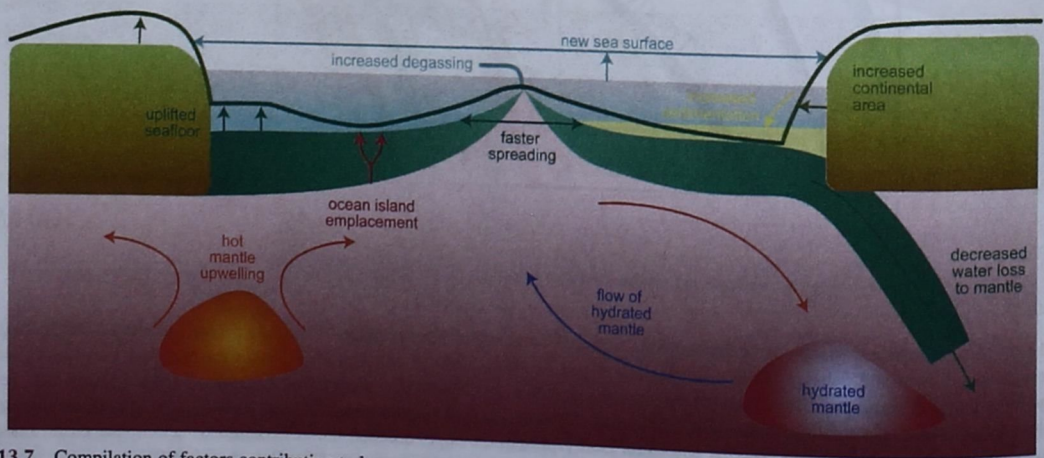

FIGURE 13.7 Compilation of factors contributing to long-term eustatic change and its magnitude. After Conrad (2013).

qualitative estimates based on the extent of flooding of paleocontinents and long-term patterns of coastal onlap [e.g., Hallam, 1992; Snedden and Liu, 2010 (after Hardenbol et al., 1998; Haq and Al-Qahtani, 2005; Haq and Schutter, 2008)]. Fig. 13.9 shows a compilation of some long-term eustatic curves derived using both geodynamic modeling and stratigraphic observations. Guillaume et al. (2016) produced an averaged long-term eustatic curve for the Phanerozoic using a variety of papers, including some older, more qualitative attempts at estimating long-term eustatic magnitudes (Vail et al., 1977; Hallam, 1992; Haq and Al-Qahtani, 2005; Haq and Schutter, 2008).

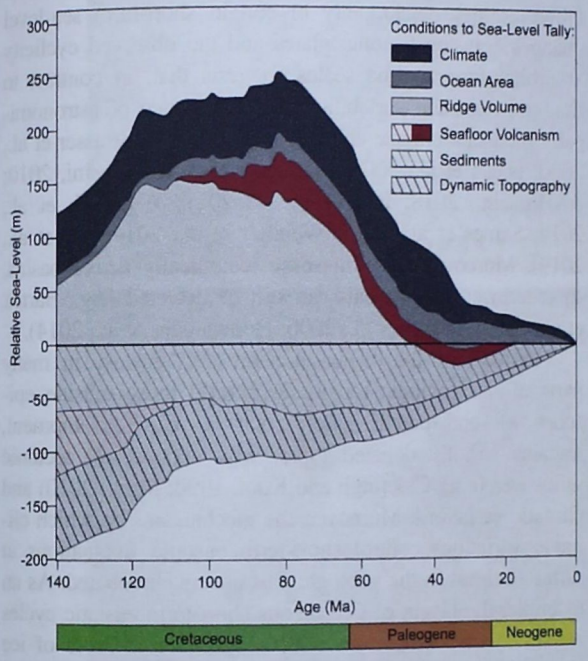

FIGURE 13.8 Relative importance of contributors to long-term term eustasy. After Conrad (2013).

Papers that include the entire Phanerozoic typically show eustatic peaks in the Late Ordovician and Late Cretaceous (although precise timing and magnitude varies) and a broad low around the Paleozoic–Mesozoic transition. This long-term periodicity has been related to tectonic supercycles of plate reorganization (Wilson Cycles) (e.g., Worsley et al., 1986; Veevers, 1990; Algeo and Seslavinsky, 1995; Miall, 2010; Nance and Murphy, 2013). Conceptually, during continental assembly remaining oceans were likely old and therefore deep leading to low sea-level. In comparison, times of continental breakup lead to new ridge formation, spreading and therefore shallower oceans and hence higher sea-level.

Karlsen et al. (2019) suggested that an imbalance between water fluxes from the mantle at ridges and into the mantle at trenches may have contributed to sea-level change since the breakup of Pangea. Thus faster slab subduction during Pangea breakup transported extra water to the mantle that may have contributed up to c. 130 m of gradual sea-level fall since 230 Ma. Cloetingh and Haq (2015) have suggested that water exchange with the mantle may also play a role in creating short-term eustatic cycles.

13.3.2.2 Magnitude

As shown in Fig. 13.9, although some broad consensus exists regarding the general timing of long-term eustatic highs and lows, estimates of magnitudes (and rates) of

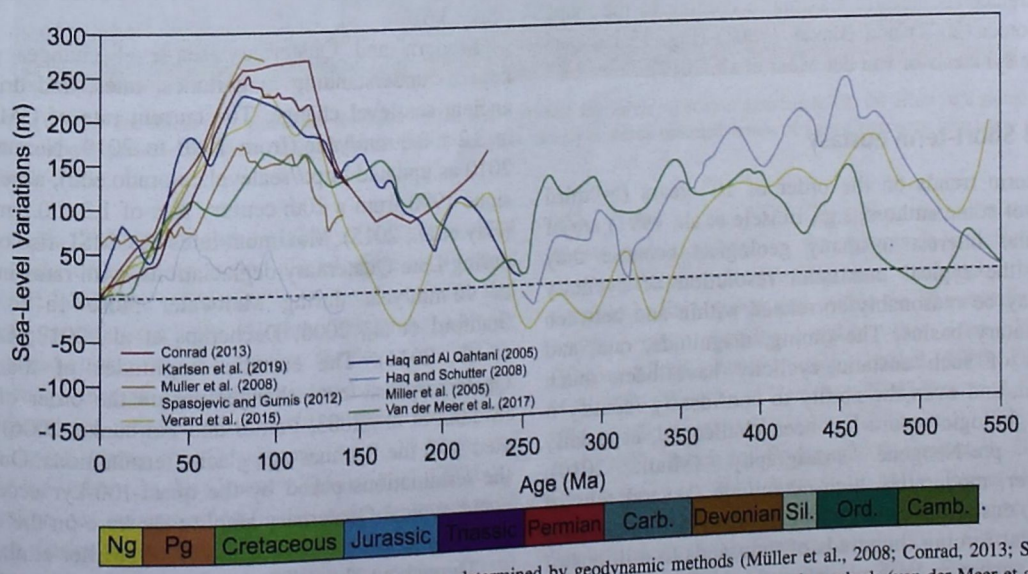

FIGURE 13.9 Long-term Phanerozoic eustatic fluctuations, as determined by geodynamic methods (Müller et al., 2008; Conrad, 2013; Spasojevic and Gurnis, 2012; Vérard et al., 2015; Karlsen et al., 2019), strontium isotope ratios as a proxy for geodynamic methods (van der Meer et al., 2017), and stratigraphic interpretations (Miller et al., 2005a; Haq and Al-Qahtani, 2005; Haq and Schutter, 2008).

change vary quite markedly; this variance occurs between model and data-driven interpretations and within each type of approach.

The magnitude of the Late Cretaceous long-term eustatic high appears to be a point of particular contention, with values estimated to be as much as c. 286 m above present-day levels by Spasojevic and Gurnis (2012) and less than 100 m by Miller et al. (2005a). Conrad (2013) argued that ridge volumes have decreased since the mid-Cretaceous, in response to a ~50% slowdown in seafloor spreading rate, resulting in a contribution of ~150 m to a total ~250 m of sea-level fall (Figs. 13.8 and 13.9). However, as elegantly demonstrated by Xu et al. (2006), differences in plate models can have a profound effect on calculations of the magnitudes of long-term eustasy. They noted that the use of the Hall (2002) Cenozoic plate model, which despite having only a c. 20% reduction in oceanic lithospheric production rates as compared to the Gordon and Jurdy (1986) plate model, resulted in halving the resultant modeled eustatic change (i.e., a fall of 125 vs 250 m for the Cenozoic).

Studies of continental flooding suggest that a Late Cretaceous peak occurred on the order of 135 ± 55 (Bond, 1979) or 150 m (Harrison, 1990), although more recent estimates have suggested only a c. 100 m peak (Rowley, 2013). McDonough and Cross (1991) calculated a Late Cenomanian sea-level elevation of 269 ± 87 m above present sea level from a backstripped shoreline in the Western Interior Seaway, although compensation for glacial isostatic effects of the last ice age may significantly reduce this estimate. Intriguingly, a sea-level rise of c. 250 m from today's mean sea level would be required to flood cratons to the extent mapped during Late Cretaceous eustatic maxima, according to the maps of Golonka (2007) and Blakey (2008) (Fig. 13.10) (see also the synthesis of van der Meer et al., 2017).

13.3.3 Short-term eustasy

Short-term trends on the order of 10^6 years (="third order" of some authors, e.g., Einsele et al., 1991) are of particular interest to many geologists because they reflect the typical maximum resolution of cyclicity that may be reasonably correlated within and between sedimentary basins. The timing, magnitude, rate, and drivers of such eustatic cyclicity have been much debated, and even the ability to confidently identify it in the geologic record has been challenged, especially within pre-Neogene stratigraphy (Miall, 2010). However, moderately high-magnitude (several tens of meters) eustatic changes occurring at or within the pace of orbital forcing (hundreds of thousands to millions of years) appear to be a prevalent feature of Phanerozoic geologic history (Miller et al., 2005a, 2011) and require appeal to driving mechanisms that occur at suitable rates (Fig. 13.6).

13.3.3.1 Drivers

Tectonics (e.g., intraplate deformation, mantle upwelling) have been viewed as an important control on short-term RSL changes (Cloetingh et al., 1985, 2013; Vakarelov et al., 2006; Petersen et al., 2010; Lovell, 2010; Miall, 2010). However, the synchroneity of certain short-term sea-level changes between tectonic plates and the observed cyclicity at orbital forcing time scales suggests that, in contrast to long-term eustatic variability, the importance of astronomically mediated climate changes is paramount (Strasser et al., 2000; Naish et al., 2009; Matthews and Al-Husseini, 2010; Al-Husseini, 2018; Boulila et al., 2011; Wagreich et al., 2014; Sames et al., 2016; Wendler et al., 2014; Liu et al., 2019). Moreover, even in some tectonically active basins, short-term eustatic signals can still be detected (e.g., Bartek et al., 1991; Strauss et al., 2006; Hohenegger et al., 2014).

Nonetheless, the origin of short-term eustasy in many parts of the geologic record, especially those outside episodes of undisputed major polar ice-cap development, remains a hotly debated topic, with support for tectonic influences (e.g., Cloetingh and Kooi, 1990; Miall, 2010) and climatic variations. Moreover, the mechanisms by which climatic variations control short-term eustatic fluctuations at different times in the geologic past are much debated. As an example, the origin of Cretaceous short-term eustatic cycles is particularly contentious with support for the role of ice sheets (glacio-eustasy) and groundwater storage (aquifer-eustasy) (e.g., Wagreich et al., 2014; Sames et al., 2016; Ray et al., 2019; Laurin et al., 2019; Davies et al., 2020) (Fig. 13.6).

Modern and Quaternary sea-level changes provide keys to understanding magnitudes, rates, and drivers of ancient sea-level change. The current rate of GMSL rise is 3.2 ± 0.3 mm/year (from 1990 to 2019; Nerem et al., 2010 as updated http://sealevel.colorado.edu), accelerating since 1990 from a 20th century rate of 1.2 ± 0.2 mm/year (Hay et al., 2015). Maximum rates of GMSL rise occurred during Late Quaternary deglaciations, with rates in excess of 40 mm/year during Meltwater Pulse 1a (c. 14 ka; Stanford et al., 2006; Dechamps et al., 2012; Lambeck et al., 2014). The eustatic amplitudes of the largest Quaternary sea-level changes are on the order of 130 m (Siddall et al., 2003; Peltier and Fairbanks, 2006) associated with the Bruhnes-age glacial terminations. Outside of the terminations paced by the quasi-100-kyr eccentricity cycle, typical Quaternary amplitudes were on the order of 50–60 m (Lisiecki and Raymo, 2005; Miller et al., 2011).

Throughout the Oligocene–Quaternary interval, short-term eustasy operated with large (more than 50 m) magnitude and often a rapid pace (over 40 mm/year = 40 m/kyr)

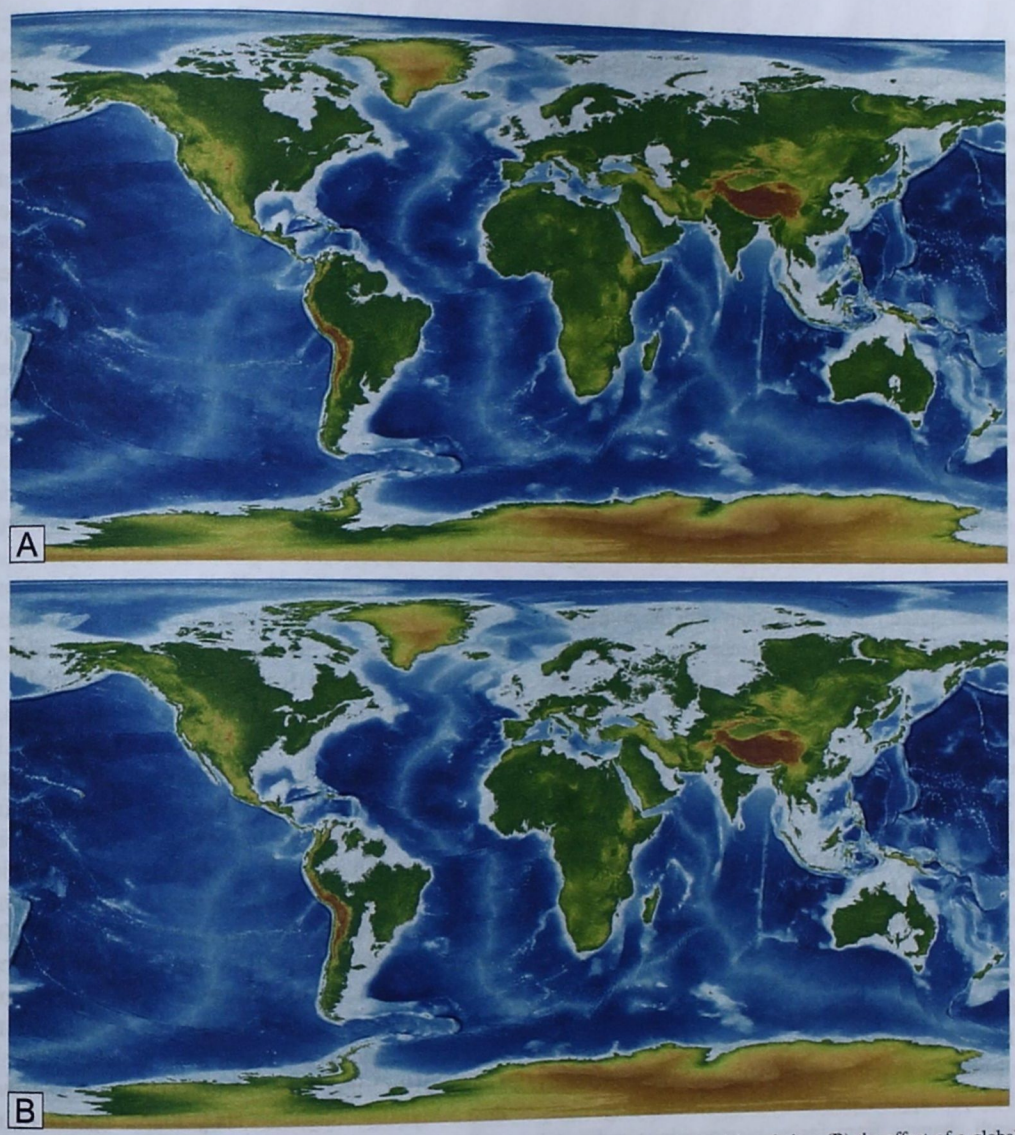

FIGURE 13.10 (A) The effect of a global sea-level rise 100 m above present-day levels on coastal inundation; (B) the effect of a global sea-level rise of 300 m above present-day levels on coastal inundation. (B) more closely matches modeled levels of Late Cretaceous inundation (Golonka, 2007; Blakey, 2008).

(Miller et al., 2020) with the c. 1.2 Myr obliquity orbital forcing cycle determining major glacial episodes (Zachos et al., 2001; Wade and Pälike, 2004; Pälike et al., 2006) and prominent eustatic cyclicity. Higher frequency orbitally forced glacio-eustasy is also evident (Miller et al., 2020). Consequently, changes in sea level were driven by changes in continental ice volume, particularly northern hemisphere (the ice ages) during the Quaternary (last 2.55 Myr) and Antarctic ice volume in the Cenozoic (Miller et al., 2005a).

Therefore our understanding of the relatively recent geologic past demonstrates that the signature of short-term glacio-eustasy is relatively large magnitude (tens—200 m) changes operating on short-term cyclicities controlled by the astronomical forcing of climate (Miller et al., 2005a,b, 2011, 2020; Naish et al., 2009). In subsequent subsections, we review our knowledge of the magnitude and duration of short-term eustasy for pre-Oligocene stratigraphy, but there seems to be little dispute that, within the Phanerozoic, glacio-eustasy was operating within the Late Paleozoic (Visean–Middle Permian) (e.g., Heckel, 1986; Dickinson et al., 1994; Wright and Vanstone, 2001; Eros et al., 2012a,b; Giles, 2009; Rygel et al., 2008; Fielding et al, 2008; Bishop et al., 2009; Horton and Poulsen, 2009; Fang et al., 2015; van Hinsbergen et al., 2015; Buso et al., 2019; Chen et al., 2019), and the latest Ordovician–Early Silurian (e.g., Hambrey, 1985; Sutcliffe et al., 2000; Finnegan et al., 2011; Ghienne, 2011; Ghienne et al., 2014; Davies et al., 2016). For these periods, glacio-eustasy has been regularly implicated as a major driver

of global sea-level change, although the precise mechanisms driving ice sheet growth and retreat are complex (Horton and Poulsen, 2009).

Could glacio-eustasy have been operating during other Phanerozoic periods, especially those that are characterized by warm or hot (greenhouse) climates? Or does an explanation for short-term eustasy during these times require other processes to dominate, such as aquifer-eustasy, or tectonic drivers, such as intraplate stress variations? To answer these questions an assessment is required of the magnitude and duration of short-term Phanerozoic eustasy, which we address in the subsequent subsections of this chapter, drawing together our conclusions in Section 13.3.3.4.

13.3.3.2 Magnitudes

A contentious topic has been the estimation of the magnitude of short-term eustatic change. Early estimates of such changes, often based on seismic onlap patterns and apparently failing to account for subsidence (e.g., Vail et al., 1977; Haq et al., 1987, 1988; Ross and Ross, 1987), were high, often in excess of 100 m per event, and quickly drew criticism (e.g., Christie-Blick, 1990; Miall, 1992; Christie-Blick and Driscoll, 1995; Miller and Mountain, 1996; Dewey and Pitman, 1998). More recent estimates have tended to revise magnitudes downward. Even so, a great deal of uncertainty exists, as exemplified by the differences in the Cretaceous short-term eustatic curves of Miller et al. (2005a) and Sahagian et al. (1996), as compared to Haq (2014) (Fig. 13.11) or the estimates of Rygel et al. (2008) as compared to Ross and Ross (1987).

There are several methodologies by which the magnitude of RSL change can be estimated within any given outcrop or subsurface sedimentary section. These methods include simple approaches involving determining likely water depth changes from facies juxtapositions and fossil assemblage changes (e.g., Brett et al., 1993, 2009; Banner and Simmons, 1994), to the study of seismic geometries and the identification of erosional and depositional relief (e.g., Johnson et al., 1991; Miall, 2010; Ray et al., 2019). Estimating RSL magnitudes from the stratigraphic record has inherent limitations (Burton et al., 1987; Immenhauser, 2009; Sames et al., 2016) arising from the complex effect of several processes, including subsidence/uplift, sediment input, compaction, and isostasy, and inherent uncertainties (e.g., estimating palaeowater depth). As a result, many published eustatic curves are unscaled and show relative magnitudes because of uncertainties in assigning numerical values in terms of magnitude (e.g., Brett et al., 2011; Nielsen, 2004, 2011; Babcock et al., 2015; see also Davies et al., 2016 for a discussion of this issue with respect to Silurian eustasy). Likewise, many local/regional RSL curves are presented unscaled and are consequently difficult to incorporate into a synthesis of eustasy.

A further complication is that a sea-level estimate from a single location or transect may not be dominated by eustasy. The interaction of controls on sedimentation operating at a variety of frequencies and magnitudes develop the local stratigraphic record (e.g., Guillocheau, 1995). Although the effect of local subsidence/uplift rates has long been acknowledged, the effects of dynamic topography (the surface expression of mantle flow originating from the upper thermal boundary of mantle convection) (Fig. 13.7) have become an increasingly important consideration (e.g., Burgess and Gurnis, 1995; Burgess, 2008; Kominz et al., 2008, Conrad and Husson, 2009; Miall, 2010, 2016; Spasojevic and Gurnis, 2012; Conrad, 2013; Rowley, 2013; Guillaume et al., 2016). However, it is worth emphasizing that dynamic topography operates on time scales typically 2 to more than 10 Myr (Moucha et al., 2008; Petersen et al., 2010), with its greatest impact on time scales greater than 5 Myr (Cloetingh and Haq, 2015). Therefore, although an important factor in considering the magnitude of long-term

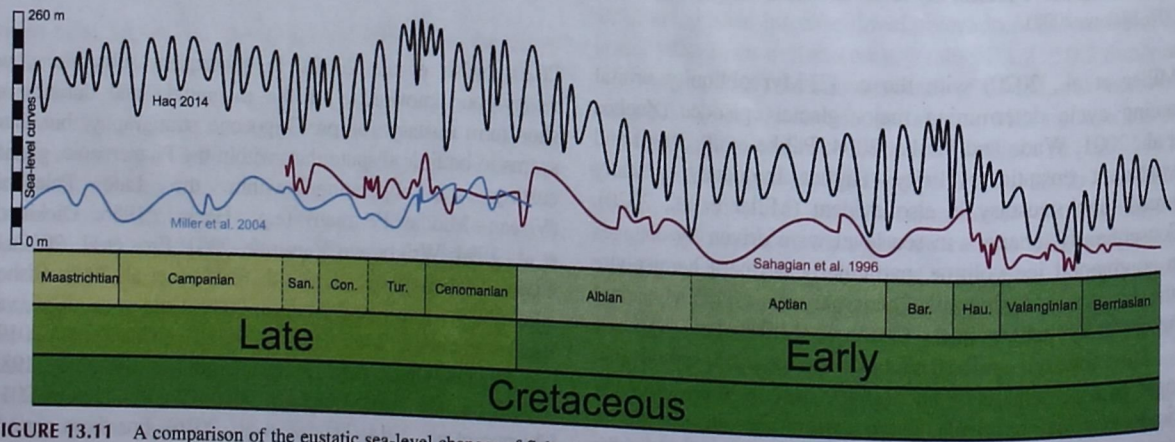

FIGURE 13.11 A comparison of the eustatic sea-level changes of Sahagian et al. (1996), Miller et al. (2004) and Haq (2014) illustrating the marked difference in magnitude estimates. From Ray et al. (2019).

eustasy, it has a reduced impact on assessing the magnitude of short-term eustatic events.

Sea-level curves produced from an assessment of local stratigraphy will effectively reflect local water depth changes (Holland and Patzkowsky, 1998; Loi et al., 2010). Three approaches can be undertaken to extract the eustatic magnitude given such circumstances: (1) backstripping; (2) use of the $\delta^{18}O$ record from foraminifera combined with an independent temperature proxy (for sediments Late Cretaceous and younger); and (3) a global synthesis of empirical estimates of eustatic sea-level change based on different types of geological observations, and incorporating data from (1) and (2) as appropriate, followed by a demonstration of synchroneity. These approaches are each discussed in turn.

13.3.3.2.1 Backstripping

Backstripping can be employed to progressively account for the effects of sediment compaction, sediment loading, and thermal subsidence (e.g., Miller et al., 2005a; Kominz et al., 2008, 2016). The residual in backstripping modeling is attributable to eustasy and nonthermal subsidence (R2 of Kominz et al., 2008, 2016) and can provide magnitude estimates for both long-term and short-term eustasy.

The sediments from the New Jersey margin of eastern North America are ideal for backstripping because sedimentation rates are well understood, and porosity-depth data provides reliable estimates of sediment compaction. This has enabled several workers (Miller et al., 2003a,b, 2004, 2005a; Kominz et al., 2003, 2008, 2016; Van Sickel et al., 2004) to show that short-term eustatic changes were in the range of 15–80 m during the Late Cretaceous to Miocene, with Cretaceous estimates on the low end of this range (15–40 m). Similar studies by Sahagian and Jones (1993) and Sahagian et al. (1996) on Middle Jurassic to Late Cretaceous sediments from the Russian Platform suggested comparable magnitudes of sea-level change to the work of the Miller-led team, indicating that estimates of short-term eustatic change as much as 160 m for same geologic time periods of study (Haq et al., 1987, 1988) or 400 m (Vail et al., 1977) are unlikely. Long-term trends can also be contrasted. Miller et al. (2005a) and Kominz et al. (2008) suggest that sea levels have fallen by c. 75–110 m from a Late Cretaceous maximum; Haq et al. (1987), however, have suggested that long-term sea level has fallen by c. 250 m during the same time period, although their long-term sea-level estimates were based entirely on those derived from the seafloor reconstructions of Pitman (1978) and Pitman and Golovchenko (1983).

It has been argued (e.g., Müller et al, 2008; Spasojevic et al., 2008; Spasojevic and Gurnis, 2012; Rowley, 2013; Haq, 2014) that the estimates of the magnitude of Late Cretaceous–Cenozoic eustatic change at all scales by Miller and his coworkers are underestimates because they have failed to account for the influence of dynamic topography, especially those related to the migration of North America over the subducted and negatively buoyant Fallon Plate during the last 70 Myr. Nonetheless, the potential effects of dynamic topography were considered by Kominz et al. (2008, 2016), which still produced eustatic magnitude estimates markedly lower than those of Haq et al. (1987), Haq (2014), and Müller et al. (2008). Backstripping estimates for eustatic changes from the Miocene of the Marion Plateau (east Australian margin) are also on the order of 50–60 m (John et al., 2004, 2011).

Loi et al. (2010) and Dabard et al. (2015) have successfully applied backstripping to Ordovician sediments in elegant studies from the North African Gondwana margin and the Armorican Massif. In their study of the Late Ordovician of the Bou Ingarf succession in Morocco, Loi et al. (2010) demonstrated that third-order (c. 1–3 Myr) eustatic magnitudes were greater than 40 m, and a fall in association with the growth of the Hirnantian ice sheet was estimated as more than 70 m (Fig. 13.12). Superimposed on these third-order magnitudes are fourth-order (400 kyr) cycles with eustatic magnitudes in the range 10–30 m. These interpretations were used to suggest that glacio-eustasy operated throughout the Katian and Hirnantian, supporting the notion of pre-Hirnantian Gondwanan ice sheets.

Dabard et al. (2015) extended this analysis into Darriwilian and Sandbian (Middle to Late Ordovician) strata through study of the Crozon Peninsula succession in Armorica, western France. Second-, third-, and fourth-order eustatic cycles were recognized. The second- and third-order cycles have magnitudes of more than 50 m, occasionally more than 80 m, whereas fourth-order cycles have magnitudes primarily in the range of 10–30 m. The authors interpret such magnitudes/periodicities as evidence for glacio-eustasy. Interestingly, the backstripping analysis in this case study highlights the effects that high subsidence rates can have on amplifying sea-level magnitudes. From the depositional model, amplitudes of fourth-order RSL change are high (c. 60 m), but backstripping suggests the eustatic component is only 30 m.

13.3.3.2.2 Oxygen isotope records

Oxygen isotope ($\delta^{18}O$) records from benthic foraminifera comprise two dominant signals: ambient temperature and $\delta^{18}O$ of seawater (Pearson, 2012). The latter parameter is affected by continental ice volume and changes attributable to fractionation from evaporation and precipitation often expressed as salinity (Miller, 2002). Therefore $\delta^{18}O$ measurements can be a useful proxy for reconstructing past ocean temperatures (Emiliani, 1955) and ice volumes (Shackleton, 1967) and, in turn, the magnitude of eustatic change driven by ice volume changes (e.g., Miller et al., 1987, 1991). As noted by Haq (2014), if the Pleistocene sea

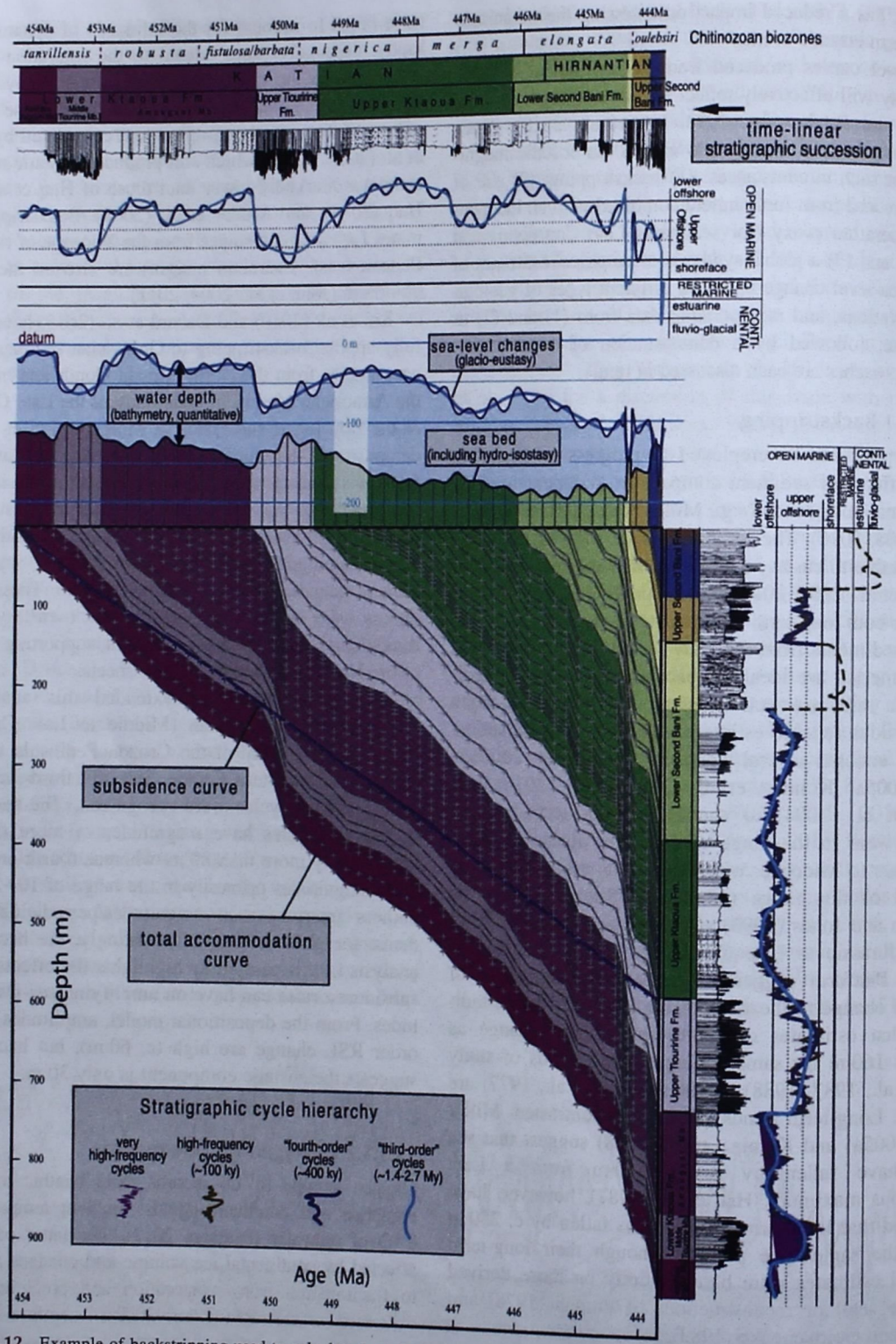

FIGURE 13.12 Example of backstripping used to calculate Late Ordovician eustatic magnitudes based on data from Morocco. After Loi et al. (2010).

level: $\delta^{18}O$ slope can be assumed to be similar across all geologic time, it may be possible to estimate the magnitude of eustatic variations using this proxy (Cramer et al., 2011 provide a comprehensive discussion of this technique). However, several problems limit this application (e.g., Wendler and Wendler, 2016). First, it is necessary to remove temperature and the local hydrological factors through the study of Mg:Ca ratios of the same samples to derive $\delta^{18}O$ of seawater ($\delta^{18}O_{sw}$) (Billups and Schrag, 2002). This carries a great deal of uncertainty for pre-Cenozoic sediments. The organic biomarker-based TEX_{86} proxy, alkenones, or clumped isotope techniques can also be used to calculate temperature (Hollis et al., 2019). Second, ice sheets become progressively depleted in ^{18}O as ice sheet elevation increases and temperatures decrease, thereby increasing $\delta^{18}O_{sw}$ by varying amounts. Third, "vital effects," the effect of the organism on changing the isotopic ratio as it metabolizes and constructs its shell, may distort values. Finally, pH variations and diagenesis can influence the $\delta^{18}O$ signal, detracting from its application in sediments older than late Mesozoic (Haq and Schutter, 2008).

Nonetheless, several workers (e.g., Stoll and Schrag, 2000; Miller et al., 1991, 2005a, 2011) have used variations in $\delta^{18}O$ to assess past ice volume and eustatic magnitudes. Combining backstripped estimates of eustatic change with those derived from $\delta^{18}O$ records, were both records are well age calibrated, can provide powerful insight into the magnitude of short-term eustatic change (e.g., Pekar et al., 2002; John et al., 2004, 2011).

Cramer et al. (2011) reconciled onshore New Jersey backstripped sea-level estimates with those obtained from deep-sea benthic foraminiferal $\delta^{18}O$ and Mg/Ca records. Because of limitations in the data, this approach, as illustrated in Fig. 13.13, was restricted to periods longer than 2 Myr and shows similar changes from both methods. It was judged to be most reliable for sediments younger than 45 Ma because of data limitations and uncertainties (especially the Mg/Ca ratio of seawater), although Miller et al. (2005a) documented specific intra–Late Cretaceous $\delta^{18}O$ increases that could be used to calculate the magnitude of specific short-term Cretaceous eustatic falls.

Ongoing studies (Fig. 13.14) are using higher resolution $\delta^{18}O$ records to compare Cenozoic changes on the Myr scale, calibrated by Milankovitch cyclicity (Miller et al., 2020). These results can be favorably compared to the backstripping results from New Jersey margin and help develop a model of variable Cenozoic Antarctic ice sheet growth and decay creating short-term eustatic changes with magnitudes most in the range 15–30 m in the Eocene, increasing to ~50 m in the Oligocene to Early Miocene (with a c. 60 m fall around the Eocene/Oligocene boundary). During the Miocene Climate Optimum (c. 17–15 Ma), magnitudes were reduced to less than 20 m as a result of greatly diminished ice sheets. Short-term eustatic magnitudes returned to c. 20–30 m during the Late Middle to late Miocene and Pliocene. Large sea-level changes with lowering of 60–120 m below present were restricted to the past 2.7 Myr, linked to full-scale continental ice sheet development in the Northern Hemisphere. Even considering the large ($\pm$ 10 to $\pm$ 20 m) errors in magnitudes, $\delta^{18}O$ records provide a useful constraint. Moreover, the timing of eustatic events can be constrained by this method when the $\delta^{18}O$ record is linked to high-resolution biostratigraphy or other chronostratigraphic proxies (see Section 13.2.2).

13.3.3.2.3 Geological synthesis

For any given time period a useful approach to estimating the magnitude limits is to make a comparative synthesis of magnitude records from local and regional studies where (1) the sea-level change is deemed to be eustatic (because of relatively tectonically stable location and the short duration of the event) and (2) the magnitude estimates are derived by clearly documented reliable means. These include, in addition to backstripping and $\delta^{18}O$ analysis, sedimentological and paleontological observations, such as erosional and depositional relief, facies juxtaposition, fossil assemblages, and seismic and stratigraphic geometries. Rygel et al. (2008) pioneered this methodology for the study of Late Paleozoic eustasy; more recently, Ray et al. (2019) followed a similar approach to determine Cretaceous eustatic magnitude limits, supported by a data sensitivity analysis.

A similar but apparently more qualitative approach was undertaken by Haq and Schutter (2008) and Haq (2014), who derive eustatic magnitude estimates by averaging local measurements from the stratigraphic sections used to build the eustatic model (see also Haq, 2017, 2018). Haq (2014) has acknowledged that such measurements will be approximations, but it is intriguing that the magnitudes of eustatic change suggested by Haq and Schutter (2008) and by Haq (2014) greatly exceed those of Rygel et al. (2008) and Ray et al. (2019), respectively, or estimates purely from backstripping (e.g., Kominz et al., 2008). Johnson (2010) noted that the largest changes suggested in the Silurian short-term eustatic curve of Johnson (2006) are only half the magnitude suggested by Haq and Schutter (2008). Many of the sea-level changes documented by Johnson (2006) are determined from the extent of transgression and regression measured against topographic relief. A simple conclusion may be that the magnitude of local water depth change in the sections selected by Haq and Schutter (2008) and Haq (2014) has been overestimated, leading to a high-value average.

Rygel et al. (2008) synthesized more than 100 papers that had documented Late Paleozoic eustatic magnitudes based mostly on physical observations (e.g., erosion and depositional relief, facies juxtapositions, and cycle thickness) in the rock record from specific successions with short temporal durations (Fig. 13.15). By doing so, they sought to

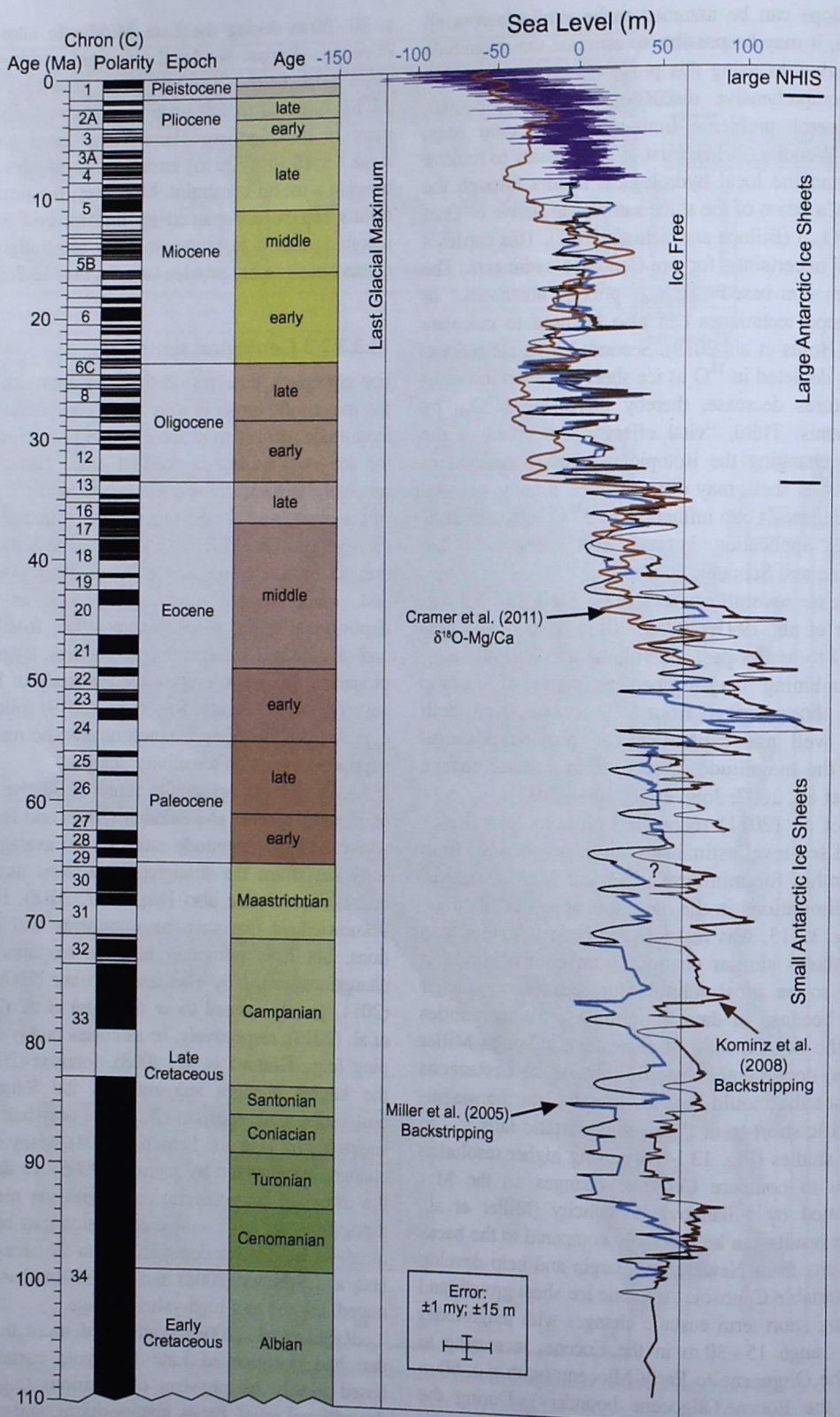

overcome the caveats and assumptions associated with each method of calculating eustatic magnitude and remove local and regional biases from the data.

They noted that at least eight intervals could each be characterized by specific magnitudes of eustasy. This supports the views of Isbell et al. (2003) and Fielding et al. (2008) that Late Paleozoic Gondwana ice sheets were dynamic and waxed and waned throughout much of the Carboniferous and Permian. Eustatic fluctuations of 20–25 m, and occasionally as much as 60 m, occurred throughout the Early Mississippian (Tournaisian), a widely recognized glacial period. Middle Mississippian (mid-Chadian–Holkerian) eustatic changes were 10–25 m, a decrease that matches a paucity of coeval glacial deposits. Late Viséan fluctuations of 10–50 m record the initial phases of ice accumulation ahead of the widespread mid-Carboniferous glacial event. The latest Mississippian–earliest Pennsylvanian was a time of widespread glaciation and eustatic magnitudes in the range of 40–100 m. A reduction in magnitudes of less than 40 m occurred in the middle Pennsylvanian, followed by an increase to 100–120 m in the late Pennsylvanian–earliest Permian; the latter corresponds to growth of Gondwanan ice sheets and the presence of northern hemisphere ice. Early–middle Permian magnitudes of 30–70 m reflect the waning stages of major glaciation. Finally, eustatic fluctuations of 10–60 m in the Late Permian reflect the late-stage glaciation, although the modest magnitude of some events may imply other driving mechanisms.

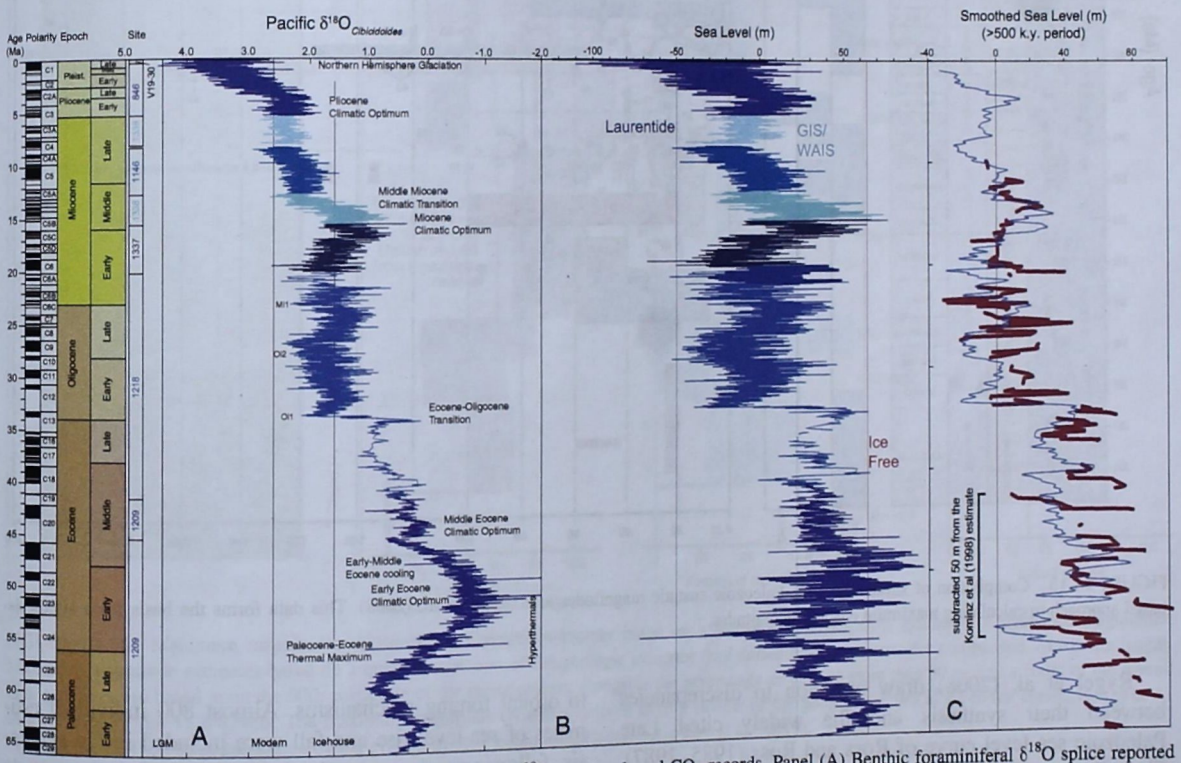

FIGURE 13.14 Summary of Cenozoic benthic foraminiferal $\delta^{18}O$, sea level, and CO_2 records. Panel (A) Benthic foraminiferal $\delta^{18}O$ splice reported to *Cibicidoides* spp. Modern is the core top value for $\delta^{18}O_{Cibicidoides}$; the Icehouse line is placed at 1.8‰ in *Cibicidoides*, with values greater requiring major ice sheets. Panel (B) Sea level obtained using a new benthic foraminiferal $\delta^{18}O$ splice and $\delta^{18}O_{seawater}$ from Mg/Ca; ice-free line (*magenta*) drawn 64 m above present, GIS-WAIS (Greenland ice sheet and West Antarctic ice sheet; *light blue*) drawn at +12 m above present; Laurentide (*dark blue*) drawn at −50 m. Panel (C) Comparison of smoothed sea-level estimates from $\delta^{18}O$ and Mg/Ca (*blue*; obtained by interpolating to 20-kyr intervals and using a 49-point Gaussian convolution filter, removing periods shorter than 490 kyr) with backstripped NJ estimates (*red*; Kominz et al., 2008, 2016). The NJ estimates for the Early to Middle Eocene were shifted by −50 m. See Miller et al. (2020) for further details.

FIGURE 13.13 Comparison of Cenozoic sea-level curves relative to modern (=0 m) using two methods: backstripping of New Jersey onshore sequences (*blue*, Miller et al., 2005a; *brown*, update of Kominz et al., 2008 using slightly different initial subsidence conditions) and $\delta^{18}O$-Mg/Ca method to extract temperature from $\delta^{18}O_{benthic}$ records (Cramer et al., 2011), with the residual $\delta^{18}O_{seawater}$ assumed to be global mean sea level as a result of ice-volume fluctuations. The Cramer record was smoothed to remove periods shorter than 2 Myr; it is truncated at 48 Ma because of uncertainties in the Mg/Ca record described by Cramer et al. (2011). The "ice-free line" is set at 64 m, the uncompensated change in water volume stored in continental ice sheets and glaciers (Fretwell et al., 2013). The Last Glacial Maximum (LGM) is set at 120 m below modern (Fairbanks, 1989). Error bars in age sea level are for backstripped estimates (Miller et al., 2005a; Kominz et al., 2008). Ice volume history and figure layout modified after Miller et al. (2011) and presented to the GTS2004, including geomagnetic polarity chrons. *NHIS*, Northern Hemisphere ice sheets.

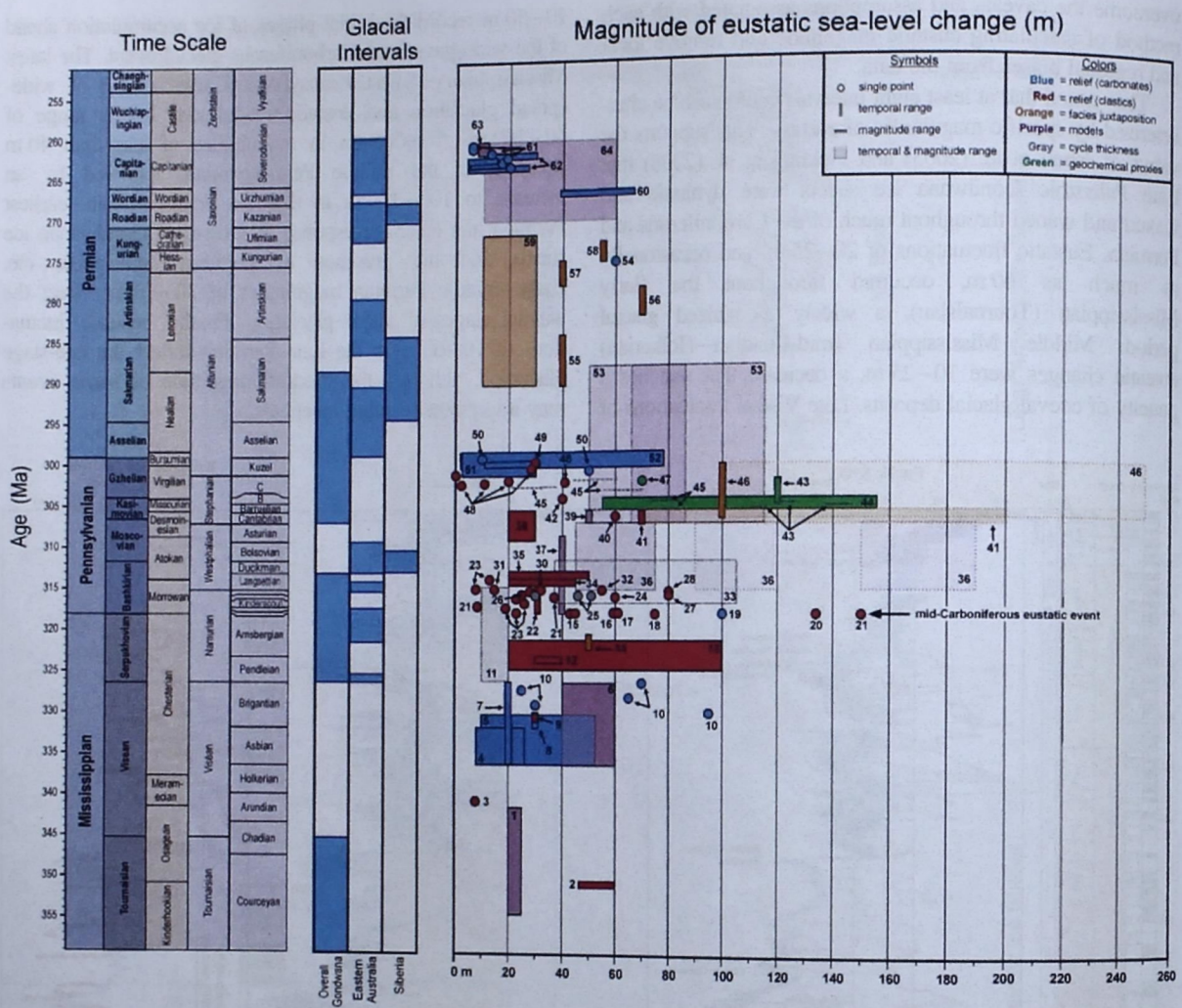

FIGURE 13.15 Compilation of short-term Late Paleozoic eustatic magnitudes after Rygel et al. (2008). This data forms the basis for a synthesis-based approach to calculating maximum eustatic magnitudes.

Rygel et al. (2008) draw attention to discrepancies between their synthesis and the widely cited Late Paleozoic sea-level curve of Ross and Ross (1985, 1987). First, Ross and Ross (1987) illustrate frequent eustatic magnitudes in excess of 100 m throughout the Late Paleozoic, a conclusion not substantiated by the Rygel et al. (2008) synthesis. Second, the timing of the highest magnitudes on the Ross and Ross (1987) curve correspond to periods of low magnitudes on the Rygel et al. (2008) synthesis and vice versa. Consequently, long-term highstands of eustasy on the Ross and Ross (1987) curve correspond to times of known maximum glaciation.

Ray et al. (2019) used records of Cretaceous sea-level change with duration of 3 Myr or less. By doing so, they reduced the influence of local tectonics and long-term drivers of eustasy (e.g., seafloor spreading and sedimentation) in favor of a short-term, climate-driven eustatic signal linked to orbital forcing mechanisms. Almost 800 individual estimates of sea-level rise and fall were included in the synthesis, following a rigorous selection process using the criteria previously described. A consensus view was extracted from this data in a stepwise manner. First, a preliminary statistical analysis of the entire dataset was undertaken to identify robust temporal trends in magnitude estimates and to establish intervals characterized by a particular range of magnitudes. After these intervals were established an in-depth review was performed of the geologic setting and methods, from which the magnitude estimates were derived in each interval. This geologic review identified the most robust studies, discounted anomalous data, and identified a robust maximum short-term magnitude for each of the time intervals. Finally, as a means of validating these geologically defined maximum short-term magnitude limits, a further statistical review focused on the upper magnitude limits.

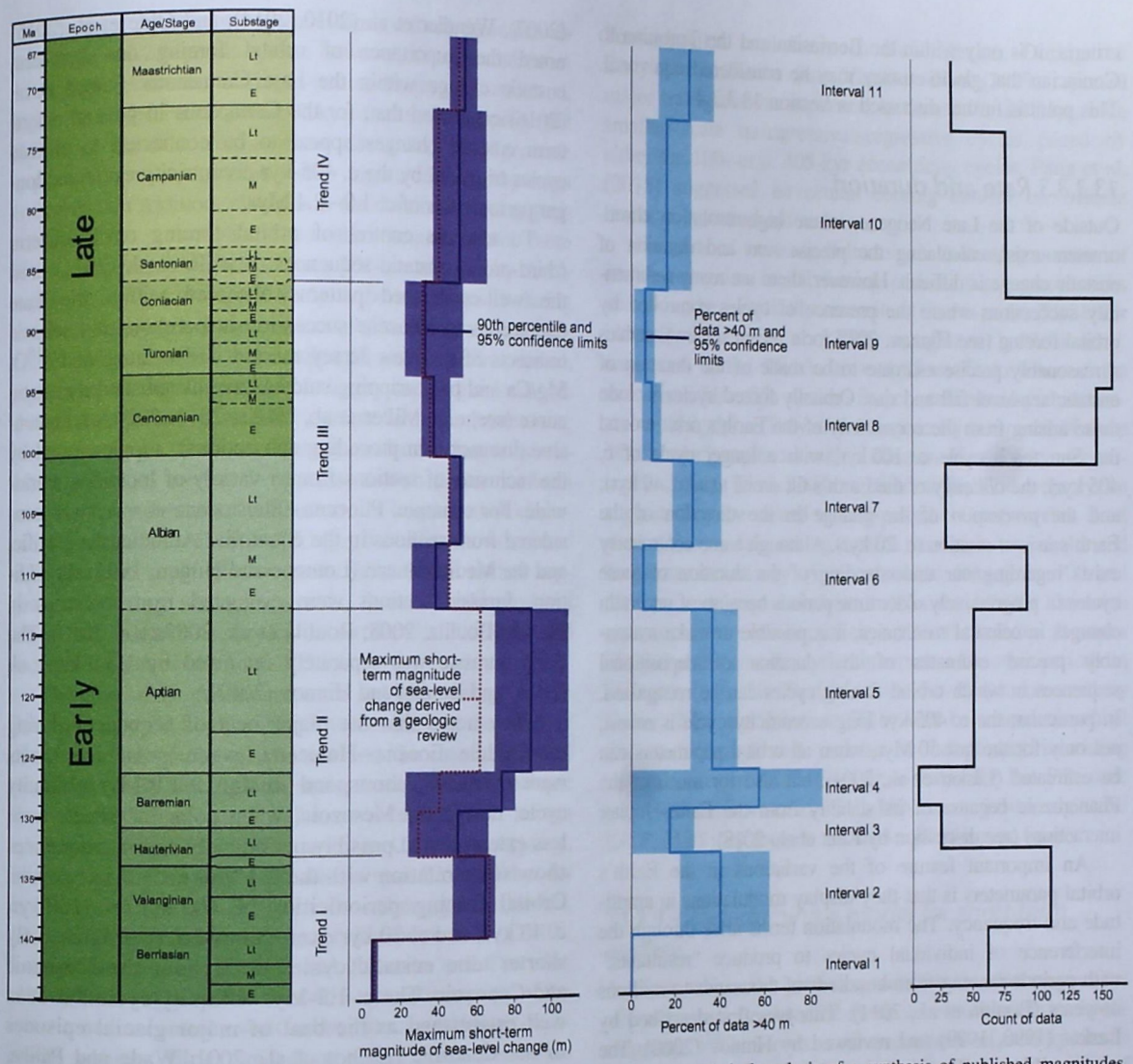

FIGURE 13.16 Maximum magnitudes of short-term Cretaceous eustasy based on a statistical analysis of a synthesis of published magnitudes. Maximum magnitude estimates based on a qualitative review of the geologic evidence (*red dotted line*) are shown for comparison. Maximum magnitude estimates are based upon the 90th percentile of the entire dataset, alongside the percentage of data of more than 40 m, and a count of the overall data for each of the 11 intervals. The maximum magnitude estimates derived from a review of the geologic record is given for comparison. The 11 intervals are derived from magnitude trends evident in the median magnitudes. After Ray et al. (2019).

The initial review of the entire Cretaceous dataset, weighing each data point equally, gave a median value for short-term eustatic change of 12 m, with the data approximating a log-normal distribution with a mean of $11.9 + 23.5/-7.9$ m (1σ); consequently, the majority of sea-level estimates are of relatively low magnitude with few examples of large magnitude. Examining *median* estimates at a stage level, following standard statistical resampling procedures, demonstrated that elevated magnitude values occurred during the Valanginian, Barremian to Aptian, and Santonian to Maastrichtian, with low magnitude values in the Berriasian, Hauterivian, and Albian to Coniacian. More specifically, *maximum* magnitude limits were derived (Fig. 13.16), which are consistent with some estimates derived from backstripping (e.g., Miller et al., 2003a,b, 2005a), but are in contrast with some of the greater magnitudes suggested by Haq (2014) (Fig. 13.11). Even though the Cretaceous eustatic estimates suggested by Ray et al. (2019) are relatively modest, 50% of the Cretaceous is associated with significant (greater than 40 m) eustatic changes that may be considered to be characteristic of glacio-eustasy (Valanginian, Aptian, Albian, and Maastrichtian). Furthermore, in the presence of significant eustatic change, the immediately older intervals of modest magnitudes (10–40 m) may be interpreted as representing the growth and demise of land-grounded icecaps. Based on these

criteria, it is only within the Berriasian and the Turonian to Coniacian that glacio-eustasy may be considered equivocal. This point is further discussed in Section 13.3.3.4.

13.3.3.3 Rate and duration

Outside of the Late Neogene, where high-resolution chronometers exist, calculating the precise rate and duration of eustatic change is difficult. However, there are many sedimentary successions where the presence of cycles controlled by orbital forcing (see Hinnov, 2018 for a recent review) enables a reasonably precise estimate to be made of the duration of eustatic sea-level fall and rise. Orbitally forced cycles include those arising from the *eccentricity* of the Earth's orbit around the Sun (each cycle c. 100 kyr, with a longer cycle of c. 405 kyr); the *obliquity* of the Earth's tilt on its axis (c. 40 kyr); and the *precession* of the change in the direction of the Earth's axis of rotation (c. 20 kyr). Although some controversy exists regarding our understanding of the duration of these cycles in progressively older time periods because of uncertain changes in celestial mechanics, it is possible to make reasonably precise estimates of the duration of depositional sequences in which orbital forcing cycles can be recognized. In particular, the c. 405-kyr long eccentricity cycle is robust, not only for the last 50 Myr, when all orbital parameters can be estimated (Laskar et al., 2004), but also for much of the Phanerozoic because of its stability from the Earth–Jupiter interactions (see discussion by Kent et al., 2018).

An important feature of the variations in the Earth's orbital parameters is that they display modulations in amplitude and frequency. The modulation terms arise through the interference of individual cycles to produce "resultants," with periods ranging from hundreds of thousands to millions of years (Boulila et al., 2011). This was first described by Laskar (1990, 1999) and reviewed by Hinnov (2000). The most well-known long-period modulation cycles are those of eccentricity (c. 2.4 Myr) and obliquity (c. 1.2 Myr).

The Kimmeridge Clay succession of southern England and northern France is one such succession in which orbital forcing has been considered to have been a major driver of the deposition sequences present. Huang et al. (2010) noted that the c. 405-kyr eccentricity cycle plays a major role in controlling the transgressive/regressive cyclicity observed in the Kimmeridge Clay (see also Boulila et al., 2008a,b,c, 2010; Simmons, 2012).

Orbital forcing has enabled the estimation of the duration of significant short-term transgressions and regressions with Cenomanian successions. Voigt et al. (2006) noted that one such transgression of a rocky shoreline in Germany, with a magnitude of 22–28 m, occurred in the *geslinianum* Zone of the Late Cenomanian with a duration of 80–180 kyr. Gale et al. (2002, 2008) noted that significant transgressions in the *rhotomagense* Zone of the Middle Cenomanian had durations of c. 150 kyr. More recently, Laurin and Sageman (2007), Wendler et al. (2010, 2014), and Olde et al. (2015) noted the importance of orbital forcing on short-term eustatic change within the Late Cretaceous. Sames et al. (2016) concluded that, for the Cretaceous in general, short-term eustatic changes appear to be connected to climate cycles triggered by the c. 405-kyr eccentricity cycle and longer periodicities of c. 1.0–2.4 Myr.

To test the control of orbital forcing on short-term (third-order) eustatic sequences, Boulila et al. (2011) used the well-established patterns observed within the Late Cretaceous to Miocene succession in borehole and seismic transects of the New Jersey margin where integrated $\delta^{18}O$, Mg/Ca and backstripping studies have established a eustatic curve (see, e.g., Miller et al., 2005a, 2011, 2020; and extensive discussion in preceding subsections), supplemented by the inclusion of sections from a variety of locations worldwide. For example, Pliocene–Pleistocene eustasy was considered from sections in the equatorial Atlantic, the Pacific, and the Mediterranean (Lourens and Hilgen, 1997). In addition, Jurassic sections were evaluated from outcrops in France (Boulila, 2008; Boulila et al., 2008a,b,c, 2010). The Early Jurassic was separately reviewed by Boulila et al. (2014) and Boulila and Hinnov (2017).

They noted that the major beat of sequences during the Middle Eocene–Holocene, when polar ice sheets were extensive, correspond to the c. 1.2-Myr obliquity cycle; during the Mesozoic, when polar ice sheets were less extensive and possibly periodically absent, sequences show some relation with the 2.4 Myr eccentricity cycle. Orbital forcing periodicities of 405 kyr, c. 100 kyr, c. 40 kyr, and c. 20 kyr exert control over progressively shorter term eustatic cycles throughout the Mesozoic and Cenozoic. The c. 1.2-Myr obliquity cycle has been well established as the beat of major glacial episodes in the Cenozoic (Zachos et al., 2001; Wade and Pälike, 2004; Pälike et al., 2006). Interesting, recent work by Liu et al. (2019), examining sequences in the East China Sea, calibrated to eustatic events worldwide, has noted that the c. 1.2-Myr obliquity cycle may exert strong control over eustatic cycles in the early Paleogene, an interval not fully studied by Boulila et al. (2011). In contrast to Boulila et al. (2011), Wendler et al. (2014) suggested that it is the c. 1.2-Myr obliquity cycle that provides control on eustasy in the Cenomanian–Turonian, modulated through aquifer-eustasy, rather than glacio-eustasy (further discussed in Section 13.3.3.1).

Integrated seismic, core, and log studies of the Miocene on the New Jersey shallow shelf by IODP Expedition 313 (Mountain et al., 2010) provide insight into the sedimentary response to icehouse conditions. The cause of the SBs is generally inferred to be sea-level change attributable to waxing and waning ice sheets in Antarctica, although sediment input determines the preservational potential of sequences.

The most prominent sequences observed are those associated with ~1.2-Myr tilt cycles; however, in areas and times when high sedimentation input and attendant rates occurred, higher order (405 and quasi-100 kyr) sequences are preserved (Miller et al., 2013a,b). In these cases, the 1.2-Myr scale sequences are composites with higher order sequences embedded. In addition, changes in the dominant forcing periodicity affect preservational potential; sequences are more likely to be preserved when strong 100-kyr eccentricity dominated forcing but are more likely to be eroded away during times the 41-kyr tilt cycle dominated (Browning et al., 2013). These studies establish that continental margin sedimentation, especially during intervals of large, rapid glacioeustatic change, acts as low-pass filter, concatenating and truncating precessional, tilt, short eccentricity, and even longer eccentricity (405 kyr) cycles. It appears, though it has not been unequivocally demonstrated because of limitations in chronostratigraphic control of ~0.5 Myr, that SBs are associated with the most rapid glacioeustatic falls. These studies suggest that during icehouse worlds, there is a hierarchical order (not fractal) of sequences on the tilt (1.2 Myr) and eccentricity scales (100 and 405 kyr).

The rate of short-term eustatic sea-level change in the Paleozoic is particularly difficult to establish in the absence of accurate chronometric proxies and the uncertainties of extending orbital forcing time scales further back in geologic time. Nonetheless, the well-known eustatically driven cyclothems (Fig. 13.17) of the Late Carboniferous (e.g., Eros et al., 2012a) were estimated to span 235–400 kyr for major cycles and 40–120 kyr for minor cycles (Heckel, 1986, 1990, 2008). More recently, Davydov et al. (2010), Falcon-Lang et al. (2011), and Schmitz and Davydov (2012) have suggested that c. 405-kyr eccentricity cycles exert a major control over Carboniferous cyclothem deposition, whereas Elrick and Scott (2010) have noted the importance of long-period obliquity c. 1.2 Myr on mid-Pennsylvanian cyclothems in New Mexico. During the Early Carboniferous (late Visean), Giles (2009) reported major transgressions separated in time by c. 2.4 Myr, with smaller scale transgressive–regressive cycles paced by either the 100- or c. 405-kyr eccentricity cycles. Fang et al. (2015) suggested an orbital forcing control on Middle Permian eustatic sequences.

For parts of the early Paleozoic an increasing number of studies recognize orbital forcing periodicities in successions deemed to be eustatically controlled (Cherns et al., 2013). For example, Dabard et al. (2015) recognize 11 "third-order" sequences in the Middle to early Late Ordovician of the Armorican Massif in western France, calibrated by chitinozoan biostratigraphy. They are each typically composed of three "forth-order" sequences with a duration of c. 405 kyr (eccentricity cycles). The 1.2-Myr duration of the third-order cycles suggests they are related to long-period obliquity cycles. Brett et al. (2011) note a strong control exerted by the short- and long-term eccentricity cycles of orbital forcing (c. 100 and 405 kyr, and longer modulations) on the Middle Devonian succession and eustatic cyclicity of North America. It seems likely that the eustatic cycles interpreted for other periods in Paleozoic (e.g., the Silurian sea-level cycles documented by Calner, 2008 and Johnson, 2010) will be related to orbital forcing. Although this remains to be proven, increasing research into orbital forcing time scales for the Paleozoic (e.g., Radzevičius et al., 2017; http://www.geolsed.ulg.ac.be/IGCP_652/) may provide the answers in the near future.

13.3.3.4 Determining a model for short-term eustasy

As discussed in the preceding subsections, the magnitudes of eustasy can be detected (with uncertainties) from backstripping, $\delta^{18}O$ records, and a synthesis of mainly stratigraphic observations (or an integration of more than one of

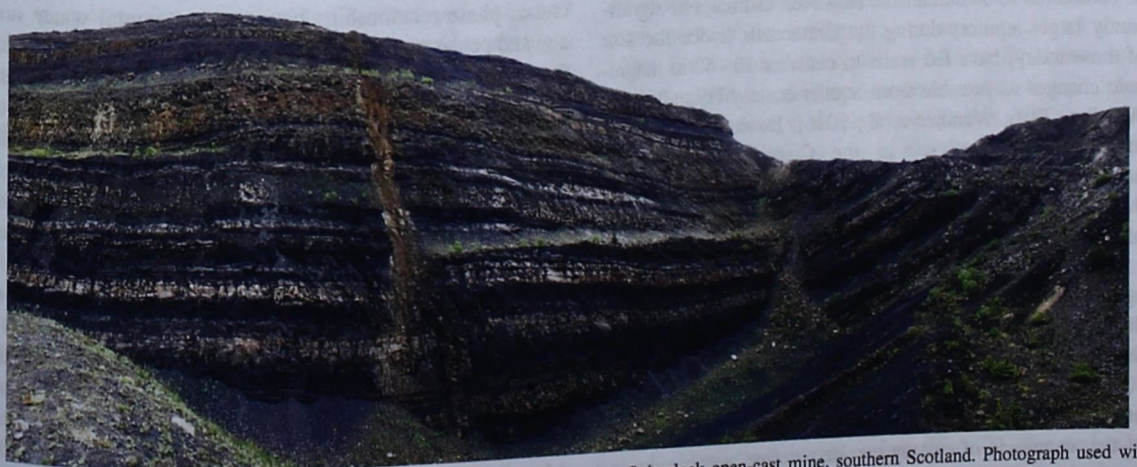

FIGURE 13.17 Carboniferous cyclothems in the Limestone Coal Formation, Spireslack open-cast mine, southern Scotland. Photograph used with kind permission of the International Appalachian Trail, Newfoundland and Labrador.

these techniques). The rate and duration of eustasy is best determined from identification of Milankovitch cyclicities within the rock record, supported by age proxies in the form of biostratigraphy and geochemical records. Based on these interpretations of the magnitude, rate, and duration of past eustasy, arguments exist for glacio-eustasy operating throughout much of the geologic record, even during times of relatively warm (greenhouse) climates (e.g., Miller et al., 2005a,b, 2011; Simmons, 2012; Davies et al., 2020), especially considering that there is increasing evidence for greater climatic instability in the geologic past than was previously thought (e.g., Hu et al., 2012).

The Cretaceous represents an increasingly well-studied period of the Earth's history when rapid, moderately high-magnitude eustatic changes were occurring (see previous section and Immenhauser, 2005; Miller et al., 2005a,b; Voigt et al., 2006; Ray et al., 2019) at a time when the Earth's climate was generally regarded as warmer than today. Two mechanisms have been proposed to explain short-term eustatic change within the Cretaceous: (1) short glacial episodes (Stoll and Schrag, 1996, 2000; Miller et al., 2005b, 2011; Maurer et al., 2013) (glacio-eustasy) and (2) the alternating charge and discharge of aquifers (Hay and Leslie, 1990; Jacobs and Sahagian, 1993; Wendler et al., 2016; Wendler and Wendler, 2016; Föllmi, 2012; Wagreich et al., 2014; Sames et al., 2016; Laurin et al., 2019) (aquifer- or limno-eustasy).

Critical to distinguishing between these two mechanisms are the upper magnitude limits of eustatic change they enable. The upper limit of glacio-eustatic magnitudes is 200 m or more (Miller et al., 2005a,b); the upper limits of aquifer-eustasy are uncertain, but significantly less than glacio-eustasy (Fig. 13.6). Jacobs and Sahagian (1993) suggested as little as 8 m as a maximum, whereas Hay and Leslie (1990) and Wagreich et al. (2014) suggested a 50 m upper limit, based on estimates of present-day aquifer storage with isostatic adjustment. The 50 m limit requires the alternate filling and emptying of all available aquifers, so it may be considered to be unrealistic. However, estimates of significantly larger aquifers during the Cretaceous (twice the size of those today) have led some to consider 10–40 m magnitude changes as possible from aquifer-eustasy (Wendler and Wendler, 2016; Wendler et al., 2016). Davies et al. (2020) modelled aquifer-eustasy in the Cretaceous considering palaeoclimate models and aquifer availability, and concluded that aquifer-eustasy was unlikely to contribute more than 5 m of eustatic change, even under the most favorable conditions.

Ray et al. (2019) and Davies et al. (2020) reviewed the options for the drivers of short-term eustasy in the Cretaceous that could also be applied in other geologic periods. Given the maximum likely contributions that thermo-eustasy (c. 10 m), aquifer-eustasy (c. 5 m), and glacio-eustasy (c. 200 m) may make to the total short-term eustatic signal, knowledge of the magnitude of eustasy can help define possible driving mechanisms. Thus short-term magnitudes of no more than 10 m may be accounted for solely by thermo-eustasy, or any combination of drivers, whereas magnitudes in excess of 15 m appear to be unachievable without a contribution from glacio-eustasy.

As magnitudes of short-term eustasy increase toward 15 m, it is more likely that glacio-eustasy makes a contribution. This is because of the environmental extremes required to drive the other two mechanisms toward their maximum capacity. For example, a 9 m short-term thermo-eustatic change requires the temperature of the oceans to change by approximately 15°C (Sundquist, 1990), which is comparable to the difference in temperature between the oceans of the warmest Late Cretaceous and the most recent major glaciation (Grossman, 2012). Clearly, repeated short-term changes of this magnitude are inconsistent with the mass of climate proxy data for much of the geologic record (e.g., O'Brien et al., 2017 for the Cretaceous).

Similarly, the enhanced hydrological cycle that appears necessary for aquifer-eustasy would require extreme episodes of aridity and humidity to operate at its maximum capacity (Davies et al., 2020). During the Cretaceous, humid-arid cycles are inferred (Föllmi, 2012; Wendler et al., 2016), but not at the extremes required to be the sole driver of short-term eustasy (Davies et al., 2020). This led Föllmi (2012) to suggest that giant lakes may have played a role but, overall, the water capacity of lakes is negligible (Wagreich et al., 2014; Sames et al., 2016).

Ray et al. (2019) concluded that during the Cretaceous, glacio-eustasy dominates the intervals of significant short-term eustatic change (Valanginian, Aptian, Albian, and Maastrichtian) and episodes of modest eustatic fluctuation preceding and proceeding. Only during the Berriasian, Turonian, and Coniacian is the likelihood of glacio-eustatic influence equivocal. Wagreich et al. (2014) noted that, notwithstanding age calibration uncertainties, Turonian eustatic signals appear to be out of phase with lacustrine water-level changes (as determined from the Songliao Basin, China). Out-of-phase relationships between continental water storage and ocean water levels can be advanced as an argument for aquifer-eustasy, although this must be tested by the study of multiple age-calibrated lacustrine successions on separate continents. Indeed, Davies et al. (2020) recently demonstrated that the greatest aquifer charge is more likely during cooler intervals, indicating that aquifer-eustasy might work in phase with both glacio- and thermo-eustasy in contrast to the current aquifer-eustasy paradigm.

The conclusions of Ray et al. (2019) and Davies et al. (2020) support a growing view that glacio-eustasy was a dominant eustatic mechanism during much of the Cretaceous, mediated by changes in volume of relatively small polar ice sheets and episodic cold spells (Miller et al., 2003a,b, 2005b; Miller, 2009; Koch and Brenner, 2009; Maurer et al., 2013; Davies et al., 2020; Lin et al., 2020). Despite ongoing perceptions in much of the geological

community that the Cretaceous was dominated by persistent warm climates (e.g., Hay, 2008; Jenkyns et al., 2012; Föllmi, 2012; Wendler and Wendler, 2016), this view is increasingly challenged by both evolving climate science (e.g., Donnadieu et al., 2011; Hu et al., 2012; Hong and Lee, 2012; Ludvigson et al., 2015; Tabor et al., 2016; Ladant and Donnadieu, 2016), the gathering of sedimentological and geochemical proxies for the presence of polar ice (e.g., Price, 1999; Alley and Frakes, 2003; Macquaker and Keller, 2005; McArthur et al., 2007; Price and Nunn, 2010; Simmons, 2012; Föllmi, 2012; Hore et al., 2015; Herrle et al., 2015; Rodríguez-López et al., 2016; Grasby et al., 2017; Rogov et al., 2017; Vickers et al, 2019; Horner et al., 2019; Alley et al., 2019), and changes in the global populations of microfossils that indicate episodes of marked cooling (e.g., Mutterlose et al., 2009; McAnena et al., 2013).

Sedimentological proxies are relatively scarce in the Late Cretaceous, but temperature proxies, such as TEX_{86}, $\delta^{18}O$, and seasonal diatom production and sediment flux, have identified a broad middle Campanian to end-Maastrichtian cooling and the presence of seasonal sea ice (Davies et al., 2009; Bowman et al., 2013; Kemp et al., 2014; O'Brien et al., 2017; Niezgodzki et al., 2019). The balance of evidence is leading to the increasing acceptance that within the Cretaceous there were at least episodes of polar glaciation (e.g., Donnadieu et al., 2011; Ladant and Donnadieu, 2016). However, this view is often in contrast with geochemical evidence (e.g., TEX_{86}, $\delta^{18}O$, Mg/Ca), which generally implies that temperatures were too warm for ice sheet growth (e.g., compare the TEX_{86} proxy data of Jenkyns et al., 2004 with the diatom productivity and sediment flux data of Davies et al., 2009). One explanation for this may be the presence of a seasonal bias in many of the proxy temperature estimates, especially at high latitudes (e.g., Davies et al., 2019a).

The relatively high magnitudes and rapid rate of sea-level change driven by glacio-eustasy can lead to the creation of spectacular incised valley systems and prominent subaerial exposure surfaces. In the Aptian, for example, such features have been documented from numerous basins around the world (van Buchem et al., 2010b; Husinec et al., 2012; Maurer et al., 2013; Peropadre et al., 2013; Millán et al., 2014; Bover-Arnal et al., 2014; Pictet et al., 2015; Horner et al., 2019). In the McMurray Formation of the Western Canadian Foreland Basin, four distinct composite channel-form bodies can be documented across an area of more than 14,000 km^2 (Horner et al., 2019). Composite channel-form bodies are up to 50 km wide and locally exceed 70 m thick. Furthermore, transgressive rock units can be correlated over a minimum of 280 km, suggesting that shorelines advanced and retreated more than 300 km, creating a distinctive stratigraphic architecture. Similar scale incised valley systems were described by Koch and Brenner (2009) from Albian/Cenomanian boundary strata (Dakota Formation) of the US Western Interior Seaway, which were attributed to have a glacio-eustatic origin.

The increased likelihood that glacio-eustasy was the dominant driver of short-term eustasy during the Cretaceous highlights the possibility that it was also an important driver in other periods previously regarded as being dominated by warm climates. Evidence for glaciation and episodic cool/cold climates is being gathered for every Phanerozoic period, even at the end of the Triassic (Schoene et al., 2010). Significant glaciation is envisaged for parts of the Cambrian (Landing and MacGabhann, 2010; Cherns et al., 2013; Babcock et al., 2015); the pre-Hirnantian Ordovician (Page et al., 2007; Cherns et al., 2013; Dabard et al., 2015; Pohl et al., 2016); the post-Llandovery Silurian (Page et al., 2007; Grahn and Caputo, 1992; Diaz-Martinez and Grahn, 2007; Caputo, 1998; Cherns et al., 2013); and the Middle Devonian to earliest Carboniferous (Caputo et al., 2008; Isaacson et al., 2008; Elrick et al., 2009; Montañez and Poulsen, 2013; Lakin et al., 2016; Elrick and Witzke, 2016).

Cold spells in the Jurassic have been suggested by, for example, Korte and Hesselbo (2011), Korte et al. (2015), Rogov and Zakharov (2010), Donnadieu et al. (2011), Dromart et al. (2003), Krencker et al. (2019), and Rogov et al. (2019) and references therein. In the pre-Oligocene Cenozoic continental ice sheets in both the southern and northern hemispheres have been envisaged by, among others, Tripati et al. (2005, 2008), and Middle to Late Eocene ice sheets appear to be incontrovertible (Peters et al., 2010; Gulick et al., 2017).

Thus a growing body of evidence exists to support the presence of volumetrically significant polar ice in what are commonly regarded as greenhouse times. What is remarkable is that short-term (third-order) eustatic sea-level change often seems to show a correlation with proxy records of paleotemperature changes (e.g., sea-level falls are associated with evidence for cooling events) (Cherns et al., 2013). Moreover, the likely (orbitally forced) pace and (at least moderate—c. 50 m or greater) magnitude of eustasy in many parts of the stratigraphic column (e.g., Brett et al., 2011; Elrick and Witzke, 2016—Middle Devonian) is at least suggestive of glacio-eustasy, even though more research is needed to firmly establish this. The increasing evidence for orbital forcing of climate, extinction events, and sedimentation patterns in, for example, the Devonian (e.g., De Vleeschouwer et al., 2017) and Ordovician (Cherns et al., 2013; Dabard et al., 2015) suggests a causal link with glacio-eustasy may soon be established.

The frequency and magnitude of eustatic events appear to be rather different for the Triassic, as compared to the rest of the geologic record (Davies and Simmons, 2018; Haq, 2018). Davies and Simmons (2018) noted eight major sequences on the Arabian Plate that they suggested may have a eustatic origin. Haq (2018) noted more eustatic events (see also Franz et al., 2014), but only six

were major with amplitudes suggested to be in excess of 75 m. Major Triassic eustatic cycles thus appear to have an unusually long, uneven periodicity, although smaller scale depositional cyclicity appears to follow orbital forcing periodicities of 20, 100, and occasionally 405 kyr (e.g., Ajdanlijsky et al., 2019). That humid/arid climate shifts were particularly dramatic in the Triassic (e.g., Preto et al., 2010; Stefani et al., 2010; Trotter et al., 2015) has led some (e.g., Jacobs and Sahagian, 1993; Wagreich et al., 2014; Li et al., 2016) to invoke aquifer-eustasy as a control on Triassic short-term eustasy. The revised aquifer-eustasy paradigm of Davies et al. (2020) is supported by the observation that Triassic warming events appear to correspond to eustatic highs and cooling to eustatic lows (Davies and Simmons, 2018; Simmons and Davies, 2018; Haq, 2018), but the magnitudes of eustatic change (e.g. Haq, 2018), whilst needing further assessment, suggest aquifer-eustasy is an unlikely driver. Therefore the driving mechanism for Triassic short-term eustasy remains enigmatic, although glacio-eustasy has been cited as the cause of end-Triassic sea-level fall (Schoene et al., 2010).

13.4 Phanerozoic eustasy: a review

Although some consensus on the timing of eustatic events is emerging, there are still significant differences between workers for most geologic periods (especially for the pre-Cenozoic). Perhaps this is not surprising, given that inherent differences exist in how eustatic change has been recognized in the geologic record, be that from stratigraphic synthesis, backstripping, or geochemical approaches (e.g., use of $\delta^{18}O$), noting that interpretation strategy of sedimentary successions and biostratigraphic calibration will inevitably differ between authors. It should also be noted that different eustatic schemes should be recalibrated to a single geologic time scale, although what is important is the position of eustatic events within standard biozonation schemes.

Given these uncertainties, we would hesitate to recommend any one particular eustatic sea-level curve over another. Instead, we simply highlight the key interpretations that are available and encourage the stratigraphic community to continue to gather data, which will help the advancement of a true consensus. It is encouraging that some stratigraphic subcommissions for the various periods of the Phanerozoic are developing consensus views on eustasy for their particular interval of geologic time. The Permian Subcommission, for example, maintains a view on transgressive and regressive cycles (http://permian.stratigraphy.org/per/per.asp).

13.4.1 Major syntheses

There are several publications, some much cited, that provide an analysis of short-term eustasy over multiple geologic periods or eras, and some of which were used in previous Geologic Time Scale publications.

Haq et al. (1987, 1988)—Summarized EPR research into Mesozoic and Cenozoic eustasy, with a sea-level curve that has been widely reproduced and cited. The data behind the eustatic model was not published, which led to criticism from some quarters (see review in Miall, 2010). Numerous short-term eustatic cycles were depicted, which some have argued (Miall, 1991, 1992) go beyond the capabilities of tools of correlation and calibration to resolve. Others have found the timing of events to be plausible, although the magnitudes to be excessive (e.g., Miller et al., 2005a; also see Ray et al., 2019 and discussion in Section 13.3.3.2). Nonetheless, and despite relatively recent updates (Haq and Al-Qahtani, 2005; Haq, 2014, 2017, 2018), the model continues to be widely regarded as the de facto statement on eustasy. The update by Haq and Al-Qahtani (2005) integrating Arabian Plate stratigraphy with minor modification was adopted for the Triassic portion of the GTS2016 compilation of Ogg et al. (2016).

Hardenbol et al. (1998)—Intended as an update to the Haq et al. (1987, 1988) Mesozoic and Cenozoic synthesis based on the study of outcrops from around Europe, synthesizing the work by a large group of experts (e.g., Hesselbo and Jenkyns, 1998). This work was adopted for the Mesozoic and Cenozoic portions of the 2012 geologic time scale compilation of Gradstein et al. (2012) and for the Jurassic and Cenozoic portions of the 2016 geologic time scale compilation of Ogg et al. (2016).

Haq and Schutter (2008)—Much cited representation of Paleozoic eustasy based on the study of multiple sections originally identified at EPR from regions thought tectonically stable. One hundred and seventy-two eustatic events were listed for the Paleozoic, varying in magnitude from a few tens of meters to ~125 m. Although commonly cited, the eustatic curve within this paper has often been found to contrast with more detailed studies on a period-by-period basis, not least in the number of cycles represented and their magnitude (see, e.g., discussion in Eros et al., 2012b and Johnson, 2010). As with the syntheses by Haq et al. (1987, 1988) for the Mesozoic and Cenozoic, details of interpretation strategy and biostratigraphic calibration are lacking, which hinders comparison and evaluation. A recalibrated version of the Silurian portion was presented by Melchin et al. (2012) in the 2012 geologic time scale compilation. This work was adopted for the Paleozoic portion of the 2016 geologic time scale compilation of Ogg et al. (2016) with minor modification.

Snedden and Liu (2010)—Recalibration of the Haq et al. (1987), Hardenbol et al. (1998), and Haq and Schutter (2008) eustatic curves to the 2008 geologic time scale. No new data appears to have been applied.

Ross and Ross (1985, 1988, 1992, 1995, 1996)—Pioneering attempts to synthesize knowledge on Paleozoic

eustasy, drawing on mainly North American stratigraphy. These papers continue to be widely cited, despite strong criticism from those who have performed more recent detailed studies (e.g., Eros et al., 2012a).

Sahagian and Jones (1993) and Sahagian et al. (1996)—An attempt to produce a sea-level curve for the Jurassic, Cretaceous, and Paleocene of the Russian Platform, by backstripping stratigraphic data from numerous wells. Because of the supposed stability of the Russian Platform, the sea-level curve is thought to be eustatic in origin. The presence of numerous unconformities within the stratigraphy may be a limitation on the provision of a continuous eustatic record.

Miller et al. (2005a)—Much cited review of Phanerozoic eustasy incorporating data from various previous studies, but with a focus on the significance of the backstripped Late Cretaceous–Cenozoic stratigraphic record of the New Jersey onshore that, in turn, was updated by Kominz et al. (2008, 2016).

Simmons et al. (2007)—Argued that the latest Precambrian–Phanerozoic Arabian Plate sequence stratigraphic model of Sharland et al. (2001) and updated by Davies et al. (2002) and Sharland et al. (2004) was essentially a eustatic model. Davies and Simmons (2018), Horbury (2018), and Lunn et al. (2019) have recently suggested updates to the Triassic part of the model, whereas Simmons and Davies (2018) and van Buchem et al. (2011) have updated parts of the Jurassic and Cretaceous model, respectively. Van Buchem et al. (2010b) and Maurer et al. (2013) paid particular attention to the Barremian and Aptian parts of this model, using detailed, high-resolution outcrop and subsurface studies and global comparisons to advance a case for glacio-eustasy, at least during the late Aptian.

There are also important syntheses for specific time periods (see also other chapters in this book). The following subsections describe some of the more recent and often-cited compilations and commentaries, noting that some examine long-term trends, whereas others can be focused on specific short-term events.

13.4.1.1 Cambrian

Babcock et al. (2015)—Provided a review of the state of knowledge of Cambrian sea-level history in the light of improved chronostratigraphy with an onlap curve for the upper part of the Cambrian–basal Ordovician. Abrupt transgressions that led to deposition of black shales or black limestones and the evolutionary inceptions of key agnostoid trilobites are suspected to be glacio-eustatic in origin. This paper drew upon information in the following detailed studies: Miller et al. (2003a, 2003b), Runkel et al. (2007), Nielsen and Schovsbo (2011), Peng et al. (2012), and Álvaro et al. (2014).

Nielsen and Schovsbo (2015)—A particularly comprehensive review of the Early–Middle Cambrian, with suggestions that their analysis of sea-level change in Baltoscandia may correspond with global patterns. The codification of sea-level events (e.g., Hawkes Bay Event) makes them particularly useful.

Lee et al. (2015)—Provided a discussion of the major sea-level fall immediately postdating the Cambrian Epoch 3—Furongian boundary that is recognized on both Laurentia and Gondwana and is thus considered to be eustatic in origin. This event had major effect on the composition of reef communities.

13.4.1.2 Ordovician

Nielsen (2004, 2011)—Presented a sea-level curve for Baltoscandia. Because of the tectonic quiescent nature of the region during the Ordovician and slow depositional rates, many parts of the curve were suspected as being eustatic in origin. The 2011 version was recalibrated to the time scale of Ogg et al. (2008) and included minor revisions in the Late Ordovician. The difficulty in estimating amplitudes was emphasized. Events were codified for ease of use. The 2004 version was used by Cooper and Sadler (2012) in the 2012 geologic time scale compilation. Note that interpretation of Ordovician sea-level change from the deeper water facies of Baltoscandia by Dronov et al. (2011) differs substantially from that of Nielsen (2004, 2011).

Videt et al. (2010)—Recognized 16 third-order cycles in the Ordovician stratigraphy of northern Gondwana (North Africa), calibrated by chitinozoan biostratigraphy, several of which they believed to be eustatic in origin based on a comparison with sea-level events on several other continents. Loi et al. (2010) and Dabard et al. (2015) presented related detail.

Munnecke et al. (2010)—Presented a comprehensive review of the challenges in recognizing eustatic changes in Ordovician sediments. They provided a compilation of published regional sea-level curves and, as subsequently noted by Dronov (2017), whereas there are good matches between some curves there are apparent mismatches, with western Gondwana and Avalonia especially, displaying differences from other continents, mostly as a result of local tectonics.

Creveling et al. (2018)—Provided a discussion of how sea-level histories at continental margins in both the near- and far-field of the Late Ordovician ice sheet can differ significantly from eustasy because of isostatic adjustments. Dietrich et al. (2018) and Pohl and Austermann (2018) provided further discussion of this topic.

13.4.1.3 Silurian

Johnson et al. (1998) and Johnson (2006, 2010)—Using comparisons of Silurian stratigraphy on multiple paleocontinents, often based on first-hand experience, Markes Johnson has been at the forefront of developing an understanding of Silurian eustasy in the manner of the pioneer

Grabau (1936a,b, 1940). His sea-level curves, the most recent being the 2006 version, are much cited. His 2010 paper is a comparison of the 2006 eustatic curve with the Silurian portion of the Haq and Schutter (2008) Paleozoic synthesis. Although driven by different approaches, 8 of 10 highstands of Johnson (2006) match 8 of 15 highstands suggested by Haq and Schutter (2008). A recalibrated version of the 2006 curve was presented by Melchin et al. (2012) in the 2012 geologic time scale compilation.

Loydell (1998, 2007)—Defined episodes of sea-level rise and fall in the Early Silurian, based primarily on the oxidation state of the strata under investigation and the graptolite fauna contained therein. The 2007 paper expanded this concept to include carbon isotope data. A recalibrated version of the 1998 curve was presented by Melchin et al. (2012) in the 2012 geologic time scale compilation. See also Page et al. (2007).

Munnecke et al. (2010)—This was a comprehensive review of the challenges in recognizing eustatic changes in Silurian sediments. They provided a compilation of published Silurian eustatic curves and, as subsequently noted by Simmons (2012), although there is a good deal of commonality, differences can be ascribed to differing interpretation strategies for recognizing sea level and eustasy and differences in biostratigraphic calibration. See also Calner (2008).

Davies et al. (2016)—This was another comprehensive review of Early Silurian sea-level change, comparing the pattern observed in the type Llandovery succession of mid-Wales with 62 other published datasets, including global and regional baselevel curves. The concept of a Eustasy Index as extracted from the commonality in this data was used to argue that eustatic changes can only be confidently identified for highstands associated with ice-sheet collapse.

13.4.1.4 Devonian

Johnson et al. (1985)—Using sections in relatively stable cratonic interiors and continental margins, they defined a series of 12 cycles in the Devonian portion of the Kaskaskia Megasequence of North America (Sloss, 1963) and subdivided them into two series of cycles (I and II) separated by the major Taghanic unconformity. This work, and an updated version (Johnson et al., 1996), has become entrenched as a standard for Devonian eustatic cyclicity, as noted by Brett et al. (2011).

House and Ziegler (1997)—This was a seminal description of Devonian eustasy in multiple worldwide sections, building the pioneering work of House (1983) and Johnson et al. (1985).

Ma et al. (2009)—Important comparison of sea-level changes as expressed in the Devonian stratigraphy of South China with other sections worldwide, leading to insights into eustasy.

Brett et al. (2011)—Presented a sea-level curve for the Middle Devonian of eastern North America that, because of the persistence of its pattern over a wide geographic area and its linkage to the short- and long-term eccentricity cycles of orbital forcing (100 and 405 kyr), was thought to be glacio-eustatic in origin. Eight third-order cycles were recognized within the Eifelian–Givetian.

Becker et al. (2012)—Presented a new curve for the GTS2012 compilation (Gradstein et al., 2012), based on a synthesis of past global curves, although without detailed explanation. Becker et al. (2020, Ch. 22: The Devonian Period, this book) developed a very detailed relative sea-level curve calibrated to ammonoid and conodont zones.

Wong et al. (2016)—Presented a revision of Frasnian sea-level curve based on decades of sequence stratigraphic analysis of outcrops in the Canadian Rocky Mountains and of the adjacent, hydrocarbon-bearing, subsurface. This study stands out for the detail of the biostratigraphic, sedimentological, and information about depositional geometries over a large area, that assist in the recognition of global patterns.

13.4.1.5 Carboniferous

Izart et al. (2003)—This was a near-global comparison of Late Carboniferous and Permian sequences, leading to the recognition of interregional stratigraphic patterns and the timing of eustatic changes.

Heckel (2008)—Regarded the late middle through late Pennsylvanian cyclothems of midcontinent North America as the result of large-scale eustatic fluctuations related to the large-scale, but short-term, waxing and waning of Gondwanan continental ice sheets, in turn moderated by long eccentricity cycles of orbital forcing.

Eros et al. (2012a)—Demonstrated the correlation of 252 cyclothems across a 250 km long depositional ramp profile of the Donets Basin, within a 33 my span of the Mississippian–Pennsylvanian. Their occurrence on orbital forcing time scales and correspondence to cyclicity in other basins suggests a glacio-eustatic origin for the RSL curve generated from this data. Ruban (2012) and Eros et al. (2012b) provide a discussion about a comparison of this work with the Paleozoic eustatic curve of Haq and Schutter (2008). See also van Hinsbergen et al. (2015).

Aretz et al. (2020, Ch. 23: The Carboniferous Period, this book) present a revised Early Carboniferous sequence stratigraphy history calibrated to European biostratigraphic zones.

13.4.1.6 Permian

Izart et al. (2003)—This was a near-global comparison of Late Carboniferous and Permian sequences, leading to the recognition of interregional stratigraphic patterns and the timing of eustatic changes.

Rygel et al. (2008)—Provided a comprehensive review of the magnitude of Late Paleozoic eustatic change, discussed in detail in the Section 13.3.3.2 on eustatic magnitudes. They are critical of the Ross and Ross (1985, 1987) curves because they cannot be replicated.

Jin et al. (2006)—Related the proposed GSSP for the base Lopingian to a major eustatic fall calibrated by a negative carbon isotope excursion and major faunal turnover. This paper is a good example of the way in which chronostratigraphy and eustasy can possibly be integrated.

13.4.1.7 Triassic

Embry (1988, 1997)—Provided seminal descriptions of the sequence stratigraphy of the Canadian Triassic succession with global comparisons to yield a eustatic signal that could also be linked to chronostratigraphic subdivision (i.e., stage and substage boundaries). See also Mørk (1994).

Gianolla and Jacquin (1998)—Provided a description of the Triassic stratigraphy of Western Europe with global comparisons (incorporated in eustatic model of Hardenbol et al., 1998).

Franz et al. (2014)—Documented evidence for eustasy from the Carnian succession of the epicontinental Central European Basin.

Haq (2018)—Provided a reappraisal of the Haq et al. (1988) and Hardenbol et al. (1998) synthesis incorporating subsequent published data from Europe, Arabia, India, Pakistan, China, and Australia (see https://www.geosociety.org/datarepository/2018/2018390.pdf—14 key references were cited, including previous syntheses). Twenty-two third-order sequences were recognized, with sea-level change amplitudes estimated as mostly varying between less than 25 m and c. 75 m. Six were estimated as exceeding 75 m.

13.4.1.8 Jurassic

Hallam (2001)—This was a much cited global compilation of stratigraphic data to extract a eustatic signal and challenged the notion of major, rapid sea-level falls within the Jurassic.

Zimmermann et al. (2015)—Reviewed the sequence stratigraphy of the Early and Middle Jurassic of the North German Basin, noting correspondence with the short-term (second-order) Boreal cyclicity described by De Graciansky et al. (1998) and Jacquin et al. (1998). The influence of local tectonics on deposition cyclicity in the Jurassic of northern Europe was emphasized (see also Underhill and Partington, 1993; Hesselbo and Jenkyns, 1998; Hesselbo, 2008), although high-frequency (fourth-order) sequences are suggested to have a glacio-eustatic origin because of their inferred periodicity and interregional correlation.

Haq (2017) —Provided a reappraisal of the Haq et al. (1988) and Hardenbol et al. (1998) synthesis incorporating subsequent published data from Europe, Arabia, India, and Argentina (see http://www.geosociety.org/datarepository/2017/2017387.pdf—15 key references were cited, including previous syntheses). Incorporation of data away from these regions was thought to be hindered by uncertainties in interregional biostratigraphic calibration. Fifty-six third-order sequences were recognized, with sea-level change amplitudes estimated as varying between less than 25 m and c. 150 m.

13.4.1.9 Cretaceous

Hoedemaeker (1995)—Used variations in ammonite diversity to recognize eustatic highs and lows in the Berriasian–Barremian stratigraphy of southeast Spain. Eustasy is implied because of correlation of the cyclicity to other parts of Europe and Russia. The duration of the cyclicity (c. 3.4 Myr, using the time scale of the publication) is intermediate between the "third-order" and "second-order" cyclicity of Haq et al. (1987, 1988) for the same period.

Haq (2014)—Provided a reappraisal of the Haq et al. (1988) and Hardenbol et al. (1998) syntheses incorporating subsequent published data from a global set of locations. Fifty-eight third-order sequences were recognized, with sea-level change amplitudes estimated as varying between less than 20 m and c. 100 m. See also Haq and Huber (2017). The review of Haq (2014) was adopted for the Cretaceous portion of the 2016 geologic time scale compilation of Ogg et al. (2016) with minor modification.

Wendler et al. (2014)—Recognized long-term obliquity and long- and short-term eccentricity orbitial forcing cycles as a primary control on mid-Cretaceous sea-level changes on the Levant margin of the Arabian Plate. This was interpreted as a eustatic pattern, with aquifer-eustasy invoked as a driving mechanism (see discussion in Section 13.3.3.1).

Scott et al. (2018)—Placed Cenomanian–Turonian flooding events as recognized in North America into a precise chronostratigraphic framework that permitted correlation with Tunisian sections. Commonality provided support to the eustatic model of Haq (2014) and Haq and Huber (2017). See also Gale et al. (2002, 2008), Galeotti et al. (2009), and Koch and Brenner (2009).

Dujoncquoy et al. (2018)—Provided a comprehensive study of the Early Cretaceous of Oman using outcrop, 3D seismic, and well log data to generate a RSL curve. Comparison of this with that from the Vocontian Basin of France (Gréselle and Pittet, 2010) suggested a eustatic origin. Reasonable comparison with the eustatic curve of Snedden and Liu (2010) was also demonstrated.

13.4.1.10 Cenozoic

Abreu and Anderson (1998)—Used a smoothed $\delta^{18}O$ isotope curve as a proxy for eustasy. Correspondence with

other eustatic curves suggested a strong glacio-eustatic signature from the Middle Eocene onward.

Sluijs et al. (2008)—Constructed a eustatic curve for the Paleocene–Eocene transition using palynological and sedimentological data from multiple sites from around the globe.

Miller et al. (1998, 2013b)—Backstripped onshore New Jersey data to provide a testable history of sea-level change. Miocene portions were tested using offshore cores collected by IODP Expedition 313 on the New Jersey shelf, as presented in Miller et al. (2013a,b), Katz et al. (2013), Browning et al. (2013), and McCarthy et al. (2013). See also Van Sickel et al. (2004) and Gasson et al. (2012).

Kominz et al. (2016)—Backstripped RSL estimates of Middle to Late Miocene sequences from the New Jersey coastal plain and three IODP shelf sites are generally internally consistent with respect to the timing of SBs and RSL variations. Coastal plain sedimentation tends to predict RSL changes that are consistent with those observed offshore. Where onshore and offshore sedimentation corresponds, the rising and falling portions of the RSL curve can be correlated, although the magnitude of offshore and onshore estimates is offset. This result requires that the New Jersey passive margin has undergone epeirogeny and, in particular, that the offshore shelf has subsided less than the coastal plain. Thus it is consistent with relative epeirogeny attributable to subduction of the Farallon Plate (Moucha et al., 2008) and arising from glacial isostatic adjustments effects of the last deglaciation (Raymo et al., 2011).

John et al. (2011)—The timing and magnitude of Miocene eustasy was calculated for the succession on the Marion Plateau, offshore northeastern Australia, as calibrated to other successions, notably offshore New Jersey. Eight sea-level falls correspond to $\delta^{18}O$ increases that reflect increased Antarctic ice volumes. From backstripping, ranges of individual sea falls were from 26–28 to 53–81 m. Overall sea level fell between 53 and 69 m and between 16.5 and 13.9 Ma.

Cramer et al. (2011)—Reconciled onshore New Jersey backstripped sea-level estimates with a different approach, using deep-sea benthic foraminiferal $\delta^{18}O$ and Mg/Ca records to extract changes in seawater $\delta^{18}O$ proportional to ice-volume and sea-level changes. Because of limitations in the data, this approach (as illustrated in Fig. 13.13) was restricted to periods longer than 2 Myr and showed similar changes from both methods. Ongoing studies use higher resolution $\delta^{18}O$ records to compare changes on the Myr scale (Miller et al., 2020).

13.5 Summary

Many challenges still exist to isolating the eustatic signal in the rock record. The basic interpretation of water depth changes or transgressive–regressive cycles in any given succession can be fraught with difficulties (Brett et al., 2011; Simmons, 2012), and eminent workers can come to differing conclusions on the interpretation of the same outcrop or well stratigraphy. If carried through multiple sections, there will inevitably be differing conclusions on the timing and magnitude of eustasy. Even assuming a consistent approach to the interpretation of changing RSL, demonstrating that the same changes can be seen in multiple sections on different paleocontinents, and are synchronous can be challenging, given the limitations of biostratigraphy and other correlation proxies (Miall, 1991, 1992, 2010). Nonetheless, stratigraphers have a variety of techniques at their disposal to develop an understanding of eustasy ranging from backstripping, to $\delta^{18}O$ (for the Cenozoic), to synthesis techniques evaluating multiple stratigraphic sections. High-resolution biostratigraphy, carbon, and strontium isotope studies and the identification of orbital forcing can provide a robust framework in which to correlate. As a consequence, knowledge of the timing, magnitude, and duration of eustasy is evolving, especially for short-term (10^5–10^6 years) cyclicity, which clearly relates to the orbital forcing of climate change.

Given the relatively high magnitudes (tens of meters) of short-term eustatic change (although not as great as suggested, e.g., by Haq et al., 1987, 1988 and Haq, 2014) and its occurrence on astronomical forcing time scales (Boulila et al., 2011), it seems likely that glacio-eustasy is the primary driver of eustasy throughout much of the Phanerozoic, even in "greenhouse" times, such as the Cretaceous (Ray et al., 2019). Aquifer-eustasy has a growing number of advocates (e.g., Sames et al., 2016) but cannot explain the higher magnitudes of eustatic change observed and the observed relationships between eustasy and climate (Davies et al., 2020). In support of the notion of the dominance of glacio-eustasy as a control on short-term sea-level changes is the growing body of direct, proxy, and circumstantial evidence that supports glaciation for parts of all periods of the Phanerozoic with the possible exception of the Triassic.

The magnitude and timing of long-term (10^7–10^8 years) eustasy was often qualitatively estimated by stratigraphic observations on the extent of continental flooding (e.g., Hallam, 1992). Progress on geodynamic modeling has enabled more quantitative approaches to be taken (e.g., Conrad, 2013; Vérard et al., 2015). Spreading ridge volume is a key factor driving long-term eustasy and this, alongside other geodynamic features, can be modeled, to derive a long-term eustatic curve (Fig. 13.9). However, the choice of plate model is key, and different plate models can derive quite different results. These different results pose some challenges when attempting to integrate long-term sea-level trends with local observations to isolate the true magnitude of short-term sea-level events.

Long-term trends can act to amplify or suppress short-term trends.

An understanding of eustasy is a powerful means of understanding the often incomplete nature of the sedimentary record. Knowledge of eustatic cyclicity is useful in determining the selection of chronostratigraphic reference sections (GSSPs) and provides a context for the evolution of the subdivisions of the geologic time scale. With this in mind, it is worth recalling that when d'Orbigny (1842) introduced the term *étage* (stage), he did so with a catastrophists' view of the Earth's history. Stages were "the expression of the boundaries which Nature has drawn with bold strokes across the globe." Stage boundaries occurred at horizons of faunal turnover, in turn caused by dramatic paleoenvironmental change. Such changes and major sea-level falls can easily be coincident (e.g., Gaskell, 1991). Thus the early definitions of stages often related to probable time gaps in proximal depositional settings caused by sea-level falls of significant magnitude and rate. We would no longer view such locations as optimal as reference sections for the boundaries of the subdivisions of the geologic time scale, preferring to place these in sections of continuous stratigraphy. These may include the distal equivalents of SBs observed in proximal settings (Simmons, 2012).

More broadly, an understanding of eustasy provides context for the subdivision of geologic time. Increasingly, the definition of stages is related to changes in the Earth system, of which eustasy is one component (e.g., Babcock et al., 2015). The biostratigraphic events that typically act as proxies for the definition of stage boundaries can be related to changes in paleoclimate, geodynamics, ocean chemistry, and eustasy.

The developments in the understanding of eustasy are not always well known within the broader geological community, as is evidenced by the continuing reference to older papers (e.g., Haq et al., 1987; Johnson et al., 1985) that have now been superseded, not only by work by their primary authors, but also by several other independent workers. Such a situation could be regarded as "chaos" (Ruban, 2016), or, more positively, as choice. The geologist interested in understanding eustasy within a given geologic period can evaluate several options and choose that which adopted a methodology they regard as robust. Moving forward, we hope that the subcommissions for each geologic period of the International Subcommission on Stratigraphy will drive the attempts to arrive at consensus view, using consistent and well-calibrated approaches.

Acknowledgments

Many of the ideas on eustasy described herein have been discussed and debated with colleagues at Neftex Petroleum Consultants (now part of Halliburton) over the last 20 years. Peter Sharland, Roger Davies, Dave Casey, and Peter Wells are thanked for driving this research in the early years. This paper is published with the permission of Halliburton to whom the authors are grateful for technical support. We thank numerous colleagues who participated in the generation of the "New Jersey sea-level curve" (especially M. Kominz, G. Mountain, P. Sugarman, and S. Pekar), the IODP paloceanographic community for their efforts in generating the $\delta^{18}O$ and Mg/Ca records, and B. Cramer for his Mg/Ca synthesis. Douwe van der Meer is thanked for his helpful comments. The contribution by Ken Miller is supported by NSF grant OCE1657013.

Bibliography

Abreu, V.S., and Anderson, J.B., 1998, Glacial eustasy during the Cenozoic: sequence stratigraphic implications. *The American Association of Petroleum Geologists Bulletin*, **82**: 1385–1400.

Ager, D.V., 1981, *The Nature of the Stratigraphic Record*, 2nd ed. John Wiley, New York, p. 122.

Ager, D.V., 1993, *The New Catastrophism: The Importance of the Rare Event in Geological History*. Cambridge University Press, Cambridge, p. 231.

Ajdanlijsky, G., Strasser, A., and Götz, A.E., 2019, Integrated bio- and cyclostratigraphy of Middle Triassic (Anisian) ramp deposits, NW Bulgaria. *Geologica Carpathica*, **70**: 325–354.

Algeo, T.J., and Seslavinsky, K.B., 1995, Reconstructing eustatic and epeirogenic trends from Paleozoic continental flooding records. *In* Haq, B.U. (ed), *Sequence Stratigraphy and Depositional Response to Eustatic, Tectonic and Climatic Forcing*. Springer, Dordrecht, pp. 209–246.

Al-Husseini, M., 2018, Arabian orbital sequences. *In* Montenari, M. (ed), *Stratigraphy and Timescales, Volume Three: Cyclostratigraphy and Astrochronology*. Elsevier, Amsterdam, pp. 219–264.

Allen, P.A., 2017, *Sediment Routing Systems*. Cambridge University Press, Cambridge, p. 407.

Alley, N.F., and Frakes, L.A., 2003, First known Cretaceous glaciation: Livingstone Tillite Member of the Cadna-owie Formation, South Australia. *Australian Journal of Earth Sciences*, **50**: 139–144.

Alley, N.F., Hore, S.B., and Frakes, L.A., 2019, Glaciations at high-latitude Southern Australia during the Early Cretaceous. *Australian Journal of Earth Sciences*, **2019**: 1–51.

Álvaro, J.J., Benziane, F., Thomas, R., Walsh, G.J., and Yazidi, A., 2014, Neoproterozoic–Cambrian stratigraphic framework of the Anti-Atlas and Ouzellagh promontory (High Atlas), Morocco. *Journal of African Earth Sciences*, **98**: 19–33.

Aretz, M., Herbig, H.G., and Wang, X.D., 2020, Chapter 23 – The Carboniferous Period. *In* Gradstein, F.M., Ogg, J.G., Schmitz, M.D., and Ogg, G.M. (eds), *The Geologic Time Scale 2020*. **Vol. 2** (this book). Elsevier, Boston, MA.

Arkell, W.J., 1933, *The Jurassic System in Great Britain*. Clarendon Press, Oxford, p. 681.

Armentrout, J.M., 1996. High resolution sequence biostratigraphy: examples from the Gulf of Mexico Plio-Pleistocene. *In* Howell, J.A., and Aitken, J.F. (eds). *High Resolution Sequence Stratigraphy: Innovations and Applications*. Geological Society, London, Special Publications, **104**: p. 65–86.

Armentrout, J.M., 2019, Tectonic events and eustatic cycle correlation: a review of biostratigraphic issues for depositional cycle chart construction and sequence dating. *In* Denne, R.A., and Kahn, A. (eds),

Geologic Problem Solving with Microfossils IV. SEPM Special Publication, **111**.

Babcock, L.E., Peng, S.-C., Brett, C.E., Zhu, M.-Y., Ahlberg, P., Bevis, M., et al., 2015, Global climate, sea-levels, and biotic events in the Cambrian Period. *Palaeoworld*, **24**: 5–15.

Banner, F.T., and Simmons, M.D., 1994, Calcareous algae and foraminifera as water-depth indicators: an example from the Early Cretaceous carbonates of northeast Arabia. *In* Simmons, M.D. (ed), *Micropalaeontology and Hydrocarbon Exploration in the Middle East*, British Micropalaeontological Society Publications Series: pp. 243–252.

Barrell, J., 1917, Rhythms and the measurement of geologic time. *Geological Society of America Bulletin*, **28**: 745–904.

Bartek, L.R., Vail, P.R., Anderson, J.B., Emmet, P.A., and Wu, S., 1991, Effect of Cenozoic ice sheet fluctuations in Antarctica on the stratigraphic signature of the Neogene. *Journal of Geophysical Research*, **96B**: 6753–6778.

Becker, R.T., Gradstein, F.M., and Hammer, O., 2012, The Devonian period. In Gradstein, F.M., Ogg, J.G., Schmitz, M.D., and Ogg, G.M. (eds), *The Geologic Time Scale 2012*, Elsevier, **2**: 559–602.

Becker, R.T., Marshall, J.E.A., and Da Silva, A.-C., 2020, Chapter 22 – The Devonian Period. *In* Gradstein, F.M., Ogg, J.G., Schmitz, M.D., and Ogg, G.M. (eds), *The Geologic Time Scale 2020*. **Vol. 2** (this book). Elsevier, Boston, MA.

Bergen, J.A., Truax III, S., de Kaenel, E., Blair, S., Browning, E., Lundquist, J., et al., 2019, BP Gulf of Mexico Neogene Astronomically-tuned Time Scale (BP GNATTS). *Geological Society of America Bulletin*, **131**: 1871–1888.

Bergström, S.M., Chen, X., Gutierrez-Marco, J.C., and Dronov, A., 2008, The new chronostratigraphic classification of the Ordovician system and its relations to major regional series and stages and to $\delta^{13}C$ chemostratigraphy. *Lethaia*, **42**: 97–107.

Billups, K., and Schrag, D.P., 2002, Paleotemperatures and ice volume of the past 27Myr revisited with paired Mg/Ca and $^{18}O/^{16}O$ measurements on benthic foraminifera. *Paleoceanography*, **17**: 1–3.

Bishop, J.W., Montañez, I.P., Gulbranson, E.L., and Brenckle, P.L., 2009, The onset of mid-Carboniferous glacio-eustasy: sedimentologic and diagenetic constraints, Arrow Canyon, Nevada. *Palaeogeography, Palaeoclimatology, Palaeoecology*, **276**: 217–243.

Blakey, R., 2008, Pennsylvanian – Jurassic sedimentary basins of the Colorado Plateau and Southern Rocky Mountains. *In* Miall, A.D. (ed), *The Phanerozoic Sedimentary Basins of the United States and Canada. Sedimentary Basins of the World*. Elsevier, **5**: 245–296.

Bond, G.C., 1979, Evidence for some uplifts of large magnitude in continental platforms. *Tectonophysics*, **61**: 285–305.

Bond, C.E., Gibbs, A.D., Shipton, Z.K., and Jones, S., 2007, What do you think this is? "Conceptual uncertainty" in geoscience interpretation. *GSA Today*, **17**: 4–11.

Boulila, S., 2008, *Cyclostratigraphie des séries sédimentaires du Jurassique supérieur (Sud-Est de la France, Nord de la Tunisie): contrôle astroclimatique, implications géochronologiques et séquentielles*. Ph.D. thesis. Pierre et Marie Curie University, Paris, France. p. 313.

Boulila, S., and Hinnov, L.A., 2017, A review of tempo and scale of the early Jurassic Toarcian OAE: implications for carbon cycle and sea level variations. *Newsletters on Stratigraphy*, **50**: 363–389.

Boulila, S., Galbrun, B., Hinnov, L.A., and Collin, P.-Y., 2008a, Orbital calibration of the Early Kimmeridgian (southeastern France): implications for geochronology and sequence stratigraphy. *Terra Nova*, **20**: 455–462.

Boulila, S., Galbrun, B., Hinnov, L.A., and Collin, P.Y., 2008b, High-resolution cyclostratigraphic analysis from magnetic susceptibility in a Lower Kimmeridgian (Upper Jurassic) marl-limestone succession (La Méouge, Vocontian Basin, France). *Sedimentary Geology*, **203**: 54–63.

Boulila, S., Hinnov, L.A., Huret, E., Collin, P.Y., Galbrun, B., Fortwengler, D., et al., 2008c, Astronomical calibration of the Early Oxfordian (Vocontian and Paris basins, France): consequences of revising the Late Jurassic time scale. *Earth and Planetary Science Letters*, **276**: 40–51.

Boulila, S., de Rafelis, M., Hinnov, L.A., Gardin, S., Galbrun, B., and Collin, P.-Y., 2010, Orbitally forced climate and sea-level changes in the paleoceanic Tethyan domain (marl-limestone alternations, Lower Kimmeridgian, SE France). *Palaeogeography, Palaeoclimatology, Palaeoecology*, **292**: 57–70.

Boulila, S., Galbrun, B., Miller, K.G., Pekar, S.F., Browning, J.V., Laskar, J., et al., 2011, On the origin of Cenozoic and Mesozoic "third-order" eustatic sequences. *Earth-Science Reviews*, **109**: 94–112.

Boulila, S., Galbrun, B., Huret, E., Hinnov, L.A., Rouget, I., Gardin, S., et al., 2014, Astronomical calibration of the Toarcian Stage: implications for sequence stratigraphy and duration of the early Toarcian OAE. *Earth and Planetary Science Letters*, **386**: 98–111.

Boulila, S., Laskar, J., Haq, B.U., Galbrun, B., and Hara, N., 2018, Long-term cyclicities in Phanerozoic sea-level sedimentary record and their potential drivers. *Global and Planetary Chang*, **165**: 128–136.

Bover-Arnal, T., Salas, R., Guimerà, J., and Moreno-Bedmar, J.A., 2014, Deep incision in an Aptian carbonate succession indicates major sea-level fall in the Cretaceous. *Sedimentology*, **61**: 1558–1593.

Bowman, V.C., Francis, J.E., and Riding, J.B., 2013, Late Cretaceous winter sea ice in Antarctica? *Geology*, **41**: 1227–1230.

Brett, C.E., Boucot, A.J., and Jones, B., 1993, Absolute depths of Silurian benthic assemblages. *Lethaia*, **26**: 25–40.

Brett, C.E., Ferretti, A., Histon, K., and Schönlaub, H.P., 2009, Silurian sequence stratigraphy of the Carnic Alps, Austria. *Palaeogeography, Palaeoclimatology, Palaeoecology*, **279**: 1–28.

Brett, C.E., Baird, G.C., Bartholomew, A.J., DeSantis, M.K., and Ver Straeten, C.A., 2011, Sequence stratigraphy and a revised sea-level curve for the Middle Devonian of eastern North America. *Palaeogeography, Palaeoclimatology, Palaeoecology*, **304**: 21–53.

Browning, J.V., Miller, K.G., Sugarman, P.J., Barron, J., McCarthy, F.M., Kulhanek, D.K., et al., 2013, Chronology of Eocene–Miocene sequences on the New Jersey shallow shelf: implications for regional, interregional, and global correlations. *Geosphere*, **9**: 1434–1456.

Burgess, P.M., 2008, Phanerozoic evolution of the sedimentary cover of the North American craton. *In* Miall, A.D. (ed), *The Sedimentary Basins of the United States and Canada*. Elsevier, 31–63.

Burgess, P.M., and Gurnis, M., 1995, Mechanisms for the formation of cratonic stratigraphic sequences. *Earth and Planetary Science Letters*, **136**: 647–663.

Burton, R., Kendall St. C., C.G., and Lerche, I., 1987, Out of our depth: on the impossibility of fathoming eustasy from the stratigraphic record. *Earth-Science Reviews*, **24**: 237–277.

Buso, V.V., Danielski Aquino, C., Gomes Paim, P.S., Alves de Souza, P., Mori, A.L., Fallgatter, C.F., et al. 2019. Late Palaeozoic glacial cycles and subcycles in western Gondwana: correlation of surface and subsurface data of the Paraná Basin, Brazil. Palaeogeography,

Palaeoclimatology, Palaeoecology, 531. Part B, article #108435: 16 pp. https://doi.org/10.1016/j.palaeo.2017.09.004.

Calner, M., 2008, Silurian global events – at the tipping point of climate change. *In* Elewa, A.M.T. (ed), *Mass Extinction*. Springer, Berlin, 21–57.

Caputo, M.V., 1998, Ordovician-Silurian glaciations and global sea-level changes. *In* Landing, E., and Johnson, M.E. (eds), *Silurian Cycles: Linkages of Dynamic Stratigraphy With Atmospheric, Oceanic, and Tectonic Changes*. New York State Museum Bulletin, **491**: 15–25.

Caputo, M.V., de Melo, J.H.G., Streel, M., and Isbell, J.L., 2008, Late Devonian and Early Carboniferous glacial records of South America. *In* Fielding, C.R., Frank, T.D., and Isbell, J.L. (eds), *Resolving the Late Paleozoic Ice Age in Time and Space*. Geological Society of America Special Paper 441. 161–173.

Carter, R.M., Abbott, S.T., Fulthorpe, C.S., Haywick, D.W., and Henderson, R.A., 1991, Application of global sea-level and sequence-stratigraphic models in Southern Hemisphere Neogene strata from New Zealand. *In* Macdonald, D.I.M. (ed), *Sedimentation, Tectonics, Eustasy: Sea-Level Changes Active Margins*. International Association of Sedimentologists Special Publication 12. 41–65.

Catuneanu, O., 2006, *Principles of Sequence Stratigraphy*. Elsevier, Amsterdam, p. 375.

Catuneanu, O., 2017, Sequence stratigraphy: guidelines for a standard methodology. *In* Montenari, M. (ed), *Stratigraphy and Timescales, Volume Two: Advances in Sequence Stratigraphy*. Elsevier, 1–58.

Catuneanu, O., 2019a, Model-independent sequence stratigraphy. *Earth-Science Reviews*, **188**: 312–388.

Catuneanu, O., 2019b, Scale in sequence stratigraphy. *Marine and Petroleum Geology*, **106**: 128–159.

Catuneanu, O., Abreu, V., Bhattacharya, J.P., Blum, M.D., Dalrymple, R.W., Eriksson, P.G., et al., 2009, Towards the standardization of sequence stratigraphy. *Earth-Science Reviews*, **92**: 1–33.

Chamberlin, T.C., 1899, An attempt to frame a working hypothesis on the cause of glacial periods on an atmospheric basis. *The Journal of Geology*, **7**: 545–584.

Chamberlin, T.C., 1909, Diastrophism as the ultimate basis for correlation. *The Journal of Geology*, **17**: 685–693.

Chen, J., Sheng, Q., Hu, K., Yao, L., Lin, W., Montañez, I.P., et al., 2019, Late Mississippian glacio-eustasy recorded in the eastern Paleo-Tethys Ocean (South China). *Palaeogeography, Palaeoclimatology, Palaeoecology*, **531**.

Cherns, L., Wheeley, J.R., Popov, L.E., Ghobadi Pour, M., Owens, R. M., and Hemsley, A.R., 2013, Long-period orbital climate forcing in the early Palaeozoic? *Journal of the Geological Society, London*, **170**: 707–710.

Christie-Blick, N., 1990, Sequence stratigraphy and sea-level changes in Cretaceous time. *In* Ginsburg, R.N., and Beaudoin, B. (eds), *Cretaceous Resources, Events and Rhythms Background and Plans for Research*. Kluwer, Dordrecht, 1–22.

Christie-Blick, N., and Driscoll, N.W., 1995, Sequence stratigraphy. *Annual Review of Earth and Planetary Sciences*, **23**: 451–478.

Christie-Blick, N., Mountain, G.S., and Miller, K.G., 1990, Seismic stratigraphy: record of sea-level change. *In* Revelle, R. (ed), *Sea-Level Change, National Research Council, Studies in Geophysics*. National Academy Press, 116–140.

Cloetingh, S., and Haq, B.U., 2015, Inherited landscapes and sea-level change. *Science*, **347**: 1258375.

Cloetingh, S., and Kooi, H., 1990, Intraplate stresses: a new perspective on QDS and Vail's third-order cycles. *In* Cross, T.A. (ed), *Quantitative Dynamic Stratigraphy*. Prentice-Hall, Englewood Cliffs, NJ, 127–148.

Cloetingh, S., McQueen, H., and Lambeck, K., 1985, On a tectonic mechanism for regional sea-level variations. *Earth and Planetary Science Letters*, **75**: 157–166.

Cloetingh, S., Burov, E., and Francois, T., 2013, Thermo-mechanical controls on intra-plate deformation and the role of plume-folding interactions in continental topography. *Gondwana Research*, **24**: 815–837.

Cogné, J.P., and Humler, E., 2006, Trends and rhythms in global seafloor generation rate. *Geochemistry, Geophysics, Geosystems*, **7**: 1–17.

Cogné, J.-P., Humler, E., and Courtillot, V., 2006, Mean age of oceanic lithosphere drives eustatic sea-level change since Pangea breakup. *Earth and Planetary Science Letters*, **245**: 115–122.

Conrad, C.P., 2013, The solid Earth's influence on sea-level. *Geological Society of America Bulletin*, **125**: 1027–1052.

Conrad, C.P., and Husson, L., 2009, Influence of dynamic topography on sea-level and its rate of change. *Lithosphere*, **1**: 110–120.

Cooper, R.A., and Sadler, P.M., 2012, The Ordovician period. *In* Gradstein, F.M., Ogg, J.G., Schmitz, M.D., and Ogg, G.M. (eds), *The Geologic Time Scale*. Elsevier, **2**: 489–524.

Cooper, R.A., Crampton, J.S., Raine, J.I., Gradstein, F.M., Morgans, H.E., Sadler, P.M., et al., 2001, Quantitative biostratigraphy of the Taranaki Basin, New Zealand: a deterministic and probabilistic approach. *The American Association of Petroleum Geologists Bulletin*, **85**: 1469–1498.

Cramer, B.S., Brett, C.E., Melchin, M.J., Männik, P., Kleffner, M.A., McLaughlin, P.I., et al., 2010a, Revised correlation of Silurian Provincial Series of North America with global and regional chronostratigraphic units and $\delta^{13}C_{carb}$ chemostratigraphy. *Lethaia*, **44**: 185–202.

Cramer, B.D., Loydell, D.K., Samtleben, C., Munnecke, A., Kaljo, D., Männik, P., et al., 2010b, Testing the limits of Paleozoic chronostratigraphic correlation via high-resolution (<500 ky) integrated conodont, graptolite, and carbon isotope ($\delta^{13}C_{carb}$) biochemostratigraphy across the Llandovery–Wenlock (Silurian) boundary: is a unified Phanerozoic time scale achievable? *Geological Society of America Bulletin*, **122**: 1700–1716.

Cramer, B.S., Miller, K.G., Barrett, P.J., and Wright, J.D., 2011, Late Cretaceous – Neogene trends in deep ocean temperature and continental ice volume: reconciling records of benthic foraminiferal geochemistry ($\delta^{18}O$ and Mg/Ca) with sea-level history. *Journal of Geophysical Research*, **116**: C12023.

Creveling, J.R., Finnegan, S., Mitrovica, J.X., and Bergmann, K.D., 2018, Spatial variation in Late Ordovician glacioeustatic sea-level change. *Earth and Planetary Science Letters*, **496**: 1–9.

Cuvier, G., and Brongniart, A., 1811, *Essai sur la géographie minéralogique des environs de Paris: avec une carte géognostique, et des coupes de terrain*. Baudouin, Paris.

d'Orbigny, A., 1842, *Paléontologie Francaise. Terrains crétacés, Céphalopodes*. Masson, Paris, p. 662.

Dabard, M.P., Loi, A., Paris, F., Ghienne, J.F., Pistis, M., and Vidal, M., 2015, Sea-level curve for the Middle to early Late Ordovician in the Armorican Massif (western France): icehouse third-order glacio-eustatic cycles. *Palaeogeography, Palaeoclimatology, Palaeoecology*, **436**: 96–111.

Davies, R.B., and Simmons, M.D., 2018, Triassic sequence stratigraphy of the Arabian Plate. *In* Pöppelreiter, M.C. (ed), *Lower Triassic to Middle Jurassic Sequence of the Arabian Plate*. EAGE (European Assoc. Geoscientists and Engineers), 101–162.

Davies, R.B., Casey, D.M., Horbury, A.D., Sharland, P.R., and Simmons, M.D., 2002, Early to mid-Cretaceous mixed carbonate-clastic shelfal systems: examples, issues and models from the Arabian Plate. *GeoArabia*, **7**: 541–598.

Davies, A., Kemp, A.E., and Pike, J., 2009, Late Cretaceous seasonal ocean variability from the Arctic. *Nature*, **460**: 254–258.

Davies, J.R., Waters, R.A., Molyneux, S.G., Williams, M., Zalasiewicz, J.A., and Vandenbroucke, T.R., 2016, Gauging the impact of glacioeustasy on a mid-latitude early Silurian basin margin, mid Wales, UK. *Earth-Science Reviews*, **156**: 82–107.

Davies, A., Hunter, S.J., Gréselle, B., Haywood, A.M., and Robson, C., 2019a, Evidence for seasonality in early Eocene high latitude sea-surface temperatures. *Earth and Planetary Science Letters*, **519**: 274–283.

Davies, R.B., Simmons, M.D., Jewell, T.O., and Wyton, J., 2019b, Regional controls on siliciclastic input into Mesozoic depositional systems of the Arabian Plate and their petroleum significance. *In* AlAnzi, H.R., Rahmani, R.A., Steel, R.J., and Soliman, O.M. (eds), *Siliciclastic Reservoirs of the Arabian Plate*. AAPG Memoir, **116**: 103–140.

Davies, A., Gréselle, B., Hunter, S.J., Baines, G., Robson, C., Haywood, A.M., et al., 2020, Assessing the impact of aquifer-eustasy on short-term Cretaceous sea-level. *Cretaceous Research*, **112**, article #104445: 12 pp. https://doi.org/10.1016/j.cretres.2020.104445.

Davydov, V.I., Crowley, J.L., Schmitz, M.D., and Poletaev, V.I., 2010, High-precision U-Pb zircon age calibration of the global Carboniferous time scale and Milankovitch band cyclicity in the Donets Basin, eastern Ukraine. *Geochemistry, Geophysics, Geosystems*, **11**: Q0AA04.

De Graciansky, P.C., Hardenbol, J., Jacquin, T., and Vail, P.R. (eds), 1998, *Mesozoic and Cenozoic Sequence Stratigraphy of European Basins*. SEPM Special Publication, **60**: 786pp.

De Vleeschouwer, D., Da Silva, A.C., Sinnesael, M., Chen, D., Day, J.E., Whalen, M.T., et al., 2017. Timing and pacing of the Late Devonian mass extinction event regulated by eccentricity and obliquity. *Nature Communications*, **8**: article #2268. https://doi.org/10.1038/s41467-017-02407-1.

Dechamps, P., Durand, N., Bard, E., Hamelin, B., Camoin, G., Thomas, A.L., et al., 2012, Ice-sheet collapse and sea-level rise at the Bølling warming 14,600 years ago. *Nature*, **483**: 559–564.

Dewey, J.F., and Pitman, W.C., 1998, Sea-level changes: mechanisms, magnitudes and rates. *In* Pindell, J.L., and Drake, C.L. (eds), *Paleogeographic Evolution and Non-glacial Eustasy, Northern South America*. SEPM Special Publication, **58**: 1–16.

Diaz-Martinez, E., and Grahn, Y., 2007, Early Silurian glaciation along the western margin of Gondwana (Peru, Bolivia and Northern Argentina): Palaeogeographic and geodynamic setting. *Palaeogeography, Palaeoclimatology, Palaeoecology*, **245** (1), 62–81.

Dickinson, W.R., Soreghan, G.S., and Giles, K.A., 1994, Glacio-eustatic origin of Permo-Carboniferous stratigraphic cycles: evidence from the southern Cordilleran foreland region. *In* Dennison, J.M., and Ettensohn, F.R. (eds), *Tectonic and Eustatic Controls on Sedimentary Cycles, Society of Sedimentary Geology, Concepts in Sedimentology and Palaeontology*. **4**: 25–34.

Dietrich, P., Ghienne, J.-F., Lajeunesse, P., Deschamps, R., and Razin, P., 2018. Deglacial sequences and Glacio-Isostatic adjustment: Quaternary compared with Ordovician glaciations. *In* Le Heron, D.P., Hogan, K.A., Phillips, E.R., Huuse, M., Busfield, M.E., and Graham, A.G.C. (eds.). *Glaciated Margins: The Sedimentary and Geophysical Archive*. Geological Society, London, Special Publications, **475**: 149–179.

Donnadieu, Y., Dromart, G., Goddéris, Y., Pucéat, E., Brigaud, B., Dera, G., et al., 2011, A mechanism for brief glacial episodes in the Mesozoic greenhouse. *Paleoceanography*, **26**: PA3212.

Donovan, A.D., Ratcliffe, K., and Zaitlin, B.A., 2010, The sequence stratigraphy family tree: understanding the portfolio of sequence methodologies, Special Publication. *In* Ratcliff, K.T., and Zaitlin, B.A. (eds), *Application of Modern Stratigraphic Techniques: Theory and Case Histories*. SEPM, **94**: 5–33.

Dromart, G., Garcia, J.-P., Picard, S., Atrops, F., Lecuyer, C., and Sheppard, S.M.F., 2003, Ice age at the Middle-Late Jurassic transition? *Earth and Planetary Science Letters*, **213**: 205–220.

Dronov, A., 2017, Ordovician sequence stratigraphy of the Siberian and Russian platforms. *In* Montenari, M. (ed), *Stratigraphy and Timescales, Volume 2: Advances in Sequence Stratigraphy*. Elsevier, 187–241.

Dronov, A.V., Ainsaar, L., Kaljo, D., Meidla, T., Saadre, T., and Einasto, R., 2011, Ordovician of Baltoscandia: facies, sequences and sea-level changes. *In* Gutiérrez-Marco, J.C., Rábano, I., and García-Bellido, D. (eds), *Ordovician of the World, Cuadernos del Museo Geominero*. Instituto Geologico y Minero de España, Madrid, 143–150.

Drummond, C.N., and Wilkinson, B.H., 1996, Stratal thickness frequencies and the prevalence of orderdness in stratigraphic sequences. *The Journal of Geology*, **104**: 1–18.

Dujoncquoy, E., Grélaud, C., Razin, P., Imbert, P., van Buchem, F., Dupont, G., et al., 2018, Seismic stratigraphy of a Lower Cretaceous prograding carbonate platform (Oman) and implications for the eustatic sea-level curve. *The American Association of Petroleum Geologists Bulletin*, **102**: 509–543.

Edwards, L.E., 1989, Supplemented graphic correlation: a powerful tool for paleontologists and nonpaleontologists. *Palaois*, **4**: 127–143.

Ehrenberg, S.N., Pickard, N.A.H., Laursen, G.V., Monibi, S., Mossadegh, Z.K., Svånå, T.A., et al., 2007, Strontium isotope stratigraphy of the Asmari Formation (Oligocene-Lower Miocene), SW Iran. *Journal of Petroelum Geology*, **30**: 107–128.

Einsele, G., Ricken, W., and Seilacher, A., 1991, Cycles and events in stratigraphy – basic concepts and terms. *In* Einsele, G., Ricken, W., and Seilacher, A. (eds), *Cycles and Events in Stratigraphy*. Springer-Verlag, 1–19.

Elrick, M., Berkyová, S., Klapper, G., Sharp, Z., Joachimski, M., and Fryda, J., 2009, Stratigraphic and oxygen isotope evidence for My-scale glaciation driving eustasy in the Early-Middle Devonian greenhouse world. *Palaeogeography, Palaeoclimatology, Palaeoecology*, **276**: 170–181.

Elrick, M., and Scott, L.A., 2010, Carbon and oxygen isotope evidence for high-frequency (104–105 yr) and My-scale glacio-eustasy in Middle Pennsylvanian cyclic carbonates (Gray Mesa Formation), central New Mexico. *Palaeogeography, Palaeoclimatology, Palaeoecology*, **285**: 307–320.

Elrick, M., and Witzke, B., 2016, Orbital-scale glacio-eustasy in the Middle Devonian detected using oxygen isotopes of conodont apatite: implications for long-term greenhouse – icehouse climatic

transitions. *Palaeogeography, Palaeoclimatology, Palaeoecology*, **445**: 50–59.

Embry, A.F., 1988, Triassic sea level changes: Evidence from the Canadian Arctic Archipelago. Sea-level changes: an integrated approach. *In* Wilgus, C.K., Hastings, B.S., Kendall St., C.G., and Posamentier, H.W. (eds), *Sea-level Changes: An Integrated Approach*. SEPM Special Publication, **42**: 249–259.

Embry, A.F., 1997, Global sequence boundaries of the Triassic and their identification in the Western Canadian Sedimentary Basin. *Bulletin of Canadian Petroleum Geology*, **45**: 415–433.

Emery, K.O., and Aubrey, D.G., 1991, Impact of sea-level/land-level change on society. *Sea-Levels, Land Levels, and Tide Gauges*. Springer, 167–174.

Emiliani, C., 1955, Pleistocene temperatures. *The Journal of Geology*, **63**: 538–578.

Eros, J.M., Montañez, I.P., Osleger, D.A., Davydov, V.I., Nemyrovska, T.I., Poletaev, V.I., et al., 2012a, Sequence stratigraphy and onlap history of the Donets Basin, Ukraine: insight into Carboniferous icehouse dynamics. *Palaeogeography, Palaeoclimatology, Palaeoecology*, **313**: 1–25.

Eros, J.M., Montañez, I.P., Davydov, V.I., Osleger, D.A., Nemyrovska, T.I., Poletaev, V.I., et al., 2012b, Reply to the comment on "Sequence stratigraphy and onlap history of the Donets Basin, Ukraine: insight into Carboniferous icehouse dynamics". *Palaeogeography, Palaeoclimatology, Palaeoecology*, **363**: 187–191.

Fairbanks, R.G., 1989, A 17,000-year glacio-eustatic sea level record: influence of glacial melting rates on the Younger Dryas event and deep-ocean circulation. *Nature*, **342**: 637.

Falcon-Lang, H.J., Heckel, P.H., Dimichele, W.A., Blake Jr., B.M., Easterday, C.R., Eble, C.F., et al., 2011, No major stratigraphic gap exists near the middle-upper Pennsylvanian (Desmoinesian-Missourian) Boundary in North America. *Palaios*, **26**: 125–139.

Fang, Q., Wu, H., Hinnov, L.A., Jing, X., Wang, X., and Jiang, Q., 2015, Geologic evidence for chaotic behaviour of the planets and its constraints on the third-order eustatic sequences at the end of the Late Paleozoic Ice Age. *Palaeogeography, Palaeoclimatology, Palaeoecology*, **440**: 848–859.

Fielding, C.R., Frank, T.D., and Isbell, J.L., 2008, The late Paleozoic ice age—a review of current understanding and synthesis of global climate patterns. *Geological Society of America Special Papers*, **441**: 343–354.

Finnegan, S., Bergmann, K., Eiler, J.M., Jones, D.S., Fike, D.A., Eisenman, I., et al., 2011, The magnitude and duration of Late Ordovician–Early Silurian glaciation. *Science*, **331**: 903–906.

Föllmi, K.B., 2012, Early Cretaceous life, climate and anoxia. *Cretaceous Research*, **35**: 230–257.

Franz, M., Nowak, K., Berner, U., Heunisch, C., Bandel, K., Röhling, H.G., et al., 2014, Eustatic control on epicontinental basins: the example of the Stuttgart Formation in the Central European Basin (Middle Keuper, Late Triassic). *Global and Planetary Chang*, **122**: 305–329.

Fretwell, P., Pritchard, H.D., Vaughan, D.G., Bamber, J.L., Barrand, N. E., Bell, R., et al., 2013, Bedmap2: improved ice bed, surface and thickness datasets for Antarctica. *Cryosphere*, **7**: 375–393.

Gale, A.S., Hardenbol, J., Hathway, B., Kennedy, W.J., Young, J.R., and Phansalkar, V., 2002, Global correlation of Cenomanian (Upper Cretaceous) sequences: evidence for Milankovitch control on sea-level. *Geology*, **30**: 291–294.

Gale, A.S., Voigt, S., Sageman, B.B., and Kennedy, W.J., 2008, Eustatic sea-level record for the Cenomanian (Late Cretaceous)—extension to the Western Interior Basin, USA. *Geology*, **36**: 859–862.

Galloway, W.E., 1989, Genetic stratigraphic sequences in basin analysis, I. Architecture and genesis of flooding-surface bounded depositional units. *American Association of Petroleum Geologists Bulletin*, **73**: 125–142.

Galeotti, S., Rusciadelli, G., Sprovieri, M., Lanci, L., Gaudio, A., and Pekar, S., 2009, Sea-level control on facies architecture in the Cenomanian–Coniacian Apulian margin (Western Tethys): a record of glacio-eustatic fluctuations during the Cretaceous greenhouse? *Palaeogeography, Palaeoclimatology, Palaeoecology*, **276**: 196–205.

Gaskell, B.A., 1991, Extinction patterns in Paleogene benthic foraminiferal faunas: relationship to climate and sea level. *Palaois*, **6**: 2–16.

Gasson, E., Siddall, M., Lunt, D.J., Rackham, O.J., Lear, C.H., and Pollard, D., 2012, Exploring uncertainties in the relationship between temperature, ice volume, and sea-level over the past 50 million years. *Reviews of Geophysics*, **50**: RG1005.

Ghienne, J.F., 2011, The Late Ordovician glacial record: state of the art. Ordovician of the World. *Cuadernos del Museo Geominero*, **14**: 13–19.

Ghienne, J.F., Desrochers, A., Vandenbroucke, T.R., Achab, A., Asselin, E., Dabard, M.P., et al., 2014, A Cenozoic-style scenario for the end-Ordovician glaciation. *Nature Communications*, **5**: 4485.

Gianolla, P., and Jacquin, T., 1998, Triassic sequence stratigraphic framework of western European basins, Special Publication. *In* de Graciansky, P.-C., Hardenbol, J., Jacquin, T., and Vail, P.R. (eds), *Mesozoic and Cenozoic Sequence Stratigraphy of European Basins*. SEPM, **60**: 719–747.

Giles, P.S., 2009, Orbital forcing and Mississippian sea-level change: time series analysis of marine flooding events in the Visean Windsor Group of eastern Canada and implications for Gondwana glaciation. *Bulletin of Canadian Petroleum Geology*, **57**: 449–471.

Golonka, J., 2007, Phanerozoic paleoenvironment and paleolithofacies maps: Mesozoic. *Geologia*, **33**: 211–264.

Gordon, R.G., and Jurdy, D.M., 1986, Cenozoic global plate motions. *Journal of Geophysical Research*, **91**: 12389–12406.

Grabau, A.W., 1936a, Revised classification of the Paleozoic System in the light of the pulsation theory. *Geological Survey of China Bulletin*, **15**: 23–51.

Grabau, A.W., 1936b, Oscillation or pulsation. *International Geological Congress*, **1**: 539–553.

Grabau, A.W., 1940, *The Rhythm of the Ages*. Henri Vetch, Peking, p. 561.

Gradstein, F.M., Ogg, J.G., Schmitz, M.D., and Ogg, G.M. (eds), 2012. *The Geologic Time Scale*. **Vols. 1 and 2**. p. 1144.

Grahn, Y., and Caputo, M.V., 1992, Early Silurian glaciations in Brazil. *Palaeogeography, Palaeoclimatology, Palaeoecology*, **99**: 9–15.

Grasby, S.E., McCune, G.E., Beauchamp, B., and Galloway, J.M., 2017, Lower Cretaceous cold snaps led to widespread glendonite occurrences in the Sverdrup Basin, Canadian High Arctic. *Geological Society of America Bulletin*, **129**: 771–787.

Gregory, J.M., Griffies, S.M., Hughes, C.W., Lowe, J.A., Church, J.A., Fukimori, I., et al., 2019, Concepts and terminology for sea level: mean, variability and change, both local and global. *Surveys in Geophysics*, **2019**: 1–39.

Gréselle, B., and Pittet, B., 2010, Sea-level reconstructions from the Peri-Vocontian Zone (South-east France) point to Valanginian glacio-eustasy. *Sedimentology*, **57**: 1640–1684.

Grossman, E.L., 2012, Oxygen isotope stratigraphy. *In* Gradstein, F.M., Ogg, J.G., Schmitz, M.D., and Ogg, G.M. (eds), *The Geologic Time Scale 2012*. Elsevier, **1**: 181–206.

Guillaume, B., Pochat, S., Monteux, J., Husson, L., and Choblet, G., 2016, Can eustatic charts go beyond first order? Insights from the Permian–Triassic. *Lithosphere*, **8**: 505–518.

Guillocheau, F., 1995, Nature, rank and origin of Phanerozoic sedimentary cycles. *Comptes rendus de l'Académie des Sciences Paris*, **320**: 1141–1157.

Gulick, S.P.S., Shevenell, A.E., Montelli, A., Fernandez, R., Smith, C., Warny, S., et al., 2017, Initiation and long-term instability of the East Antarctic Ice Sheet. *Nature*, **552**: 225–229.

Hall, R., 2002, Cenozoic geological and plate mode evolution of SE Asia and the SW Pacific: computer-based reconstructions, model and animations. *Journal of Asian Earth Sciences*, **20**: 353–434.

Hallam, A., 1963, Major epeirogenic and eustatic changes since the Cretaceous and their possible relationship to crustal structure. *American Journal of Science*, **261**: 397–423.

Hallam, A., 1992, *Phanerozoic Sea-Level Changes*. Columbia University Press, p. 224.

Hallam, A., 2001, A review of the broad pattern of Jurassic sea-level changes and their possible causes in the light of current knowledge. *Palaeogeography, Palaeoclimatology, Palaeoecology*, **167**: 23–37.

Hambrey, M.J., 1985, The Late Ordovician—Early Silurian glacial period. *Palaeogeography, Palaeoclimatology, Palaeoecology*, **51**: 273–289.

Haq, B.U., 2014, Cretaceous eustasy revisited. *Global and Planetary Chang*, **113**: 44–58.

Haq, B.U., 2017, Jurassic sea-level variations: a reappraisal. *GSA Today*, **28**: 4–10.

Haq, B.U., 2018, Triassic eustatic variations reexamined. *GSA Today*, **28**: 4–9.

Haq, B.U., and Al-Qahtani, A.M., 2005, Phanerozoic cycles of sea-level change on the Arabian Platform. *GeoArabia*, **10**: 127–160.

Haq, B.U., and Huber, B.T., 2017, Anatomy of a eustatic event during the Turonian (Late Cretaceous) hot greenhouse climate. *Science China Earth Sciences*, **60**: 20–29.

Haq, B.U., and Schutter, S.R., 2008, A chronology of Paleozoic sea-level changes. *Science*, **322**: 64–68.

Haq, B.U., Hardenbol, J., and Vail, P.R., 1987, Chronology of fluctuating sea levels since the Triassic (250 million years ago to present). *Science*, **235**: 1156–1167.

Haq, B.U., Hardenbol, J., and Vail, P.R., 1988, Mesozoic and Cenozoic chronostratigraphy and eustatic cycles, Special Publication. *In* Wilgus, C.K., Ross, C.A., and Posamentier, H. (eds), *Sea-level Changes: An Integrated Approach*. SEPM, **42**: 71–108.

Hardenbol, J., Thierry, J., Farley, M.B., Jacquin, T., de Graciansky, P.C., and Vail, P.R., 1998, Mesozoic and Cenozoic sequence chronostratigraphic framework of European basins. *In* de Graciansky, P.C., Hardenbol, J., Jacquin, T., and Vail, P.R. (eds), *Mesozoic and Cenozoic Sequence Stratigraphy of European Basins*. SEPM Special Publication 60. 3–13.

Harrison, C.G.A., 1990, Long-term eustasy and epeirogeny in continents. *In* Revelle, R. (ed), *Sea-Level Change, National Research Council, Studies in Geophysics*. National Academy Press, 141–158.

Hay, W.W., 2008, Evolving ideas about the Cretaceous climate and ocean circulation. *Cretaceous Research*, **29**: 725–753.

Hay, W.W., and Leslie, M.A., 1990, Could possible changes in global groundwater reservoir cause eustatic sea-level fluctuations? *In* Revelle, R. (ed), *Sea-Level Change, National Research Council, Studies in Geophysics*. National Academy Press, 161–170.

Hay, C.C., Morrow, E., Kopp, R.E., and Mitrovica, J.X., 2015, Probabilistic reanalysis of twentieth-century sea-level rise. *Nature*, **517**: 481.

Heckel, P.H., 1986, Sea-level curve for Pennsylvanian eustatic marine transgressive-regressive depositional cycles along midcontinent outcrop belt, North America. *Geology*, **14**: 330–334.

Heckel, P.H., 1990, Evidence for global (glacio-eustatic) control over Upper Carboniferous (Pennsylvanian) cyclothems in midcontinent North America, Special Publication. *In* Hardman, R.F.P., and Brooks, J. (eds), *Tectonic Events Responsible for Britain's Oil and Gas Reserves*. Geological Society, London, **55**: 35–47.

Heckel, P.H., 2008, Pennsylvanian cyclothems in Midcontinent North America as far-field effects of waxing and waning of Gondwana ice sheets, Special Paper. *In* Fielding, C.R., Frank, T.D., and Isbell, J.L. (eds), *Resolving the Late Paleozoic Ice Age in Time and Space. Geological Society of America*, **441**: 275–289.

Heller, P.L., Anderson, D.L., and Angevine, C.L., 1996, Is the middle Cretaceous pulse of rapid sea-floor spreading real or necessary? *Geology*, **24**: 491–494.

Herrle, J.O., Schröder-Adams, C.J., Davis, W., Pugh, A.T., Galloway, J.M., and Fath, J., 2015, Mid-Cretaceous High Arctic stratigraphy, climate, and oceanic anoxic events. *Geology*, **43**: 403–406.

Hesselbo, S.P., 2008, Sequence stratigraphy and inferred relative sea-level change from the onshore British Jurassic. *The Proceedings of the Geologists' Association*, **119**: 19–34.

Hesselbo, S.P., and Jenkyns, H.C., 1998, British Lower Jurassic sequence stratigraphy, Special Publication. *In* De Graciansky, P.C., Hardenbol, J., Jacquin, T., and Vail, P.R. (eds), *Mesozoic and Cenozoic Sequence Stratigraphy of European Basins*. SEPM, **60**: 561–581.

Hinnov, L.A., 2000, New perspectives on orbitally forced stratigraphy. *Annual Review of Earth and Planetary Sciences*, **28**: 419–475.

Hinnov, L.A., 2018, Cyclostratigraphy and Astrochronology in 2018. *In* Montenari, M. (ed), *Stratigraphy and Timescales, Volume Three: Cyclostratigraphy and Astrochronology*. Elsevier, 1–80.

Hoedemaeker, P.J., 1995, Ammonite evidence for long-term sea-level fluctuations between the 2nd and 3rd order in the lowest Cretaceous. *Cretaceous Research*, **16**: 231–241.

Hohenegger, J., Ćorić, S., and Wagreich, M., 2014, Timing of the middle Miocene Badenian stage of the central Paratethys. *Geologica Carpathica*, **65**: 55–66.

Holland, S.M., and Patzkowsky, M.E., 1998, Sequence stratigraphy and relative sea-level history of the Middle and Upper Ordovician of the Nashville Dome, Tennessee. *Journal of Sedimentary Research*, **68**: 684–699.

Hollis, C.J., Dunkley Jones, T., Anagnostou, E., Bijl, P.K., Cramwinckel, M. J., Cui, Y., et al., 2019, The DeepMIP contribution to PMIP4: methodologies for selection, compilation and analysis of latest Paleocene and early Eocene climate proxy data, incorporating version 0.1 of the DeepMIP database. *Geoscientific Model Development Discussions*, **2019**: 1–98.

Hong, S.K., and Lee, Y.I., 2012, Evaluation of atmospheric carbon dioxide concentrations during the Cretaceous. *Earth and Planetary Science Letters*, **327**: 23–28.

Horbury, A., 2018, Petroleum geology and its relation to stratigraphic architecture of the Triassic to Middle Jurassic (Induan to Aalenian) interval on the Arabian Plate. *In* Pöppelreiter, M.C. (ed), *Lower Triassic to Middle Jurassic Sequence of the Arabian Plate*. EAGE (European Association of Geoscientists and Engineers), 49–100.

Hore, S.B., Reid, A.J., and Hill, S.M., 2015, Definition and age of the enigmatic Sprigg Diamictite Member, northern Flinders Ranges, South Australia. *MESA Journal*, **77**: 42–54.

Horner, S.C., Hubbard, S.M., Martin, H.K., Hagstrom, C.A., and Leckie, D.A., 2019, The impact of Aptian glacio-eustasy on the stratigraphic architecture of the Athabasca Oil Sands, Alberta, Canada. *Sedimentology*, **66**: 1600–1642.

Horton, D.E., and Poulsen, C.J., 2009, Paradox of late Paleozoic glacioeustasy. *Geology*, **37**: 715–718.

House, M.R., 1983, Devonian eustatic events. *Proceedings of the Ussher Society*, **5**: 396–405.

House, M.R., and Ziegler, W., 1997, Devonian eustatic fluctuation in North Eurasia. *Courier Forschungsinstitut Senckenberg*, **199**: 13–23.

Hu, X., Wagreich, M., and Yilmaz, I.O., 2012, Marine rapid environmental/climatic change in the Cretaceous greenhouse world. *Cretaceous Research*, **38**: 1–6.

Huang, C., Hesselbo, S.P., and Hinnov, L., 2010, Astrochronology of the Late Jurassic Kimmeridge Clay (Dorset, England) and implications for Earth system processes. *Earth and Planetary Science Letters*, **289**: 242–255.

Husinec, A., Harman, C.A., Regan, S.P., Mosher, D.A., Sweeney, R.J., and Read, J.F., 2012, Sequence development influenced by intermittent cooling events in the Cretaceous Aptian greenhouse, Adriatic platform, Croatia. *The American Association of Petroleum Geologists Bulletin*, **96**: 2215–2244.

Immenhauser, A., 2005, High-rate sea-level change during the Mesozoic: new approaches to an old problem. *Sedimentary Geology*, **175**: 277–296.

Immenhauser, A., 2009, Estimating palaeo-water depth from the physical rock record. *Earth-Science Reviews*, **96**: 107–139.

Immenhauser, A., and Matthews, R.K., 2004, Albian sea-level cycles in Oman: the "Rosetta Stone" approach. *GeoArabia*, **9**: 11–46.

Isaacson, P.E., Diaz-Martinez, E., Grader, G.W., Kalvoda, J., Babek, O., and Devuyst, F.X., 2008, Late Devonian–earliest Mississippian glaciation in Gondwanaland and its biogeographic consequences. *Palaeogeography, Palaeoclimatology, Palaeoecology*, **268**: 126–142.

Isbell, J.L., Miller, M.F., Wolfe, K.L., and Lenaker, P.A., 2003, Timing of late Paleozoic glaciation in Gondwana: was glaciation responsible for the development of Northern Hemisphere cyclothems? *Geological Society of America Special Paper*, **370**: 5–24.

Izart, A., Stephenson, R., Vai, G.B., Vachard, D., Le Nindre, Y., Vaslet, D., et al., 2003, Sequence stratigraphy and correlation of late Carboniferous and Permian in the CIS, Europe, Tethyan area, North Africa, Arabia, China, Gondwanaland and the USA. *Palaeogeography, Palaeoclimatology, Palaeoecology*, **196**: 59–84.

Jacobs, D.K., and Sahagian, D.L., 1993, Climate-induced fluctuations in sea-level during non-glacial times. *Nature*, **361**: 710.

Jacquin, T., Dardeau, G., Durlet, C., de Graciansky, P.C., and Hantzpergue, P., 1998, The North Sea cycle: an overview of 2nd-order transgressive/regressive facies cycles in Western Europe, Special Publication. *In* De Graciansky, P.C., Hardenbol, J., Jacquin, T., and Vail, P.R. (eds), *Mesozoic and Cenozoic Sequence Stratigraphy of European Basins*. SEPM, **60**: 445–446.

Jarvis, I.A.N., Gale, A.S., Jenkyns, H.C., and Pearce, M.A., 2006, Secular variation in Late Cretaceous carbon isotopes: a new $\delta^{13}C$ carbonate reference curve for the Cenomanian–Campanian (99.6–70.6 Ma). *Geological Magazine*, **143**: 561–608.

Jenkyns, H.C., Forster, A., Schouten, S., and Sinninghe Damsté, J.S., 2004, High temperatures in the late Cretaceous Arctic Ocean. *Nature*, **432**: 888.

Jenkyns, H.C., Schouten-Huibers, L., Schouten, S., and Sinninghe Damsté, J.S., 2012, Warm Middle Jurassic–Early Cretaceous high-latitude sea-surface temperatures from the Southern Ocean. *Climate of the Past*, **8**: 215–226.

Jervey, M.T., 1988, Quantitative geological modelling of siliciclastic rock sequences and their seismic expression. *In* Wilgus, C.K., Hastings, B.S., Kendall, C.G. St. C., Posamentier, H.W., Ross, C.A., and Van Wagoner, J.C. (eds), *Sea level Changes – an Integrated Approach. SEPM Special Publication*, **42**: 47–69.

Jin, Y., Shen, S., Henderson, C.M., Wang, X., Wang, W., Wang, Y., et al., 2006, The Global Stratotype Section and Point (GSSP) for the boundary between the Capitanian and Wuchiapingian stage (Permian). *Episodes*, **29**: 253–262.

John, C.M., Karner, G.D., and Mutti, M., 2004, $\delta^{18}O$ and Marion Plateau backstripping: combining two approaches to constrain late middle Miocene eustatic amplitude. *Geology*, **32**: 829–832.

John, C.M., Karner, G.D., Browning, E., Leckie, R.M., Mateo, Z., Carson, B., et al., 2011, Timing and magnitude of Miocene eustasy derived from the mixed siliciclastic-carbonate stratigraphic record of the northeastern Australian margin. *Earth and Planetary Science Letters*, **304**: 455–467.

Johnson, M.E., 1992, A.W. Grabau's embryonic sequence stratigraphy and eustatic curve. *In* Dott Jr., R.H. (ed), *Eustasy: The Ups and Downs of a Major Geological Concept. Geological Society of America Memoir*, **180**: 43–54.

Johnson, M.E., 2006, Relationship of Silurian sea-level fluctuations to oceanic episodes and events. *GFF*, **128**: 115–121.

Johnson, M.E., 2010, Tracking Silurian eustasy: alignment of empirical evidence or pursuit of deductive reasoning? *Palaeogeography, Palaeoclimatology, Palaeoecology*, **296**: 276–284.

Johnson, J.G., Klapper, G., and Sandberg, C.A., 1985, Devonian eustatic fluctuations in Euramerica. *Geological Society of America Bulletin*, **96**: 567–587.

Johnson, M.E., Kaljo, D.L., and Jiayu, R., 1991, Silurian eustasy. *Special Papers in Palaeontology*, **44**: 145–163.

Johnson, J.G., Klapper, G., and Elrick, M., 1996, Devonian transgressive-regressive cycles and biostratigraphy, northern Antelope Range, Nevada: establishment of reference horizons for global cycles. *Palaois*, **11**: 3–14.

Johnson, M.E., Rong, J.Y., and Kershaw, S., 1998, Calibrating Silurian eustasy against the erosion and burial of coastal paleotopography. *In* Landing, E., and Johnson, M.E. (eds), *Silurian Cycles: Linkages of Dynamic Stratigraphy With Atmospheric, Oceanic and Tectonic Changes. New York State Museum Bulletin*, **491**: 3–13.

Karlsen, K.S., Conrad, C.P., and Magni, V., 2019, Deep water cycling and sea-level change since the breakup of Pangea. *Geochemistry, Geophysics, Geosystems*, **20**: 2919–2935.

Katz, M.E., Browning, J.V., Miller, K.G., Monteverde, D.H., Mountain, G.S., and Williams, R.H., 2013, Paleobathymetry and sequence stratigraphic interpretations from benthic foraminifera: insights on New Jersey shelf architecture *Geosphere*, **9**: 1488–1513.

Kemp, D.B., Robinson, S.A., Crame, J.A., Francis, J.E., Ineson, J., Whittle, R.J., et al., 2014, A cool temperate climate on the Antarctic Peninsula through the latest Cretaceous to early Paleogene. *Geology*, **42**: 583–586.

Kent, D.V., Olsen, P., Rasmussen, C., Lepre, C., Mundil, R., Irmis, R., et al., 2018, Empirical evidence for stability of the 405 kyr Jupiter-Venus eccentricity cycle over hundreds of millions of years. *Proceedings of the National Academy of Science*, **115** (24): 6153–6158.

Kirschner, J.P., Kominz, M.A., and Mwakanyamale, K.E., 2010, Quantifying extension of passive margins: implications for sea-level change. *Tectonics*, **29**: TC4006.

Koch, J.T., and Brenner, R.L., 2009, Evidence for glacioeustatic control of large, rapid sea-level fluctuations during the Albian-Cenomanian: Dakota formation, eastern margin of western interior seaway, USA. *Cretaceous Research*, **30**: 411–423.

Kominz, M.A., Van Sickel, W.A., Miller, K.G., and Browning, J.V., 2003. Sea-level estimates for the latest 100 million years: one-dimensional backstripping of onshore New Jersey boreholes. *In* Armentrout, J. (ed), Sequence Stratigraphic models for Exploration and Production: Evolving Methodology, Emerging Models, and Application Histories. *Proceedings of the 22nd Annual GCSSEPM Foundation Bob F. Perkins Research Conference, 2002, Houston, 303–315.*

Kominz, M.A., Browning, J.V., Miller, K.G., Sugarman, P.J., Mizintseva, S., and Scotese, C.R., 2008, Late Cretaceous to Miocene sea-level estimates from the New Jersey and Delaware coastal plain coreholes: an error analysis. *Basin Research*, **20**: 211–226.

Kominz, M.A., Miller, K.G., Browning, J.V., Katz, M.E., and Mountain, G.S., 2016, Miocene relative sea-level on the New Jersey shallow continental shelf and coastal plain derived from one-dimensional backstripping: a case for both eustasy and epeirogeny. *Geosphere*, **12**: 1437–1456.

Korte, C., and Hesselbo, S.P., 2011, Shallow-marine carbon-and oxygen-isotope and elemental records indicate icehouse-greenhouse cycles during the Early Jurassic. *Paleoceanography*, **26**: PA4219.

Korte, C., Hesselbo, S.P., Ullmann, C.V., Dietl, G., Ruhl, M., Schweigert, G., et al., 2015, Jurassic climate mode governed by ocean gateway. *Nature Communications*, **6**: 10015.

Krencker, F.-N., Lindström, S., and Bodin, S., 2019, A major sea-level drop briefly precedes the Toarcian oceanic anoxic event: implications for Early Jurassic climate and carbon cycle. *Scientific Reports*, **9**: article # 12518.

Ladant, J.-B., and Donnadieu, Y., 2016, Palaeogeographic regulation of glacial events during the Cretaceous supergreenhouse. *Nature Communications*, **7**: article # 12771.

Lakin, J.A., Marshall, J.E.A., Troth, I., and Harding, I.C., 2016. Greenhouse to icehouse: a biostratigraphic review of latest Devonian–Mississippian glaciations and their global effects. *In* Becker, R.T., Königshof, P., and Brett, C.E. (eds). *Devonian Climate, Sea Level and Evolutionary Events*. Geological Society, London, Special Publications, **423**: 439–464.

Lambeck, K., Rouby, H., Purcell, A., Sun, Y., and Sambridge, M., 2014, Sea level and global ice volumes from the Last Glacial Maximum to the Holocene. *Proceedings of the National Academy of Sciences of the United States of America*, **111**: 15296–15303.

Landing, E., and MacGabhann, B.A., 2010, First evidence for Cambrian glaciation provided by sections in Avalonian New Brunswick and Ireland: additional data for Avalon–Gondwana separation by the earliest Palaeozoic. *Palaeogeography, Palaeoclimatology, Palaeoecology*, **285**: 174–185.

Laskar, J., 1990, The chaotic motion of the solar system: a numerical estimate of the size of the chaotic zones. *Icarus*, **88**: 266–291.

Laskar, J., 1999, The limits of Earth orbital calculations for geological time-scale use. *Philosophical Transactions of the Royal Society of London. Series A*, **357**: 1735–1759.

Laskar, J., Robutel, P., Joutel, F., Gastineau, M., Correia, A.C.M., and Levrard, B., 2004, A long-term numerical solution for the insolation quantities of the Earth. *Astronomy & Astrophysics*, **428**: 261–285.

Laurin, J., and Sageman, B.B., 2007, Cenomanian–Turonian coastal record in SW Utah, USA: orbital-scale transgressive–regressive events during Oceanic Anoxic Event II. *Journal of Sedimentary Research*, **77**: 731–756.

Laurin, J., Barclay, R.S., Sageman, B.B., Dawson, R.R., Pagani, M., Schmitz, M., et al., 2019, Terrestrial and marginal-marine record of the mid-Cretaceous Oceanic Anoxic Event 2 (OAE 2): high-resolution framework, carbon isotopes, CO_2 and sea-level change. *Palaeogeography, Palaeoclimatology, Palaeoecology*, **524**: 118–136.

Lee, J.H., Chen, J., and Chough, S.K., 2015, The middle–late Cambrian reef transition and related geological events: a review and new view. *Earth-Science Reviews*, **145**: 66–84.

Li, M., Huang, C., Hinnov, L., Ogg, J., Chen, Z.Q., and Zhang, Y., 2016, Obliquity-forced climate during the Early Triassic hothouse in China. *Geology*, **44**: 623–626.

Lin, W., Bhattacharya, J.P., Jicha, B.R., Singer, B.S. and Matthews, W., 2020, Has Earth ever been ice-free? Implications for glacio-eustasy in the Cretaceous greenhouse age using high-resolution sequence stratigraphy. *Geological Society of America Bulletin*: B35582.1.

Lisiecki, L.E., and Raymo, M.E., 2005, A Pliocene-Pleistocene stack of 57 globally distributed benthic $\delta^{18}O$ records. *Paleoceanography*, **20**: 1–17.

Liu, Y., Huang, C., Ogg, J.G., Algeo, T.J., Kemp, D.B., and Shen, W., 2019, Oscillations of global sea-level elevation during the Paleogene correspond to 1.2-Myr amplitude modulation of orbital obliquity cycles. *Earth and Planetary Science Letters*, **522**: 65–78.

Loi, A., Ghienne, J.F., Dabard, M.P., Paris, F., Botquelen, A., Christ, N., et al., 2010, The Late Ordovician glacio-eustatic record from a high-latitude storm-dominated shelf succession: the Bou Ingarf section (Anti-Atlas, Southern Morocco). *Palaeogeography, Palaeoclimatology, Palaeoecology*, **296**: 332–358.

Lourens, L.J., and Hilgen, F.J., 1997, Long-periodic variations in the Earth's obliquity and their relation to third-order eustatic cycles and late Neogene glaciations. *Quaternary International*, **40**: 43–52.

Lovell, B., 2010, A pulse in the planet: regional control of high-frequency changes in relative sea-level by mantle convection. *Journal of the Geological Society*, **167**: 637–648.

Loydell, D.K., 1998, Early Silurian sea-level changes. *Geological Magazine*, **135**: 447–471.

Loydell, D.K., 2007, Early Silurian positive $\delta^{13}C$ excursions and their relationship to glaciations, sea-level changes and extinction events. *The Journal of Geology*, **42**: 531–546.

Luber, T.L., Bulot, L.G., Redfern, J., Nahim, M., Jeremiah, J., Simmons, M., et al., 2019, A revised chronostratigraphic framework for the Aptian of the Essaouira-Agadir Basin, a candidate type section for the NW African Atlantic Margin. *Cretaceous Research*, **93**: 292–317.

Ludvigson, G.A., Joeckel, R.M., Murphy, L.R., Stockli, D.F., Gonzalez, L.A., Suarez, C.A., et al., 2015, The emerging terrestrial record of Aptian-Albian global change. *Cretaceous Research*, **56**: 1–24.

Lunn, G.A., Miller, S., and Samarrai, A., 2019, Dating and correlation of the Baluti Formation, Kurdistan, Iraq: implications for the regional recognition of a Carnian "marker dolomite", a review of the Triassic to Early Jurassic sequence stratigraphy of the Arabian Plate. *Journal of Petroelum Geology*, **42**: 5–36.

Ma, X.P., Liao, W., and Wang, D., 2009. The Devonian System of China, with a discussion on sea-level change in South China. *In* Königshof, P. (ed.). *Devonian Change: Case Studies in Palaeogeography and Palaeoecology*. Geological Society, London, Special Publications, **314**: 241–262.

Macquaker, J.H., and Keller, M.A., 2005, Mudstone sedimentation at high latitudes: ice as a transport medium for mud and supplier of nutrients. *Journal of Sedimentary Research*, **75**: 696–709.

Maloney, J.M., Bentley, S.J., Xu, K., Obelcz, J., Georgiou, I.Y., and Miner, M.D., 2018, Mississippi River subaqueous delta is entering a stage of retrogradation. *Marine Geology*, **400**: 12–23.

Matthews, R.K., and Al-Husseini, M.I., 2010, Orbital-forcing glacio-eustasy: a sequence-stratigraphic time scale. *GeoArabia*, **15**: 155–167.

Maurer, F., Van Buchem, F.S., Eberli, G.P., Pierson, B.J., Raven, M. J., Larsen, P.H., et al., 2013, Late Aptian long-lived glacio-eustatic lowstand recorded on the Arabian Plate. *Terra Nova*, **25**: 87–94.

McAnena, A., Flögel, S., Hofmann, P., Herrle, J.O., Griesand, A., Pross, J., et al., 2013, Atlantic cooling associated with a marine biotic crisis during the mid-Cretaceous period. *Nature Geoscience*, **6**: 558.

McArthur, J.M., Janssen, N.M.M., Reboulet, S., Leng, M.J., Thirlwall, M.F., and Van de Schootbrugge, B., 2007, Palaeotemperatures, polar ice-volume, and isotope stratigraphy (Mg/Ca, $\delta^{18}O$, $\delta^{13}C$, $^{87}Sr/^{86}Sr$): the Early Cretaceous (Berriasian, Valanginian, Hauterivian). *Palaeogeography, Palaeoclimatology, Palaeoecology*, **248**: 391–430.

McArthur, J.M., Howarth, R.J., and Shields, G.A., 2012, Strontium isotope stratigraphy. *In* Gradstein, F.M., Ogg, J.G., Schmitz, M.D., and Ogg, G.M. (eds), *The Geologic Time Scale 2012*, Elsevier, **1**: 127–144.

McCarthy, F.M., Katz, M.E., Kotthoff, U., Browning, J.V., Miller, K.G., Zanatta, R., et al., 2013, Sea-level control of New Jersey margin architecture: palynological evidence from Integrated Ocean Drilling Program Expedition 313. *Geosphere*, **9**: 1457–1487.

McDonough, K.J., and Cross, T.A., 1991, Late Cretaceous sea level from a paleoshoreline. *Journal of Geophysical Research: Solid Earth*, **96** (B4), 6591–6607.

Melchin, M.J., Sadler, P.M., and Cramer, B.D., 2012, The Silurian period. *In* Gradstein, F.M., Ogg, J.G., Schmitz, M.D., and Ogg, G.M. (eds), *The Geologic Time Scale 2012*. Elsevier, **2**: 525–558.

Miall, A.D., 1991, Stratigraphic sequences and their chronostratigraphic correlation. *Journal of Sedimentary Petrology*, **61**: 497–505.

Miall, A.D., 1992, The Exxon global cycle chart: an event for every occasion? *Geology*, **20**: 787–790.

Miall, A.D., 2010, *The Geology of Stratigraphic Sequences*, 2nd ed. Springer-Verlag, p. 522.

Miall, A.D., 2016, *Stratigraphy. A Modern Synthesis*. Springer, p. 454.

Miall, A.D., and Miall, C.E., 2001, Sequence stratigraphy as a scientific enterprise: the evolution and persistence of conflicting paradigms. *Earth-Science Reviews*, **54**: 321–348.

Millán, M.I., Weissert, H.J., and López-Horgue, M.A., 2014, Expression of the Late Aptian cold snaps and the OAE1b in a highly subsiding carbonate platform (Aralar, northern Spain). *Palaeogeography, Palaeoclimatology, Palaeoecology*, **411**: 167–179.

Miller, K.G., 2002, The role of ODP in understanding the causes and effects of global sea level change. *JOIDES Journal*, **28** (1), 23–28.

Miller, K.G., 2009, Broken greenhouse windows. *Nature Geoscience*, **2**: 465–466.

Miller, K.G., and Mountain, G.S., 1996, Drilling and dating New Jersey Oligocene-Miocene sequences: ice volume, global sea level, and Exxon records. *Science*, **271**: 1092–1095.

Miller, K.G., Fairbanks, R.G., and Mountain, G.S., 1987, Tertiary oxygen isotope synthesis, sea level history, and continental margin erosion. *Paleoceanography*, **2**: 1–19.

Miller, K.G., Wright, J.D., and Fairbanks, R.G., 1991, Unlocking the ice house: Oligocene-Miocene oxygen isotopes, eustasy, and margin erosion. *Journal of Geophysical Research: Solid Earth*, **96** (B4), 6829–6848.

Miller, K.G., Mountain, G.S., Browning, J.V., Kominz, M., Sugarman, P.J., Christie-Blick, N., et al., 1998, Cenozoic global sea-level, sequences, and the New Jersey Transect: results from coastal plain and slope drilling. *Reviews of Geophysics*, **36**: 569–601.

Miller, J.F., Evans, K.R., Loch, J.D., Ethington, R.L., Stitt, J.H., Holmer, L., et al., 2003a, Stratigraphy of the Sauk III (Cambrian-Ordovician) in the Ibex Area, Western Millard County, Utah and Central Texas. *Brigham Young University of Geological Studies*, **47**: 23–141.

Miller, K.G., Sugarman, P.J., Browning, J.V., Kominz, M.A., Hernández, J.C., Olsson, R.K., et al., 2003b, Late Cretaceous chronology of large, rapid sea-level changes: glacioeustasy during the greenhouse world. *Geology*, **31**: 585–588.

Miller, K.G., Sugarman, P.J., Browning, J.V., Kominz, M.A., Olsson, R.K., Feigenson, M.D., et al., 2004, Upper Cretaceous sequences and sea-level history, New Jersey Coastal Plain. *Geological Society of America Bulletin*, **116**: 368–393.

Miller, K.G., Kominz, M.A., Browning, J.V., Wright, J.D., Mountain, G.S., Katz, M.E., et al., 2005a, The Phanerozoic record of global sea-level change. *Science*, **310**: 1293–1298.

Miller, K.G., Wright, J.D., and Browning, J.V., 2005b, Visions of ice sheets in a greenhouse world. *Marine Geology*, **217**: 215–231.

Miller, K.G., Mountain, G.S., Wright, J.D., and Browning, J.V., 2011, A 180-million-year record of sea-level and ice volume variations from continental margin and deep-sea isotopic records. *Oceanography*, **24**: 40–53.

Miller, K.G., Browning, J.V., Mountain, G.S., Bassetti, M.A., Monteverde, D., Katz, M.E., et al., 2013a, Sequence boundaries are impedance contrasts: core-seismic-log integration of Oligocene–Miocene sequences, New Jersey shallow shelf. *Geosphere*, **9**: 1257–1285.

Miller, K.G., Mountain, G.S., Browning, J.V., Katz, M.E., Monteverde, D., Sugarman, P.J., et al., 2013b, Testing sequence stratigraphic models by drilling Miocene foresets on the New Jersey shallow shelf. *Geosphere*, **9**: 1236–1256.

Miller, K.G., Lombardi, C.J., Browning, J.V., Schmelz, W.J., Gallegos, G., Mountain, G.S., et al., 2018, Back to basics of sequence stratigraphy: Early Miocene and mid-Cretaceous examples from the New Jersey paleoshelf. *Journal of Sedimentary Research*, **88**: 148–176.

Miller, K.G., Browning, J.V., Schmelz, W.J., Kopp, R.E., Mountain, G.S., and Wright, J.D. 2020. Cenozoic sea-level and cryospheric evolution from deep-sea $\delta^{18}O$ and continental margin records. *Science Advances*. 6 (20), article #eaaz1346: 15 pp. https://advances.sciencemag.org/content/6/20/eaaz1346.full.

Milne, G.A., Gehrels, W.R., Hughes, C.W., and Tamisiea, M.E., 2009, Identifying the causes of sea-level change. *Nature Geoscience*, **2**: 471.

Montañez, I.P., and Poulsen, C.J., 2013, The Late Paleozoic ice age: an evolving paradigm. *Annual Review of Earth and Planetary Sciences*, **41**: 629–656.

Mørk, A., 1994, Triassic transgressive – regressive cycles of Svalbard and other Arctic areas: a mirror of stage subdivision. Recent developments on Triassic stratigraphy. *Mémoires de Géologie, Lausanne*, **22**: 69–82.

Moucha, R., Forte, A.M., Mitrovica, J.X., Rowley, D.B., Quéré, S., Simmons, N.A., et al., 2008, Dynamic topography and long-term sea-level variations: there is no such thing as a stable continental platform. *Earth and Planetary Science Letters*, **271**: 101–108.

Mountain, G., Proust, J.-N., and the Expedition 313 Science Party, 2010. The New Jersey margin scientific drilling project (IODP Expedition 313): untangling the record of global and local sea-level changes. *Scientific Drilling*, **10**: 26–34. https://sd.copernicus.org/articles/10/26/2010/sd-10-26-2010.pdf.

Müller, R.D., Sdrolias, M., Gaina, C., Steinberger, B., and Heine, C., 2008, Long-term sea-level fluctuations driven by ocean basin dynamics. *Science*, **319**: 1357–1362.

Müller, R.D., Seton, M., Zahirovic, S., Williams, S.E., Matthews, K.J., Wright, N.M., et al., 2016, Ocean basin evolution and global-scale plate reorganization events since Pangea breakup. *Annual Review of Earth and Planetary Sciences*, **44**: 107–138.

Munnecke, A., Calner, M., Harper, D.A.T., and Servais, T., 2010, Ordovician and Silurian sea-water chemistry, sea-level, and climate: a synopsis. *Palaeogeography, Palaeoclimatology, Palaeoecology*, **296**: 389–413.

Mutterlose, J., Bornemann, A., and Herrle, J., 2009, The Aptian-Albian cold snap: evidence for "mid" Cretaceous icehouse interludes. *Neues Jahrbuch für Geologie und Paläontologia Abhandlungen*, **252**: 217–225.

Myers, K.J., and Milton, N.J., 1996, Concepts and principles of sequence stratigraphy. *In* Emery, D., and Myers, K.J. (eds), *Sequence Stratigraphy*. Blackwell, Oxford, 11–44.

Naish, T., Powell, R., Levy, R., Wilson, G., Scherer, R., Talarico, F., et al., 2009, Obliquity-paced Pliocene West Antarctic ice sheet oscillations. *Nature*, **458**: 322.

Nance, R.D., and Murphy, J.B., 2013, Origins of the supercontinent cycle. *Geoscience Frontiers*, **4**: 439–448.

Neal, J., and Abreu, V., 2009, Sequence stratigraphy hierarchy and the accommodation succession method. *Geology*, **37**: 779–782.

Nerem, R.S., Chambers, D., Choe, C., and Mitchum, G.T., 2010, Estimating Mean Sea Level Change from the TOPEX and Jason Altimeter Missions. *Marine Geodesy*, **33**: 435.

Newell, A.J., 2000, Fault activity and sedimentation in a marine rift basin (Upper Jurassic, Wessex Basin, UK). *Journal of the Geological Society*, **157**: 83–92.

Nielsen, A.T., 2004, Ordovician sea level changes: a Baltoscandian perspective. *In* Webby, B.D., Paris, F., Droser, M.L., and Percival, I.G. (eds), *The Great Ordovician Biodiversification Event*. Columbia University Press, New York, 84–93.

Nielsen, A.T., 2011, A re-calibrated revised sea-level curve for the Ordovician of Baltoscandia. *In* Gutiérrez-Marco, J.C., Rábano, I., and García-Bellido, D. (eds), *Ordovician of the World, Cuadernos del Museo Geominero*. Instituto Geologico y Minero de España, Madrid, 399–401.

Nielsen, A.T., and Schovsbo, N.H., 2011, The Lower Cambrian of Scandinavia: depositional environment, sequence stratigraphy and palaeogeography. *Earth-Science Reviews*, **107**: 207–310.

Nielsen, A.T., and Schovsbo, N.H., 2015, The regressive Early-Mid Cambrian 'Hawke Bay Event' in Baltoscandia: epeirogenic uplift in concert with eustasy. *Earth-Science Reviews*, **151**: 288–350.

Niezgodzki, I., Tyszka, J., Knorr, G., and Lohmann, G., 2019, Was the Arctic Ocean ice free during the latest Cretaceous? The role of CO_2 and gateway configurations. *Global and Planetary Change*, **177**: 201–212.

O'Brien, C.L., Robinson, S.A., Pancost, R.D., Damste, J.S.S., Schouten, S., Lunt, D.J., et al., 2017, Cretaceous sea-surface temperature evolution: constraints from TEX_{86} and planktonic foraminiferal oxygen isotopes. *Earth-Science Reviews*, **172**: 224–247.

Ogg, J.G., Ogg, G., and Gradstein, F.M., 2008, *The Concise Geologic Time Scale*. Cambridge University Press, Cambridge, 177 pp.

Ogg, J.G., Ogg, G., and Gradstein, F.M., 2016, *A Concise Geologic Time Scale 2016*. Elsevier, Amsterdam, 234 pp.

Olde, K., Jarvis, I., Uličný, D., Pearce, M.A., Trabucho-Alexandre, J., Čech, S., et al., 2015, Geochemical and palynological sea-level proxies in hemipelagic sediments: a critical assessment from the Upper Cretaceous of the Czech Republic. *Palaeogeography, Palaeoclimatology, Palaeoecology*, **435**: 222–243.

Oxford, M.J., Hart, M.B., and Watkinson, M.P., 2004, Foraminiferal characterisation of mid-upper Jurassic sequences in the Wessex Basin (United Kingdom). *Rivista Italiana di Paleontologia e Stratigrafia*, **110**: 209–218.

Page, A.A., Zalasiewicz, J.A., Williams, M., and Popov, L.E., 2007, Were transgressive black shales a negative feedback modulating glacioeustasy in the Early Palaeozoic Icehouse? *In* Williams, M., Haywood, A.M., Gregory, F.J., and Schmidt, D.N. (eds), *Deep-Time Perspectives on Climate Change: Marrying the Signal From Computer Models and Biological Proxies*. The Micropalaeontological Society, Special Publications. The Geological Society, London, 123–156.

Pälike, H., Norris, R.D., Herrle, J.O., Wilson, P.A., Coxall, H.K., Lear, C.H., et al., 2006, The heartbeat of the Oligocene climate system. *Science*, **314**: 1894–1898.

Pearson, P.N., 2012, Oxygen isotopes in foraminifera: overview and historical review. *The Paleontological Society Papers*, **18**: 1–38.

Pekar, S.F., Christie-Blick, N., Kominz, M.A., and Miller, K.G., 2002, Calibration between eustatic estimates from backstripping and oxygen isotopic records for the Oligocene. *Geology*, **30**: 903–906.

Peltier, W.R., and Fairbanks, R.G., 2006, Global glacial ice volume and Last Glacial Maximum duration from an extended Barbados sea level record. *Quaternary Science Reviews*, **25**: 3322–3337.

Pemberton, S.G., Bhattacharya, J.P., MacEachern, J.A., and Pemberton, E.A., 2016, Unsung Pioneers of Sequence Stratigraphy: Eliot Blackwelder, Joseph Barrell, Amadeus Grabau, John Rich and Harry Wheeler. *Stratigraphy*, **13**: 223–243.

Peng, S., Babcock, L.E., and Cooper, R.A., 2012, The Cambrian Period. *In* Gradstein, F.M., Ogg, J.G., Schmitz, M.D., and Ogg, G.M. (eds), *The Geologic Time Scale 2012*. Elsevier, **2**: 437–488.

Peropadre, C., Liesa, C.L., and Meléndez, N., 2013, High-frequency, moderate to high-amplitude sea-level oscillations during the late Early Aptian: insights into the Mid-Aptian event (Galve sub-basin, Spain). *Sedimentary Geology*, **294**: 233–250.

Peters, S.E., Carlson, A.E., Kelly, D.C., and Gringerich, P.D., 2010, Large-scale glaciation and deglaciation of Antarctica during the Late Eocene. *Geology*, **38**: 723–726.

Petersen, K.D., Nielsen, S.B., Clausen, O.R., Stephenson, R., and Gerya, T., 2010, Small-scale mantle convection produces stratigraphic sequences in sedimentary basins. *Science*, **329**: 827–830.

Pictet, A., Delanoy, G., Adatte, T., Spangenberg, J.E., Baudouin, C., Boselli, P., et al., 2015, Three successive phases of platform demise during the early Aptian and their association with the oceanic anoxic Selli episode (Ardèche, France). *Palaeogeography, Palaeoclimatology, Palaeoecology*, **418**: 101–125.

Pitman III, W.C., 1978, Relationship between eustasy and stratigraphic sequences of passive margins. *Geological Society of America Bulletin*, **89**: 1389–1403.

Pitman III, W.C., and Golovchenko, X., 1983, The effect of sea-level change on the shelf edge and slope of passive margins. *In* Stanley, D.I. (ed), The Shelfbreak: Critical Interface on Continental Margins. *Society of Economic Paleontologists and Mineralogists Special Publication*, **33**: 41–58.

Pohl, A., and Austermann, J., 2018, A sea-level fingerprint of the Late Ordovician ice-sheet collapse. *Geology*, **46**: 595–598.

Pohl, A., Donnadieu, Y., Le Hir, G., Ladant, J.B., Dumas, C., Alvarez-Solas, J., et al., 2016, Glacial onset predated Late Ordovician climate cooling. *Paleoceanography*, **31**: 800–821.

Posamentier, H.W., and Vail, P.R., 1988, Eustatic controls on clastic deposition II—sequence and systems tract models. *In* Wilgus, C.K., Ross, C.A., and Posamentier, H. (eds), *Sea-Level Changes: An Integrated Approach*. SEPM Special Publication, **42**: 125–154.

Preto, N., Kustatscher, E., and Wignall, P.B., 2010, Triassic climates—state of the art and perspectives. *Palaeogeography, Palaeoclimatology, Palaeoecology*, **290**: 1–10.

Price, G.D., 1999, The evidence and implications of polar ice during the Mesozoic. *Earth-Science Reviews*, **48**: 183–210.

Price, G.D., and Nunn, E.V., 2010, Valanginian isotope variation in glendonites and belemnites from Arctic Svalbard: transient glacial temperatures during the Cretaceous greenhouse. *Geology*, **38**: 251–254.

Radzevičius, S., Tumakovaitė, B., and Spiridonov, A., 2017, Upper Homerian (Silurian) high-resolution correlation using cyclostratigraphy: an example from western Lithuania. *Acta Geologica Polonica*, **67**: 307–322.

Ray, D.C., van Buchem, F.S.P., Baines, G., Davies, A., Gréselle, B., Simmons, M.D., et al., 2019. The magnitude and cause of short-term eustatic Cretaceous sea-level change: a synthesis. *Earth-Science Reviews*, 197, article #102901: 20 pp. https://doi.org/10.1016/j.earscirev.2019.102901.

Raymo, M.E., Mitrovica, J.X., O'Leary, M.J., DeConto, R.M., and Hearty, P.J., 2011, Departures from eustasy in Pliocene sea-level records. *Nature Geoscience*, **4**: 328–332.

Rodríguez-López, J.P., Liesa, C.L., Pardo, G., Meléndez, N., Soria, A.R., and Skilling, I., 2016, Glacial dropstones in the western Tethys during the late Aptian–early Albian cold snap: palaeoclimate and palaeogeographic implications for the mid-Cretaceous. *Palaeogeography, Palaeoclimatology, Palaeoecology*, **452**: 11–27.

Rogov, M.A., and Zakharov, V.A., 2010, Jurassic and Lower Cretaceous glendonites occurrences and their implication for Arctic paleoclimate reconstructions and stratigraphy. *Frontiers in Earth Science*, **17**: 345–347.

Rogov, M.A., Ershova, V.B., Shchepetova, E.V., Zakharov, V.A., Pokrovsky, B.G., and Khudoley, A.K., 2017, Earliest Cretaceous (late Berriasian) glendonites from Northeast Siberia revise the timing of initiation of transient Early Cretaceous cooling in the high latitudes. *Cretaceous Research*, **71**: 102–112.

Rogov, M.A., Zverkov, N.G., Zakharov, V.A., and Arkhangelsky, M.S., 2019, Marine reptiles and climates of the Jurassic and Cretaceous of Siberia. *Stratigraphy and Geological Correlation*, **27**: 398–423.

Ross, C.A., and Ross, J.R., 1985, Late Paleozoic depositional sequences are synchronous and worldwide. *Geology*, **13**: 194–197.

Ross, C.A., and Ross, J.R.P., 1987, Late Palaeozoic sea levels and depositional sequences. *Cushman Foundation Foraminiferal Research Special Publication*, **24**: 137–149.

Ross, C.A., and Ross, J.R.P., 1988, Late Paleozoic transgressive-regressive deposition. *In* Wilgus, C.K., Ross, C.A., and Posamentier, H. (eds), *Sea-Level Changes: An Integrated Approach. SEPM Special Publication*, **42**: 227–247.

Ross, J.R.P., and Ross, C.A., 1992, Ordovician sea-level fluctuations. *In* Webby, B.D., and Laurie, J.R. (eds), *Global Perspectives on Ordovician Geology*. Balkema, Rotterdam, 327–335.

Ross, C.A., and Ross, J.R.P., 1995, North American depositional sequences and correlations. *In* Cooper, J.D., Droser, M.L., and Finney, S.F. (eds), *Ordovician Odyssey: Short Papers for the Seventh International Symposium on the Ordovician System*. The Pacific Section for the Society of Sedimentary Geology, Fullerton, p. 309–314.

Ross, C.A., and Ross, J.R.P., 1996, Silurian sea-level fluctuations, Special Paper. *In* Witzke, B.J., Ludvigson, G.A., and Day, J. (eds), *Palaeozoic Sequence Stratigraphy: Views From the North American Craton*. Geological Society of America, Special Paper, **306**: 187–192.

Rovere, A., Stocchi, P., and Vacchi, M., 2016, Eustatic and relative sea-level changes. *Current Climate Change Reports*, **2**: 221–231.

Rowley, D.B., 2002, Rate of plate creation and destruction: 180Ma to present. *Geological Society of America Bulletin*, **114**: 927–933.

Rowley, D.B., 2013, Sea-level: Earth's dominant elevation – implications for duration and magnitudes of sea-level variations. *The Journal of Geology*, **121**: 445–454.

Ruban, D.A., 2012, Comment on "Sequence stratigraphy and onlap history of the Donets Basin, Ukraine: insight into Carboniferous icehouse dynamics" by Eros, J.M., Montañez, I.P., Osleger, D.A., Davydov, V.I., Nemyrovska, T.I., Poletaev, V.I., Zhykalyak, M. V., 2012. Sequence stratigraphy and onlap history of the Donets Basin, Ukraine: insight into Carboniferous icehouse dynamics. [Palaeogeography, Palaeoclimatology, Palaeoecology 313, 1-25]. *Palaeogeography, Palaeoclimatology, Palaeoecology*, **363–364**: 184–186.

Ruban, D.A., 2016, A "chaos" of Phanerozoic eustatic curves. *Journal of African Earth Sciences*, **116**: 225–232.

Ruban, D.A., Conrad, C.P., and van Loon, A.J., 2010, The challenge of reconstructing the Phanerozoic sea-level and the Pacific Basin tectonics. *Geologos*, **16**: 235–243.

Runkel, A.C., Miller, J.F., McKay, R.M., Palmer, A.R., and Taylor, J.F., 2007, High-resolution sequence stratigraphy of lower Paleozoic sheet sandstones in central North America: the role of special conditions of cratonic interiors in development of stratal architecture. *Geological Society of America Bulletin*, **119**: 860–881.

Rygel, M.C., Fielding, C.R., Frank, T.D., and Birgenheier, L.P., 2008, The magnitude of Late Paleozoic glacioeustatic fluctuations: a synthesis. *Journal of Sedimentary Research*, **78**: 500–511.

Sadler, P.M., 2004, Quantitative biostratigraphy – achieving finer resolution in global correlation. *Annual Review of Earth and Planetary Sciences*, **32**: 187–213.

Sahagian, D., and Jones, M., 1993, Quantified Middle Jurassic to Paleocene eustatic variations based on Russian Platform stratigraphy: stage level resolution. *Geological Society of America Bulletin*, **105**: 1109–1118.

Sahagian, D., Pinous, O., Olferiev, A., and Zakharov, V., 1996, Eustatic curve for the Middle Jurassic - Cretaceous based on Russian Platform and Siberian stratigraphy zonal resolution. *The American Association of Petroleum Geologists Bulletin*, **80**: 1433–1458.

Saltzman, M.R., and Thomas, E., 2012, Carbon isotope stratigraphy. *In* Gradstein, F.M., Ogg, J.G., Schmitz, M.D., and Ogg, G.M. (eds), *The Geologic Time Scale 2012*. Elsevier, **1**: 207–232.

Sames, B., Wagreich, M., Wendler, J.E., Haq, B.U., Conrad, C.P., Melinte-Dobrinescu, M.C., et al., 2016, Short-term sea-level changes in a greenhouse world—a view from the Cretaceous. *Palaeogeography, Palaeoclimatology, Palaeoecology*, **441**: 393–411.

Schlager, W., 2004, Fractal nature of stratigraphic sequences. *Geology*, **32**: 185–188.

Schlager, W., 2005, Carbonate sedimentology and sequence stratigraphy. *SEPM Concepts Sedimentology Paleontology*, **8**: 200.

Schlager, W., 2010, Ordered hierarchy versus scale invariance in sequence stratigraphy. *International Journal of Earth Sciences*, **99**: 139–151.

Schmitz, M.D., and Davydov, V.I., 2012, Quantitative radiometric and biostratigraphic calibration of the Pennsylvanian–Early Permian (Cisuralian) time scale and pan-Euramerican chronostratigraphic correlation. *Geological Society of America Bulletin*, **124**: 549–577.

Schoene, B., Guex, J., Bartolini, A., Schaltegger, U., and Blackburn, T. J., 2010, Correlating the end-Triassic mass extinction and flood basalt volcanism at the 100 ka level. *Geology*, **38**: 387–390.

Scott, R.W., Oboh-Ikuenobe, F.E., Benson Jr, D.G., Holbrook, J.M., and Alnahwi, A., 2018, Cenomanian-Turonian flooding cycles: US Gulf Coast and Western Interior. *Cretaceous Research*, **89**: 191–210.

Seton, M., Gaina, C., Müller, R.D., and Heine, C., 2009, Mid-Cretaceous seafloor spreading pulse: fact or fiction? *Geology*, **37**: 687–690.

Shackleton, N., 1967, Oxygen isotope analyses and Pleistocene temperatures re-assessed. *Nature*, **215**: 15.

Sharland, P.R., Archer, R., Casey, D.M., Davies, R.B., Hall, S., Heward, A., et al. 2001, Arabian Plate sequence stratigraphy. *GeoArabia Special Publication*, **2**: 387 pp.

Sharland, P.R., Casey, D.M., Davies, R.B., Simmons, M.D., and Sutcliffe, O.E., 2004, Arabian Plate sequence stratigraphy: updates to SP2. *GeoArabia*, **9**: 199–214.

Siddall, M., Rohling, E.J., Almogi-Labin, A., Hemleben, C., Meischner, D., Schmelzer, I., et al., 2003, Sea-level fluctuations during the last glacial cycle. *Nature*, **423**: 853.

Simmons, M.D., 2012, Sequence stratigraphy and sea-level change. *In* Gradstein, F.M., Ogg, J.G., Schmitz, M.D., and Ogg, G.M. (eds), *The Geologic Time Scale 2012*. Elsevier, **1**: 239–268.

Simmons, M.D., 2015, Age is an interpretation. *In* Cullum, A., and Martinius, A.W. (eds), *52 Things You Should Know About Palaeontology*, Agile Libre, Canada. 26–27.

Simmons, M.D., 2018, *Great Geologists*. Halliburton, Abingdon, p. 141.

Simmons, M.D., and Davies, R.B., 2018, Triassic to Middle Jurassic stratigraphy of the Arabian Plate: an introduction. *In* Pöppelreiter, M.C. (ed), *Lower Triassic to Middle Jurassic Sequence of the Arabian Plate*. EAGE (European Association of Geoscientists and Engineers), 9–32.

Simmons, M.D., Sharland, P.R., Casey, D.M., Davies, R.B., and Sutcliffe, O.E., 2007, Arabian Plate sequence stratigraphy: potential implications for global chronostratigraphy. *GeoArabia*, **12**: 101–130.

Sloss, L.L., 1963, Sequences in the cratonic interior of North America. *Geological Society of America Bulletin*, **74**: 93–113.

Sluijs, A., Brinkhuis, H., Crouch, E.M., John, C.M., Handley, L., Munsterman, D., et al., 2008, Eustatic variations during the Paleocene-Eocene greenhouse world. *Paleoceanography*, **23**: PA4216.

Snedden, J.W., and Liu, C., 2010, A compilation of Phanerozoic sea-level change, coastal onlaps and recommended sequence designations. *Search and Discovery Article, American Association of Petroleum Geologists*, article # 40594.

Spasojevic, S., Liu, L.J., Gurnis, M., and Müller, R.D., 2008, The case for dynamic subsidence of the U.S. east coast since the Eocene. *Geophysical Research Letters*, 35, article #, L08305: 6 pp, https://doi.org/10.1029/2008GL033511.

Spasojevic, S., and Gurnis, M., 2012, Sea-level and vertical motion of continents from dynamic earth models since the Late Cretaceous. *The American Association of Petroleum Geologists Bulletin*, **96**: 2037–2064.

Stanford, J.D., Rohling, E.J., Hunter, S.E., Roberts, A.P., Rasmussen, S. O., Bard, E., et al., 2006, Timing of meltwater pulse 1a and climate responses to meltwater injections. *Paleoceanography*, **21**: PA4103.

Stefani, M., Furin, S., and Gianolla, P., 2010, The changing climate framework and depositional dynamics of Triassic carbonate platforms from the Dolomites. *Palaeogeography, Palaeoclimatology, Palaeoecology*, **290**: 43–57.

Stoll, H.M., and Schrag, D.P., 1996, Evidence for glacial control of rapid sea level changes in the Early Cretaceous. *Science*, **272**: 1771–1774.

Stoll, H.M., and Schrag, D.P., 2000, High-resolution stable isotope records from the Upper Cretaceous rocks of Italy and Spain: glacial episodes in a greenhouse planet? *Geological Society of America Bulletin*, **112**: 308–319.

Strasser, A., Hillgärtner, H., Hug, W., and Pittet, B., 2000, Third-order depositional sequences reflecting Milankovitch cyclicity. *Terra Nova*, **12**: 303–311.

Strauss, P., Harzhauser, M., Hinsch, R., and Wagreich, M., 2006, Sequence stratigraphy in a classic pull-apart basin (Neogene, Vienna Basin). A 3D seismic based integrated approach. *Geologica Carpathica*, **57**: 185–197.

Suess, E., 1888, *Das antlitz der erde*. F. Tempsky, Vienna, 772 pp.

Suess, E., 1906, *In* Sollas, W.J. (ed), *The Face of the Earth*, translated by Sollas, W.J., Clarendon Press, Oxford: 556 pp.

Sun, S.Q., 1989, A new interpretation of the Corallian cycles of the Dorset coast. *The Journal of Geology*, **24**: 139–158.

Sundquist, E.T., 1990, Long-term aspects of future atmospheric CO_2 and sea-level changes. *In* Revelle, R. (ed), *Sea-Level Change, National*

Research Council, Studies in Geophysics. National Academy Press, Washington, DC, 193–207.

Sutcliffe, O.E., Dowdeswell, J.A., Whittington, R.J., Theron, J.N., and Craig, J., 2000, Calibrating the Late Ordovician glaciation and mass extinction by the eccentricity cycles of Earth's orbit. *Geology*, **28**: 967–970.

Tabor, C.R., Poulsen, C.J., Lunt, D.J., Rosenbloom, N.A., Otto-Bliesner, B.L., Markwick, P.J., et al., 2016, The cause of Late Cretaceous cooling: a multimodel-proxy comparison. *Geology*, **44**: 963–966.

Torsvik, T.H., Steinberger, B., Gurnis, M., and Gaina, C., 2010, Plate tectonics and net lithosphere rotation over the past 150 My. *Earth and Planetary Science Letters*, **291**: 106–112.

Tripati, A.K., Backman, J., Elderfield, H., and Ferretti, P., 2005, Eocene bipolar glaciation associated with global carbon cycle changes. *Nature*, **436**: 341–346.

Tripati, A.K., Eagle, R.A., Morton, A., Dowdeswell, J.A., Atkinson, K.L., Bahé, Y., et al., 2008, Evidence for glaciation in the Northern Hemisphere back to 44Ma from ice-rafted debris in the Greenland Sea. *Earth and Planetary Science Letters*, **265**: 112–122.

Trotter, J.A., Williams, I.S., Nicora, A., Mazza, M., and Rigo, M., 2015, Long-term cycles of Triassic climate change: a new $\delta^{18}O$ record from conodont apatite. *Earth and Planetary Science Letters*, **415**: 165–174.

Underhill, J.R., and Partington, M.A., 1993, Use of genetic sequence stratigraphy in defining and determining a regional tectonic control on the "Mid-Cimmerian unconformity" – implications for North Sea basin development and the global sea level chart. *In* Weimer, P., and Posamentier, H.W. (eds), *Siliciclastic Sequence Stratigraphy*. American Association of Petroleum Geologists Memoir, **58**: 449–484.

Vail, P.R., 1987, Seismic stratigraphy interpretation using sequence stratigraphy: Part 1: Seismic stratigraphy interpretation procedure. *In* Bally, A.W. (ed), Atlas of Seismic Stratigraphy. *AAPG Studies in Geology*, **27**: 1–10.

Vail, P.R., 1992, The evolution of seismic stratigraphy and the global. *In* Dott Jr., R.H. (ed), Eustasy: The Historical Ups and Downs of a Major Geological Concept. *Geological Society of America Memoir*, **180**: 83–92.

Vail, P.R., Mitchum Jr., R.M., Todd, R.G., Widmier, J.M., Thompson III, S., Sangree, J.B., et al., 1977, Seismic stratigraphy and global changes of sea-level. *In* Payton, C.E. (ed), Seismic Stratigraphy – Applications to Hydrocarbon Exploration. *American Association of Petroleum Geologists Memoir*, **26**: 49–212.

Vakarelov, B.K., Bhattacharya, J.P., and Nebrigic, D.D., 2006, Importance of high-frequency tectonic sequences during greenhouse times of Earth history. *Geology*, **34**: 797–800.

van Buchem, F.S.P., and Simmons, M.D., 2017, Stratigraphic sweet spots—exploration insights from a eustatic model. *In* Hart, B., Rosen, N.C., West, D., D'Agostino, A., Messina, C., Hoffman, M., and Wild, R. (eds), *Sequence Stratigraphy: The Future Defined*. GCSSEPM, 247–265.

van Buchem, F.S.P., Allan, T.L., Laursen, G.V., Lotfpour, M., Moallemi, A., Monibi, S., et al., 2010a. Regional stratigraphic architecture and reservoir types of the Oligo-Miocene deposits in the Dezful Embayment (Asmari and Pabdeh Formations) SW Iran. *In* van Buchem, F.S.P., Gerdes, K.D., and Esteban, M., (eds). *Mesozoic and Cenozoic Carbonate Systems of the Mediterranean and the Middle East: Stratigraphic and Diagenetic Reference Models*, Geological Society, London, Special Publications, **329**: 219–263.

van Buchem, F.S.P., Al-Husseini, M.I., Maurer, F., Droste, H.J., and Yose, L.A., 2010b, Sequence-stratigraphic synthesis of the Barremian–Aptian of the eastern Arabian Plate and implications for the petroleum habitat. *In* van Buchem, F.S.P., Al-Husseini, M.I., Maurer, F., and Droste, H. (eds), *Barremian-Aptian Stratigraphy and Hydrocarbon Habitat of the Eastern Arabian Plate*. GeoArabia Special Publication, **4**: 9–48.

van Buchem, F.S.P., Simmons, M.D., Droste, H.J., and Davies, R.B., 2011, Late Aptian to Turonian stratigraphy of the eastern Arabian Plate–depositional sequences and lithostratigraphic nomenclature. *Petroleum Geoscience*, **17**: 211–222.

van der Meer, D.G., van Saparoea, A.V.D.B., Van Hinsbergen, D.J.J., Van de Weg, R.M.B., Godderis, Y., Le Hir, G., et al., 2017, Reconstructing first-order changes in sea-level during the Phanerozoic and Neoproterozoic using strontium isotopes. *Gondwana Research*, **44**: 22–34.

van Hinsbergen, D.J.J., Abels, H.A., Bosch, W., Boekhout, F., Kitchka, A., Hamers, M., et al., 2015, Sedimentary geology of the middle Carboniferous of the Donbas region (Dnieper-Donets Basin, Ukraine). *Scientific Reports*, **5**: article #9099: 8 pp. https://doi.org/10.1038/srep09099.

Van Sickel, W.A., Kominz, M.A., Miller, K.G., and Browning, J.V., 2004, Late Cretaceous and Cenozoic sea-level estimates: backstripping analysis of borehole data, onshore New Jersey. *Basin Research*, **16**: 451–465.

Van Wagoner, J.C., Posamentier, H.W., Mitchum, R.M., Vail, P.R., Sarg, J.F., Loutit, T.S., et al. 1988. An overview of the fundamentals of sequence stratigraphy and key definitions. *In* Wilgus, C.K., Hastings, B.S., Kendall, C.G. St., and Posamentier, H.W. (eds). *Sea-level Changes: An Integrated Approach*. SEPM Special Publication, **42**: 39–45.

Van Wagoner, J.C., Mitchum, R.M., Campion, K.M., and Rahmanian, V.D., 1990, Siliciclastic sequence stratigraphy in well logs, cores, and outcrops: concepts for high-resolution correlation of time and facies. *American Association of Petroleum Geologists, Methods in Exploration*, **7**: 55.

Veevers, J.J., 1990, Tectonic-climatic supercycle in the billion-year plate-tectonic eon: Permian Pangean icehouse alternates with Cretaceous dispersed-continents greenhouse. *Sedimentary Geology*, **68**: 1–16.

Vérard, C., Hochard, C., Baumgartner, P.O., and Stampfli, G.M., 2015, 3D palaeogeographic reconstructions of the Phanerozoic versus sea-level and Sr-ratio variations. *Journal of Palaeogeography*, **4**: 64–84.

Vickers, M.L., Price, G.D., Jerrett, R.M., Sutton, P., Watkinson, M.P., and FitzPatrick, M., 2019, The duration and magnitude of Cretaceous cool events: evidence from the northern high latitudes. *Geological Society of America Bulletin*, **131** (11-12), 1979–1994.

Videt, B., Paris, F., Rubino, J.L., Boumendjel, K., Dabard, M.P., Loi, A., et al., 2010, Biostratigraphical calibration of third order Ordovician sequences on the northern Gondwana platform. *Palaeogeography, Palaeoclimatology, Palaeoecology*, **296**: 59–375.

Voigt, S., Gale, A.S., and Voigt, T., 2006, Sea-level change, carbon cycling and palaeoclimate during the Late Cenomanian of northwest Europe: an integrated palaeoenvironmental analysis. *Cretaceous Research*, **27**: 836–858.

Wade, B.S., and Pälike, H., 2004, Oligocene climate dynamics. *Paleoceanography*, **19**: PA4019.

Wagreich, M., Lein, R., and Sames, B., 2014, Eustasy, its controlling factors, and the limn-eustatic hypothesis – concepts

inspired by Eduard Suess. *Austrian Journal of Earth Sciences*, **107**: 115–131.

Wendler, J.E., and Wendler, I., 2016, What drove sea-level fluctuations during the mid-Cretaceous greenhouse climate? *Palaeogeography, Palaeoclimatology, Palaeoecology*, **441**: 412–419.

Wendler, J.E., Lehmann, J., and Kuss, J., 2010. Orbital time scale, intra-platform basin correlation, carbon isotope stratigraphy and sea-level history of the Cenomanian–Turonian Eastern Levant platform, Jordan. *In* Homberg, C., and Bachman, M. (eds). *Evolution of the Levant Margin and Western Arabia Platform Since the Mesozoic*. Geological Society, London, Special Publications, **341**: 171–186.

Wendler, J.E., Meyers, S.R., Wendler, I., and Kuss, J., 2014, A million-year-scale astronomical control on Late Cretaceous sea-level. *Newsletters on Stratigraphy*, **47**: 1–19.

Wendler, J.E., Wendler, I., Vogt, C., and Kuss, J., 2016, Link between cyclic eustatic sea-level change and continental weathering: evidence for aquifer-eustasy in the Cretaceous. *Palaeogeography, Palaeoclimatology, Palaeoecology*, **441**: 430–437.

Wong, P.K., Weissenberger, J.A.W., and Gilhooly, M.G., 2016, Revised regional Frasnian sequence stratigraphic framework, Alberta Outcrop and subsurface. *In* Playton, T.E., Kerans, C., and Weissenberger, J.A.W. (eds), *New Advances in Devonian Carbonates: Outcrop Analogs, Reservoirs, and Chronostratigraphy*. SEPM Special Publication, **107**: 16–79.

Worsley, T.R., Nance, D., and Moody, J.B., 1986, Tectonic cycles and the history of the Earth's biogeochemical and paleoceanographic record. *Paleoceanography*, **1**: 233–263.

Wright, V.P., and Vanstone, S.D., 2001, Onset of Late Palaeozoic glacio-eustasy and the evolving climates of low latitude areas: a synthesis of current understanding. *Journal of the Geological Society*, **158**: 579–582.

Xu, X., Lithow-Bertelloni, C., and Conrad, C.P., 2006, Global reconstructions of Cenozoic seafloor ages: implications for bathymetry and sea-level. *Earth and Planetary Science Letters*, **243**: 552–564.

Zachos, J., Pagani, M., Sloan, L., Thomas, E., and Billups, K., 2001, Trends, rhythms, and aberrations in global climate 65Ma to present. *Science*, **292**: 686–693.

Zimmermann, J., Franz, M., Heunisch, C., Luppold, F.W., Mönnig, E., and Wolfgramm, M., 2015, Sequence stratigraphic framework of the Lower and Middle Jurassic in the North German Basin: epicontinental sequences controlled by Boreal cycles. *Palaeogeography, Palaeoclimatology, Palaeoecology*, **440**: 395–416.